EFFECT OF PRECORROSION BY GALVANOSTATIC ANODIC POLARIZATION AND TEMPERATURE ON THE FORMATION RATE OF IRON (II) CARBONATE FILM

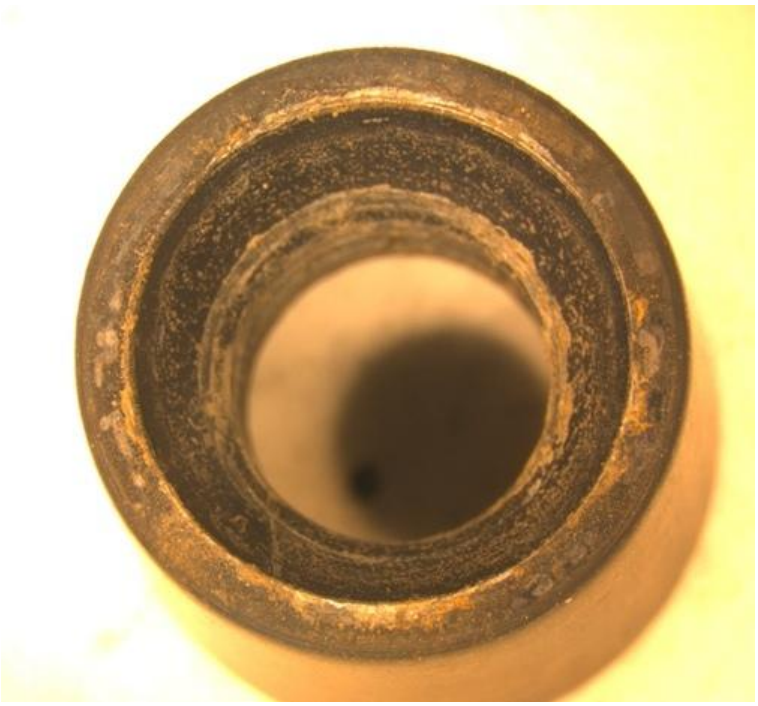

Master Thesis
by

Winia Farida Illa Biidznihi

University of Stavanger

December, 2011

University of Stavanger

Faculty of Science and Technology

MASTER'S THESIS

Study program/ Specialization: ENVIRONMENTAL TECHNOLOGY/OFFSHORE ENVIRONMENTAL ENGINEERING	Fall semester, 2011 Open / ~~Restricted access~~
Writer: WINIA FARIDA ILLA BIIDZNIHI	…… (Writer's signature)
Faculty supervisor: TOR HENNING HEMMINGSEN External supervisor(s):	
Titel of thesis: EFFECT OF PRECORROSION BY GALVANOSTATIC ANODIC POLARIZATION AND TEMPERATURE ON THE FORMATION RATE OF IRON (II) CARBONATE FILM	
Credits (ECTS): 30	
Key words: CO_2 CORROSION, Fe_3C, $FeCO_3$, EIS, CATHODIC SWEEPS, OCP, Rp/Ec TREND, SEM ANALYSIS, MEG	Pages: 64…… + enclosure: 35 …… Stavanger, 15 December/2011 Date/year

Preface

I would like to thank all those who helped me throughout my master's studies, helped me to complete this thesis and supported me in every possible way. I would like to say directly special thanks to:

- Professor Tor Henning Hemmingsen, my supervisor and my mentor, for his continuous guidance, knowledge sharing and support throughout my master's studies.
- Tonje Berntsen and Marion Seiersten from IFE.
- Torleiv Bilstad and the lab staff in Environmental and Chemistry.
- Staff at Mechanical department who made cell for the experiment.
- My partner lab; Dian Ekawati, Nushjarin Laethaisong, Valera Brailovskiy and Tamara Korto who helped and supported me during experiment and my other Indonesia friends who study and being together in Norway.
- Yanuar Priyadi, my beloved husband and Aliana, my lovely daughter. Thank you for their kindness, their love, their support, their patience, waits me for finishing my study.
- Last but not least, my parents, Widaningsih and Achmad Ali Basyah, my grandmother Rochmah and all family in Indonesia for loving me, believing in me and supporting me to pursuit my dreams.

Abstract

Corrosion on the inside walls of steel pipelines and process equipment is mostly caused by CO_2 which can cause property damage on the production and the transport of oil and natural gas. In order to control corrosion of steel in CO_2 environment, it is important to consider the formation of surface film and their influence on the corrosion rate. Iron (II) carbonate ($FeCO_3$) is an insoluble corrosion product which forms a film that potentially can be act as protective layer on the corroding surface. The presence of Fe_3C structure seems to be important in order to make the protective film which reduces the corrosion rate. In order to form the protective $FeCO_3$ formation film, a forced precorrosion is stimulated anodic current in order to enrich the amount of exposed Fe_3C (carbide) which facilitates the $FeCO_3$ formation film. The specimens which were used on these experiments are X65, St52 and St33 in base solution 1 g/kg NaCl and 50% wt MEG under precorrosion. Furthermore, 100 mmol/kg $NaHCO_3$ was added in the solution after precorrosion. The three steel qualities have different chemical composition especially the carbon (C), chromium (Cr), manganese (Mn) and silicon (Si) fraction which may show the different corrosion rate trend. The precorrosion times used in these experiments are 24 and 48 hours with temperatures of 40°C and 80°C, followed by free CO_2 corrosion for 216 hours. Electrochemical impedance spectroscopy, potentiodynamic cathodic sweeps, open circuit potential and Rp/Ec trend are methods used to follow the corrosion of these steels. In addition, SEM picture with EDS analysis is conducted to describe the electrode surface.

Keywords: CO_2 corrosion, Fe_3C, $FeCO_3$, EIS scan, Cathodic sweep, OCP, Rp/Ec trend, SEM Picture With EDS Analysis, MEG

Table of Contents

Preface i
Abstract ii
Table of Contents iii
List of Figures vi
List of Tables ix
1. INTRODUCTION 1
1.1. Background 1
1.2. Master thesis purpose 3
1.3 Structure of report 3
2. THEORY 4
2.1. Electrochemistry of CO_2 corrosion 4
2.2. Iron carbide 4
2.3. Iron (II) carbonate 4
2.4. Protective scales 5
2.4.1. The effect of temperature 5
2.5. Methods 6
2.5.1. Galvanostatic anodic polarization 6
2.5.2. NaCl solution 6
2.5.3. $NaHCO_3$ addition 6
2.5.4. Mono Ethylene Glycol (MEG) 7
2.5.5. The effect of Fe^{2+} concentration 7
2.5.6. Electrochemical impedance spectroscopy 8
2.5.7. Potentiodynamic cathodic 9
2.5.8. Rp/Ec trend 10
3 EXPERIMENTAL 11
3.1 Temperature regulation 11
3.2 Chemicals 12
3.3 Specimens and electrodes 12
3.4 Gamry software 12
3.5 Experimental procedures 14
3.6 Precorrosion 15
3.7 Analyzing the Fe^{2+} concentration 15
3.7.1 Developer solution (1 L) 15

3.7.2 Electrochemical Impedance Spectroscopy (EIS) Analysis 16
3.7.3 Potentiodynamic cathodic 16
3.7.4 Rp/Ec Trend 17
3.7.5 Scanning Electron Microscope with EDS Analysis 17
4 RESULT AND DISCUSSIONS 18
4.1 Galvanostatic anodic polarization 18
4.1.1 X65 steel 18
4.1.2 St52 steel 20
4.1.3 St33 steel 22
4.1.4 Summary comparison of 3 steels 24
4.2 Fe^{2+} Analysis 25
4.3 Electrochemical impedance spectroscopy 27
4.4.1 EIS scan results of 3 steels 27
4.4.2 Summary of EIS scan results 32
4.4 Potentiodynamic cathodic 33
4.4.1 24 hours at 40°C 34
4.4.2 48 Hours at 40°C 35
4.4.3 24 Hours at 80°C 36
4.4.4 48 hours at 80°C 38
4.4.5 The summary of potential trends for X65, St52 and St33 steels at 40°C and 80°C 39
4.5 Open circuit potential 40
4.5.1 24 hours at 40°C 40
4.5.2 48 hours at 40°C 41
4.5.3 24 hours at 80°C 42
4.5.4 48 hours at 80°C 42
4.6 Rp/Ec Trend 43
4.6.1 24 Hours at 40°C 43
4.6.2 48 Hours at 40°C 44
4.6.3 24 Hours at 80°C 45
4.6.4 48 Hours at 80°C 46
4.6.7 Summary of Rp trend from X65, St52 and St33 steels 47
4.7 SEM and EDS Analysis 48
5 CONCLUSIONS 52
6 RECOMMENDATION FOR FURTHER WORK 52

7 REFERENCES 53
8 APPENDIX 55
8.1 Chemical composition of steels 55
8.1.1 X65 steel 55
8.1.2 St52 steel 56
8.1.3 St33 steel 57
8.2 Fe2+ Concentration Analysis 58
8.2.1 Standard Calibration Curve 58
8.2 Fe^{2+} concentration results of X65, St52 and St33 steels 59
8.3 Electrochemical Impedance Spectroscopy 61
8.4 Rp/Ec Trend 63
8.4.1 X65 steel 63
8.4.2 St52 Steel 65
8.4.3 St33 steel 67
8.5 SEM Analysis 69
8.5.1 X65 steel at forced precorrosion 24 hours and 40°C 69
8.5.2 St52 steel at forced precorrosion 24 hours and 40°C 74
8.5.3 St33 steel at forced precorrosion 24 hours and 40°C 77
8.5.4 St33 steel at forced precorrosion 24 hours and 80°C 80
8.5.5 St33 steel at forced precorrosion 48 hours and 80°C 85

List of Figures

Fig. 1.1. An overview of planned activities on Master Thesis 2
Fig. 2.1 Morphologies observed for protective and non protective corrosion layers 5
Fig. 2.2 Nyquist Plot 8
Fig. 2.3 Theoretical cathodic polarization scan 9
Fig. 3.1 Julabo TW 20 Water Bath 11
Fig. 3.2 Yellow Line ET Basic Water Bath 11
Fig. 3.3 Counter electrode (Platinum) 13
Fig. 3.4 Reference Saturated Calomel Electrode (SCE) 13
Fig. 3.5 Corrosion cells connected to Gamry potentiostat 14
Fig. 3.6 Experimental procedures 15
Fig. 4.1 Potentials of X65 steel with applied current at 0.25 mA for 24 hours exposure time 19
Fig. 4.2 Potentials of X65 steel with applied current at 0.25 mA for 48 hours exposure time 20
Fig. 4.3 Potentials of St52 steel with applied current at 0.25 mA for 24 hours exposure time 21
Fig. 4.4 Potentials of St52 steel with applied current at 0.25 mA for 48 hours exposure time 22
Fig. 4.5 Potentials of St33 steel with applied current at 0.25 mA for 24 hours exposure time at different temperature 23
Fig. 4.6 Potentials of St33 steel with applied current at 0.25 mA for 48 hours exposure time at different temperature 24
Fig. 4.7 Nyquist plots result of X65 steel in precorroded 48 hours at 40°C after 216 hours of immersion in solution 27
Fig. 4.8 Nyquist plots result of St52 steel in precorroded 48 hours at 40°C after 216 hours of immersion in solution 28
Fig. 4.9 Nyquist plots result of St33 steel in precorroded 24 hours at 40°C after 192 hours of immersion in solution 29
Fig. 4.10 Nyquist plots result of St33 steel in precorroded 48 hours at 40°C after 216 hours of immersion in solution. 29
Fig. 4.11 Nyquist plots result of St52 steel in precorroded 24 hours at 80°C after 216 hours of immersion in solution 30
Fig. 4.12 Nyquist plots result of St33 steel in precorroded 24 hours at 80°C after 216 hours of immersion in solution 31
Fig. 4.13 Nyquist plots result of St33 steel in precorroded 48 hours at 80°C after 216 hours of immersion in solution 31
Fig. 4.14 Potentiodynamic cathodic sweeps of X65 steel (Precorroded 24 Hours at 40^0C) after 2-216 hours 34
Fig. 4.15 Potentiodynamic cathodic sweeps of St52 steel (Precorroded: 24 Hours at 40^0C) after 2-192 hours 34
Fig. 4.16 Potentiodynamic cathodic sweeps of St33 steel (Precorroded: 24 Hours at 40^0C) after 2-96 hours 35
Fig. 4.17 Potentiodynamic cathodic sweeps of X65 steel (Precorroded: 48 Hours at 40^0C) after 2-216 hours 35
Fig. 4.18 Potentiodynamic cathodic sweeps of St52 steel (Precorroded: 48 Hours at 40^0C) after 2-216 hours 36
Fig. 4.19 Potentiodynamic cathodic sweeps of St33 steel (Precorroded: 48 Hours at 40^0C) after 2-216 hours 36
Fig. 4.20 Potentiodynamic cathodic sweeps of X65 steel (Precorroded: 24 Hours at 80^0C) after 2-192 hours 37

Fig. 4.21 Potentiodynamic cathodic sweeps of St52 steel (Precorroded: 24 Hours at 80^{0}C) after 2-96 hours 37
Fig. 4.22 Potentiodynamic cathodic sweeps of St33 steel (Precorroded: 24 Hours at 80^{0}C) after 2-216 hours 38
Fig. 4.23 Potentiodynamic cathodic sweeps of X65 steel (Precorroded: 48 Hours at 80^{0}C) after 2-216 hours 38
Fig. 4.24 Potentiodynamic cathodic sweeps of St52 steel (Precorroded: 48 Hours at 80^{0}C) after 2-216 hours 39
Fig. 4.25 Potentiodynamic cathodic sweeps of St33 steel (Precorroded: 48 Hours at 80^{0}C) after 2-216 hours 39
Fig. 4.26 OCP of X65, St52 and St33 steels (Precorroded 24 hours at 40^{0}C) vs Time 41
Fig. 4.27 OCP of X65, St52 and St33 steels (Precorroded 48 hours at 40^{0}C) vs Time 41
Fig. 4.28 The potential of X65, St52 and St33 steels (Precorroded 24 hours at 80°C) vs Time 42
Fig. 4.29 The potential of X65, St52 and St33 steels (Precorroded 48 hours at 80°C) vs Time 43
Fig. 4.30 The corrosion rate of X65, St52 and St33 steels (Precorroded: 24 hours at 40°C) vs Time 44
Fig. 4.31 The corrosion rate of X65, St52 and St33 steels (Precorroded 48 hours at 40°C) vs Time 45
Fig. 4.32 The corrosion rate of X65, St52 and St33 steels (Precorroded 24 hours at 80oC) vs Time 46
Fig. 4.33 The corrosion rate of X65, St52 and St33 steels (Precorroded 48 hours at 80^{0}C) vs Time 47
Fig. 4.34 SEM picture with EDS analysis of X65 at forced precorrosion time 24 hours and temperature 40^{0}C after 216 hours exposure time 48
Fig. 4.35 SEM picture with EDS analysis of St52 at forced precorrosion time 24 hours and temperature 40^{0}C after 192 hours exposure time 49
Fig. 4.36 SEM picture with EDS analysis of St33 at forced precorrosion time 24 hours and temperature 40^{0}C after 75 hours exposure time 50
Fig. 4.37 SEM picture with EDS analysis of St33 at forced precorrosion time 24 hours and temperature 80^{0}C after 216 hours exposure time 50
Fig. 4.38 SEM picture with EDS analysis of St52 at forced precorrosion time 48 hours and temperature 80^{0}C after 216 hours exposure time 51
Fig. 8.1 Chemical composition of X65 steel 55
Fig. 8.2 Chemical composition of St52 steel 56
Fig. 8.3 Chemical composition of St33 steel 57
Fig. 8.4 Fe2+ Concentration vs Absorbance 58
Fig. 8.5 Fe2+ concentration of X65, St52, and St33 steels (Precorroded: 24 hours at 40^{0}C) vs Time 59
Fig. 8.6 Fe2+ concentration of 3 (three) steels (48 hours Precorrosion Times at 40^{0}C) vs Time 59
Fig. 8.7 Fe2+ concentration of 3 (three) steels (24 hours Precorrosion Times at 80^{0}C) vs Time 60
Fig. 8.8 Fe2+ concentration of 3 (three) steels (48 hours Precorrosion Times at 80^{0}C) vs Time 60
Fig. 8.9 Nyquist plots of impedance diagrams of X65 in precorroded 24 hours at 40°C after 216 hours of immersion in solution 61
Fig. 8.10 Nyquist plots of impedance diagram result of X65 in precorroded 24 hours at 80°C after 216 hours of immersion in solution 61

Fig. 8.11 Nyquist plots of impedance diagram result of X65 in precorroded 48 hours at 80°C after 216 hours of immersion in solution 62
Fig. 8.12 Nyquist plots of impedance diagram result of St52 steel in precorroded 24 hours at 40°C after 216 hours of immersion in solution 62
Fig. 8.13 Nyquist plots of impedance diagram result of St52 steel in precorroded 48 hours at 80°C after 216 hours of immersion in solution 63
Fig. 8.14 Corrosion rate of X65 steel (Precorroded 24 hours at 40^0C) vs Time 63
Fig. 8.15 Corrosion rate of X65 steel (Precorroded 48 hours at 40^0C) vs Time 64
Fig. 8.16 Corrosion rate of X65 steel (Precorroded 24 hours at 80^0C) vs Time 64
Fig. 8.17 Corrosion rate of X65 Steel (Precorroded 48 hours at 80^0C) vs Time 65
Fig. 8.18 Corrosion rate of St52 Steel (Precorroded 24 hours at 40^0C) vs Time 65
Fig. 8.19 Corrosion rate of St52 steel (Precorroded 48 hours at 40^0C) vs Time 66
Fig. 8.20 Corrosion rate of St52 steel (Precorroded 24 hours at 80^0C) vs Time 66
Fig. 8.21 Corrosion rate of St52 steel (Precorroded 48 hours at 80^0C) vs Time 67
Fig. 8.22 Corrosion rate of St33 steel (Precorroded 48 hours at 80^0C) vs Time 67
Fig. 8.23 Corrosion rate of St33 steel (Precorroded 48 hours at 40^0C) vs Time 68
Fig. 8.24 Corrosion rate of St33 (Precorroded 24 hours at 80^0C) vs Time 68
Fig. 8.25 Corrosion rate of St33 (Precorroded 48 hours at 80^0C) vs Time 69

List of Tables

Table 3.1 Chemical composition which used in experiment..... 12
Table 3.2 Chemical composition of specimen: X65 steel, St33 Steel and St52 Steel (from material certificate, received from IFE, 2011) 12
Table 4.1 The experiment results of X65 steel with variation of Precorrosion times and temperature..... 18
Table 4.2 The experiment results of St52 steel with variation of Precorrosion times and temperatures 21
Table 4.3 The experiment results of St33 steel with variation of precorrosion time and temperature..... 22
Table 4.4 The trend of potentials for X65, St52 and St33 at 40°C and 80°C 24
Table 4.5 Iron analysis results of X65, St52 and St33 steels with variation of corrosion time at forced precorrosion 24 or 48 hours at 40°C or 80°C..... 26
Table 4.6 The Rs, Rp and corrosion rate values of X65, St52 and St33 steels for 24 hours and 48 hours precorrosion time at 40°C and 80°C..... 33
Table 4.7 The trend of potentials from potentiodynamic cathodic scan for X65, St52 and St33 at 40°C and 80°C..... 40
Table 4.8 The corrosion rate results of X65, St52 and St33 steels with Variation of Precorrosion Time and Temperature..... 48

1. INTRODUCTION

1.1. Background

The corrosive conditions found in well stream carrying pipelines are mainly constituted by CO_2, H_2S and free water. Most fields at Norwegian Sector have low H_2S concentration and CO_2 is the dominating species in corrosion. Therefore, the general corrosion on the inside walls of steel pipelines and process equipment is caused by CO_2 which significantly causes material degradation (such as cracking, pitting, localized attack, weight loss) and affect to the production and transport of oil and natural gas [1-4]. One of a good way to control CO_2 corrosion is by applied protective scale $FeCO_3$ formation film on surface steel which commonly known for reducing the corrosion rate. The objective was to promote protective $FeCO_3$ film by high bicarbonate concentrations and study the effect of precorrosion and temperature on the formation of $FeCO_3$ film.

$FeCO_3$ (iron carbonate) is a main solid corrosion product in the CO_2 corrosion process which may form in wet CO_2 system, deposit on surface steel and act as protective scale which will provide reduction in the corrosion rate [5]. However, the formation $FeCO_3$ film can be protective or non protective depends on the conditions under which they are formed, such as; temperature, pH, CO_2 partial pressure, water chemistry etc [6]. In order to make the protective $FeCO_3$ formation film, the precorrosion was applied to obtain the amount of exposed Fe_3C (carbide) which necessary to promote $FeCO_3$ formation film. The terms of precorrosion here is defined as applying 0.25 mA/cm^2 anodic current by galvanostatic anodic polarization in order to increase the corrosion rate and to achieve a uniformly corroded surface in specimen. X65, St52 and St33 were used on these experiments and have different chemical properties especially in carbon (C), manganese (Mn) and silicon (Si) which may show the different corrosion rate trend. The precorrosion time which applied on these experiments were about 24 hours or 48 hours. The differences of precorrosion times may show different results of potential on the corrosion process and the effect of precorrosion times on Fe_3C formation on surface steels.

Temperature 40°C and 80°C were applied on these experiments to study the effect of temperature on formation rate $FeCO_3$ film. Furthermore, with the variation of precorrosion time and temperature gives different corrosion rate results from each specimen. Fe^{2+} concentration analysis, electrochemical impedance spectroscopy, potentiodynamic cathodic sweeps, open circuit potential and Rp/Ec trend were methods used to follow the corrosion of these steels. In addition, SEM picture with EDS analysis was conducted to describe the electrode surface of Fe_3C and $FeCO_3$ on the surface steels. An overview of planned activities in order to see the effect of temperature in schematic diagram set up in Fig. 1.1.

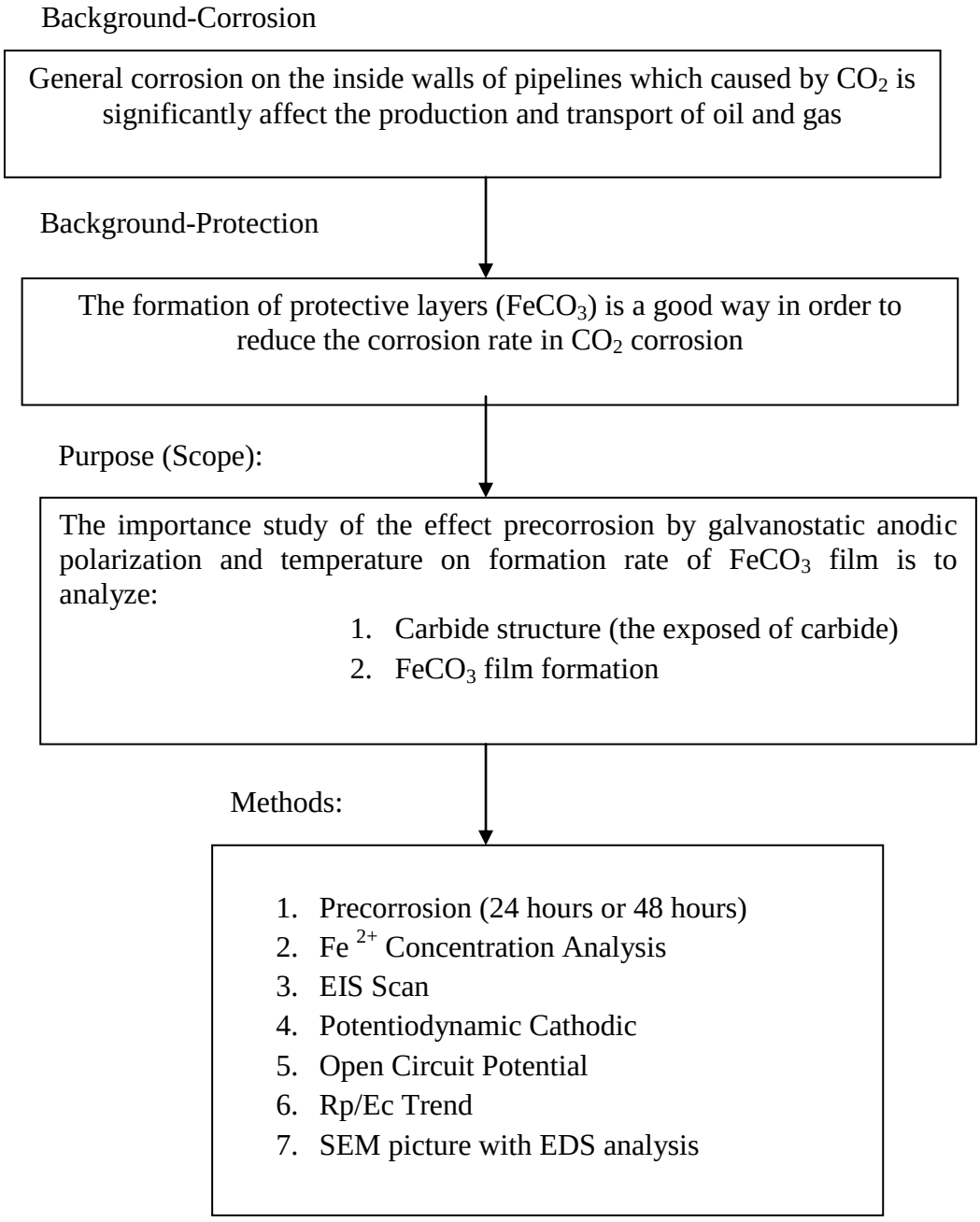

Fig. 1.1. An overview of planned activities on Master Thesis

1.2. Master thesis purpose

The purpose of the Master thesis is to form and analyze the protective iron (II) carbonate film which provides a reduction in corrosion rate. Study of the effect of precorrosion and temperature on formation $FeCO_3$ film was done. Several methods for analyzing protective iron (II) carbonate film were conducted by; Fe^{2+} concentration analysis, EIS scan, Potentiodynamic cathodic scan, OCP, Rp/Ec trend, SEM picture with EDS analysis. Therefore, in relation with iron (II) carbonate formation film, the parts of the experiments that had been analyzed were:

a. The effect of precorrosion time for Fe_3C formation which important to promote $FeCO_3$
b. The effect of temperature with variation of forced precorrosion time for $FeCO_3$ formation
c. The effect of chemical composition from carbon steel type due to corrosion rate

1.3 Structure of report

The report of Master thesis has been divided into 8 sections. The introduction is covered in section 1. Theory and experimental part are covered in section 2 and 3 respectively. Section 4 provides the results and discussion of the experiments. Section 5 provides conclusion and recommendation for further work is explained in section 6. Furthermore, references and appendix are followed in section 7 and 8 respectively.

2. THEORY

2.1. Electrochemistry of CO_2 corrosion

Aqueous CO_2 corrosion of carbon steel is an electrochemical process which involves the anodic dissolution of iron and the cathodic evolution of hydrogen [6]. The dissolved CO_2 in water or aqueous solutions caused negative impacts, especially in offshore oil and gas industry because resulted in severe corrosion on the steel pipelines and process equipment which used in the extraction, production and transport of oil and natural gas. Carbon dioxide is known to cause sweet corrosion due to its acidic properties, but there is another advantage that carbon dioxide is also known to form iron carbonate scale on carbon steel which may inhibit corrosion and reduce the corrosion rate [7]. The electrochemistry reaction of CO_2 corrosion is presented in Eq. (1):

$$Fe + CO_2 + H_2O = FeCO_3 + H_2 \qquad (1)$$

The formation of scales such $FeCO_3$ is often accompanied in electrochemical reaction as presented in Eq. 1. The formation $FeCO_3$ film can be protective or non protective depending on the conditions under which they are formed.

2.2. Iron carbide

Fe_3C (carbide) is a former part of the original steel in the non-oxidized state that accumulates on the surface as corrosion of the iron proceeds [8]. The formation of iron carbide can accelerate corrosion due to galvanic effects. It is because, Fe_3C act as an electronic conductor that leads to the possibility of galvanic coupling between the steel substrate and Fe_3C [9]. Therefore, iron carbide will remain on the surface when iron corroded. The presence of Fe_3C structure seems to be important in order to make the protective film which provides corrosion rate reduction.

2.3. Iron (II) carbonate

Iron (II) carbonate ($FeCO_3$) is an insoluble corrosion product which forms a film that potentially can be act as protective layer on the corroding surface [10]. According to the previous experiments, Iron (II) carbonate ($FeCO_3$) is important in the formation of protective layers [8, 11-13].

The equilibrium that describes the formation of iron (II) carbonate is [6]:

$$FeCO_3 = Fe^{2+} + CO_3^{2-} \qquad (2)$$

The precipitation rate determines the scale growth and its protectiveness of $FeCO_3$ because when $FeCO_3$ precipitates at the steel surface, the corrosion process can be slow down by [6]:

- Presenting a diffusion barrier for the species involved in corrosion process
- Covering (inhibiting) a portion of the steel surface

$FeCO_3$ can precipitate not only on the steel but also directly on the Fe_3C as a result of the ambient concentration in Fe^{2+} and the additional HCO_3^- anions produced on Fe_3C by the cathodic reduction of CO_2. The protective and non protective layers are depends on the presence and absence of Fe_3C in contact with steel; if Fe_3C is presence and in contact with steel, then the layer is protective. On the other hand, if Fe_3C is absence, then the layer is non protective. The non protective and protective layers are shown in Fig. 2.1.

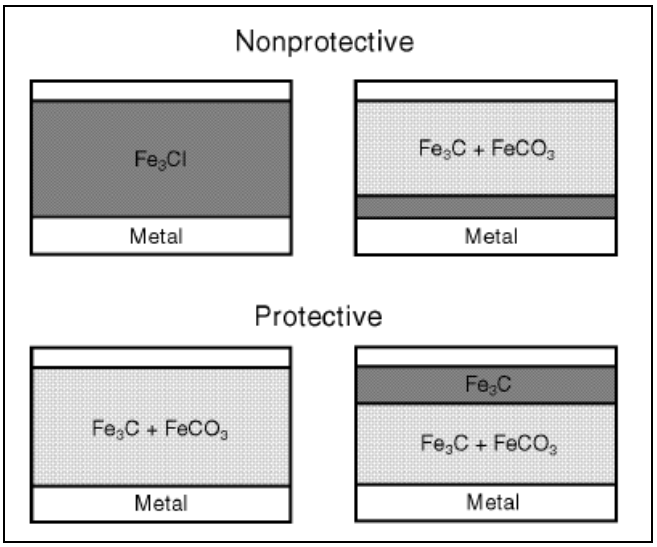

Fig. 2.1 Morphologies observed for protective and non protective corrosion layers
Source: J.L. Crolet, et.al (1998) [33]

2.4. Protective scales

There are so many factors that influences on the formation of protective $FeCO_3$ film, such as; temperature, pH, CO_2 partial pressure, water chemistry etc [6]. However, the main concern on this master thesis is the effect of temperature on the formation rate of $FeCO_3$ film which will be discussed below.

2.4.1. The effect of temperature

Temperature gives significantly effect to the corrosion rate, because an increase in temperature will cause a higher corrosion rate [14]. However, temperature also accelerates the corrosion products which will be formed on the carbon steel surface and make a protective film. Based on previous experiment [7], the protective properties of the film will improve when the temperature is increased. It is showed by temperature below 60°C, the film is easily removable, while a stable protective film is formed above temperature 60°C.
According to Dugstad [8], the morphology of the surface films is temperature dependent; a) Below 40^oC, surface films present an open porous structure and are formed mainly of Fe_3C with some $FeCO_3$ and alloying elements of the steel. In this temperature, the corrosion rate decreases with time for the first three days, but increases again for the next six days, an effect attributed to Fe_3C, which is suggested to increase the cathodic reaction, b) at 60^oC, the films present an inner porous part mainly of Fe_3C with more $FeCO_3$ accumulated in outer part. However, the formation of $FeCO_3$ did not reduce corrosion rate significantly, c) at 80^oC, a dense protective $FeCO_3$ film is formed close to the metal and it decreases the corrosion rate quickly (20-40 hours).

Temperature 40°C and 80°C were applied on these experiments to study the effect of temperature on formation rate $FeCO_3$ film.

2.5. Methods

Fe^{2+} concentration analysis, Electrochemical Impedance Scan (EIS), Potentiodynamic cathodic scan, Open Circuit Potential (OCP), Rp/Ec trend and Scanning Electron Microscopy (SEM) with EDS (Energy Dispersive Spectrometer) analysis were several methods which were used for analyzing protective iron (II) carbonate film.

2.5.1. Galvanostatic anodic polarization

Galvanostatic anodic polarization is useful to stimulate corrosion and achieve a uniformly corroded surface with iron carbide (Fe_3C) [15]. The effect of Fe_3C causes an increasing of cathodic area which reflected in the increasing of corrosion rate with time (the longer precorrosion times, the more Fe_3C present) and also be longer surface area [16]. Furthermore, the amount of exposed carbide on the galvanostatically "precorroded" surface will influence the formation rate of $FeCO_3$ film and further will affect the corrosion rate.

2.5.2. NaCl solution

NaCl in a CO_2 system will prevent passivation and be a promoter of pitting [17]. According to previous experiment [7], the corrosion rate increased with decreasing NaCl concentration on rotated electrodes. The condition may cause by the difficulties to form protective film at low salinity and on the other hand, the corrosion product showed a more porous product with increased NaCl concentration.

2.5.3. $NaHCO_3$ addition

An added amount of bicarbonate (pH), partial pressure of CO_2, temperature and the Fe^{2+} concentration are several methods which influences the precipitation of $FeCO_3$. Therefore, $NaHCO_3$ addition is useful to stimulate iron carbonate film on the steels as well as to be an efficient remedy in fighting corrosion in gas/condensate pipelines. This technique is commonly referred to as pH-stabilization [5]. The required concentration of bicarbonate is based on experimental data and field experience [18].
The equilibrium reactions are presented in Eqs.3 and 4.

$$H_2CO_3 = HCO_3^- + H^+ \qquad (3)$$

$$HCO_3^- = CO_3^{2-} + H^+ \qquad (4)$$

2.5.4. Mono Ethylene Glycol (MEG)

The addition of MEG to the solution will provide changes in the solution properties such as CO_2 solubility decreases, solution viscosity increases which lead to decreased CO_2 diffusivity, water activity decreases and solution polarity decreases [19]. Furthermore, added MEG is useful to control gas hydrate formation and minimize the effect on corrosion as well.

2.5.5. The effect of Fe^{2+} concentration

The protective films and low corrosion rates can be predicted from Fe^{2+} concentration; the increase of Fe^{2+} concentration results in higher supersaturation, which consequently accelerates the precipitation rate and leads to higher surface scaling tendency [20]. The statement is proven from previous experiments [21-23], that the CO_2 corrosion rates can be significantly reduced when $FeCO_3$ film precipitates on the steel surface (protective film). The precipitation process involves both nucleation and particle growth. The nucleation phase is believed to be exponentially dependant on the saturation ratio, while particle growth has an approximately linear relation to this parameter. Particle growth is the dominating precipitation process at low supersaturation, meaning that a surface film might not form since the driving force for the nucleation is high saturation ratio. The growth rate of $FeCO_3$ must be equal or greater than the corrosion rate in order to obtain a film, which requires a high supersaturation initially close to the steel surface where the corrosion process provides Fe^{2+} [24].
The increase in Fe^{2+} concentration in solution leads to faster and denser film formation. Typically, Fe^{2+} concentration needs to be increased to >1 ppm to make formation of Iron (II) carbonate protective films likely [25]. In order to initiate the growth of $FeCO_3$ film, the solution must be supersaturated with Iron (II) carbonate which implies that the saturation ratio/supersaturation of $FeCO_3$ must be > 1 [26].
The increased C_{Fe}^{2+} gives higher supersaturation [27] is showed in Eq. (5):

$$S = \frac{C_{Fe}^{2+} C_{CO3}^{2-}}{Ksp} \qquad (5)$$

C_{Fe}^{2+}= ionic product/activity of Fe^{2+}, C_{CO3}^{2-} = ionic product/activity of CO_3^{2-}, S= Supersaturation, Ksp = Solubility product of $FeCO_3$ at given temperature. The solubility products of $FeCO_3$ ($\log_{10}$ Ksp) for 40°C = -11.27 and 80°C = -12.57 [28].
The higher supersaturation will lead to a higher precipitation as given in Eq. (6):

$$R_{gr} = K_{gr} (S-1)^2 \qquad (6)$$

Where R_{gr} = growth rate, K_{gr}= growth rate constant, S= supersaturation

The scaling tendency [29] is given in Eq. (7):

$$ST = \frac{R_{gr}}{CR} \qquad (7)$$

Where R_{gr} = relative rates of precipitation, CR= corrosion prior to any film formation, ST = scaling tendency.
ST << 1, leading to porous and unprotective films because the rapidly corroding metal surface opens voids under the film much faster than precipitation can fill them out.
ST >> 1, unity conditions become favorable for formation of dense protective iron (II) carbonate films.

2.5.6. Electrochemical impedance spectroscopy

Electrochemical Impedance Spectroscopy (EIS) is a technique which useful for studying formation and protection ability of scales [29]. The low frequency data are on the right side of the plot shows the impedance characters of diffusion processes occurs clearly and high frequency data are on the left side of the plot which could be considered as capacitance of double electrode layer between the corrosion scale and electrode [30].

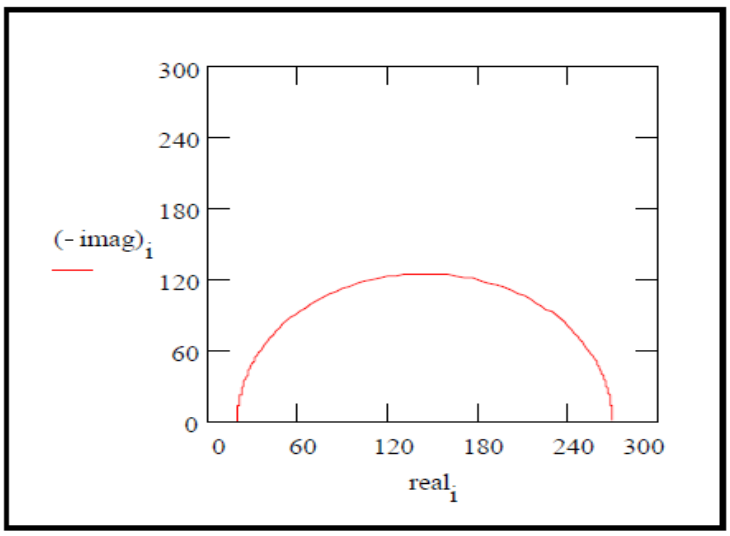

Fig. 2.2 Nyquist Plot

The different information about the corrosion system is provided by the use of EIS scan impedance technique [7]:

- Electrolyte resistance, Rs, which can be high when a low saline solution is used
- Polarization resistance, Rp, often called charge transfer resistance, which is used to calculate the corrosion rate given as B/Rp
- Warburger impedance, which gives information on diffusion controlled processes
- Absorption impedance, which gives information of degree of adsorption of species capacitance, C_{dl}, which gives information on film properties
- Thickness measurements of dielectric layer or scale
- Study of the corrosion mechanism

2.5.7. Potentiodynamic cathodic

Potentiodynamic polarization is a technique where the potential of the electrode is varied at selected rate by application of a current through the electrolyte. Through the DC polarization technique, information on corrosion rate, pitting suspecibillity, passivity as well as cathodic behavior of an electrochemical system may be obtained [31].
A schematic cathodic polarization scan is shown in Fig. 2.3. In a cathodic potentiodynamic scan, the potential is varied from point 1 in the negative direction to point 2. The open circuit potential is located at point A. Depending on the pH and the dissolved oxygen concentration in the solution, region B may represent the oxygen reduction reaction. Since this reaction is limited by how fast oxygen may diffuse in solution (mass transport controlled) there will be an upper limit on the rate of this reaction, known as limiting current density. Further decrease in the applied potential result in no change in the reaction rate, and hence the measured current remains the same (region C). Eventually, the applied potential becomes sufficiently negative for another cathodic reaction to become operative, such as shown at point D. As the potential and hence driving force becomes increasingly large, this reaction may become dominant, as shown in region E. This additional reaction is typically the reduction of other species in the environment (such as the hydrogen evolution reaction, also known as the water reduction reaction).

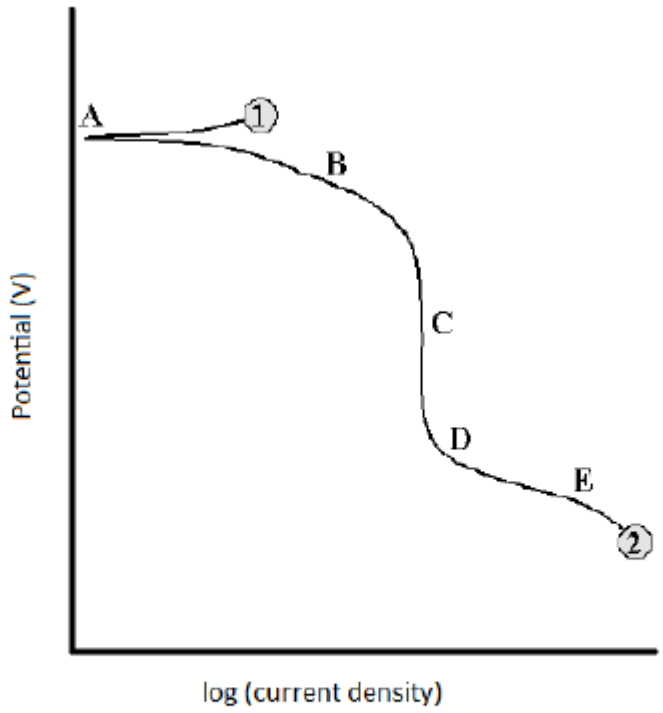

Fig. 2.3 Theoretical cathodic polarization scan

2.5.8. Rp/Ec trend

Rp is Polarization Resistance and Ec is Corrosion Potential. Rp/Ec trend purpose is to follow changes in the corrosion rate of a sample versus time. The Rp/Ec trend script makes a series of polarization resistance measurements at fixed time intervals. The resulting data is very useful for metal or inhibitor screening studies and for on-line monitoring.
Basically, the polarization resistance technique is used to obtain a rapid estimate of the corrosion rate of a metal in a solution. It is particularly applicable to long term monitoring because it involves small (< 20mV) excursions relative to Eoc. Such small excursions are less likely to change the sample than the manipulation, yields an estimate of Icorr which can be used to calculate a corrosion rate. Estimation of Icorr requires kinetic parameters, Betas, which must be calculated or estimated from other data [32].

3 EXPERIMENTAL

The purpose of the experiments is to observe the effect of galvanostatic anodic polarization which resulting in increasing on the concentration of exposed carbides and observe the effect of temperature on the formation rate of $FeCO_3$ film. There are two main outputs from experiment; 1) Carbide structure formation, 2) $FeCO_3$ film formation. The parameters of the experiment are:

3.1 Temperature regulation

Temperature is an important parameter in the experiments because temperatures significantly influence the formation of $FeCO_3$ film. The experiment is conducted at 40^{o}C and 80^{o}C, and water bath is used to achieve the required temperature for the experiment. In this experiment, the water bath that being used are; 1) Julabo TW 20, 2) Yellow Line ET Basic as shown in Figs 3.1 and 3.2.

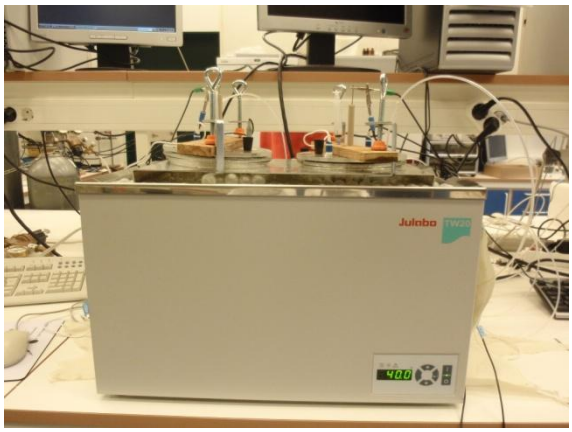

Fig. 3.1 Julabo TW 20 Water Bath

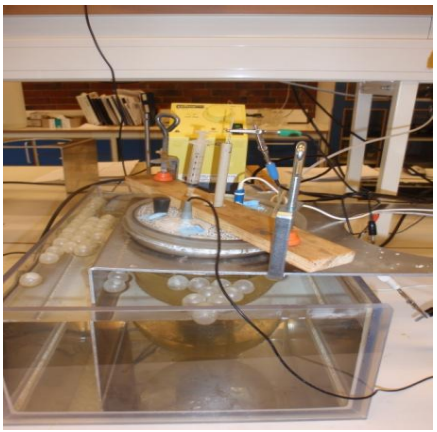

Fig. 3.2 Yellow Line ET Basic Water Bath

3.2 Chemicals

Base solution were 1 g/kg NaCl, 50 wt% MEG in CO_2 purging under precorrosion process. Furthermore, 100 mmol/kg $NaHCO_3$ was added under corrosion process.

Table 3.1 Chemical composition which used in experiment

No	Chemicals	Description
a	1 g/kg NaCl in distilled water	NaCl which used in this experiment is EMSURE ACS, ISO, Reag. Ph.Eur Sodium Chloride for analysis from Merck KGaA.
b	50 wt% MEG (50% aqueous MEG in distilled water)	Mono Ethylene Glycol (MEG) that used is 97% purity of MEG delivered by IFE.
c	1 atm CO_2	CO_2 on gas cylinder which used for experiment has serial number 500204 CO_2 30 kg (UN 1013 karbondioksid), from Yara Praxair AS.
d	100 mmol/kg $NaHCO_3$ in distilled water	$NaHCO_3$ which used in this experiment is Merck Pro Analyse $NaHCO_3$ (Molecular weight: 84.01 g/mol) from E Merck, D-6100 Darmstadt, F.R. Germany.

3.3 Specimens and electrodes

There were three specimens used in the experiments; 1) X65 steel, 2) St33 Steel, and 3) St52 Steel. The chemical composition of each steel is presented on Table 3.1 and the certificate is available in Appendix.

Table 3.2 Chemical composition of specimen: X65 steel, St33 Steel and St52 Steel (from material certificate, received from IFE, 2011)

Specimen	Element												
	C	Si	Mn	S	P	Cr	Ni	V	Mo	Cu	Al	Sn	Nb
X65	0.08	0.25	1.54	0.001	0.019	0.04	0.03	0.045	0.01	0.02	0.038	0.001	0.043
St33	0.07	0.19	0.87	0.004	0.012	0.56	0.01	0.032	0.01	0.01	0.035	0.001	-
St52	0.13	0.38	1.29	0.008	0.015	0.07	0.09	0.035	0.01	0.34	0.05	0.015	-

3.4 Gamry software

Gamry Software is used to measure and control corrosion of specimens during experiment. Gamry versions which used in this experiment are computers inserted a potentiostatic card using software; 1) Gamry Instruments Framework Version 5.61 (2010), 2) Gamry Instruments Framework Version 5.50 (2008).

The setup is according to standard method of Gamry:

1. Specimen is connected to cell cables; blue (working sense) and green (working).
2. Counter electrode (platinum), is connected to cell cables; red (counter) and orange (counter sense) with diameter 4 x 5 mm + 2.

Fig. 3.3 Counter electrode (Platinum)

3. Reference electrode (Saturated Calomel Electrode/SCE) is connected to cell cable; white (reference) applied in +245 mV vs. SHE.

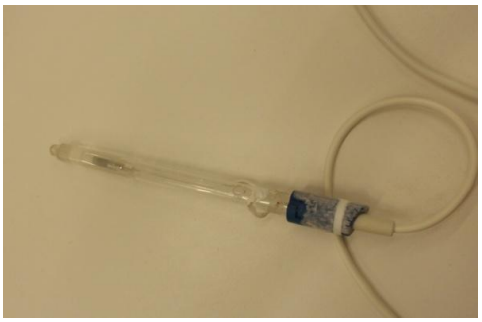

Fig. 3.4 Reference Saturated Calomel Electrode (SCE)

In the experiment, all electrodes (working electrode, counter electrode, reference electrode) that already connected to cell cable connections to a Gamry Potensiotat (PC3) in Potentiostat/Galvanostat/ZRA mode and immersed in the electrolyte which shown in the Fig. 3.5.

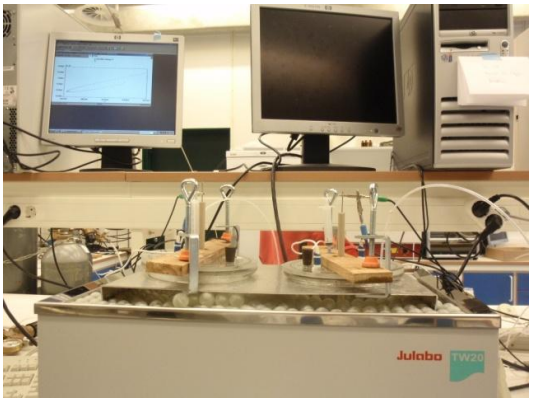

Fig. 3.5 Corrosion cells connected to Gamry potentiostat

3.5 Experimental procedures

The experiment procedures are described below:

1. Base solution is purged with CO_2 in 2 hours before the electrode is exposed to the solution. The pH is checked.
2. The specimen is polished to 1000 mesh, weighed, rinsed with ethanol prior to immersion according to the procedure provided.
3. E_{corr} is measured and a potentiodynamic cathodic sweep is performed to -300 mV vs E_{corr} in order to "activate" the surface of the electrode. Sweep rate 0.5 mV/s.
4. The specimen is galvanostatically polarized in the anodic direction at given current densities and exposure times.
5. Fe^{2+} concentration is measured at regular intervals (2, 10, 24, 48, 96, 192 and 216 hours days) for later calculation of the supersaturation of $FeCO_3$.
6. EIS scan is performed at same intervals as Fe^{2+} measurements.
7. Potentiodynamic sweep is performed in the cathodic direction (same intervals).
8. Rp/Ec trend is measured between every set of EIS/potentiodynamic sweeps to monitor the corrosion rate and -potential.
9. The specimen is removed from the solution and immediately rinse carefully with isopropanol according to the procedure provided. Specimen is weighed and preserved for SEM-analyses at IFE for selected samples.

The experimental procedures are presented in Fig. 3.6.

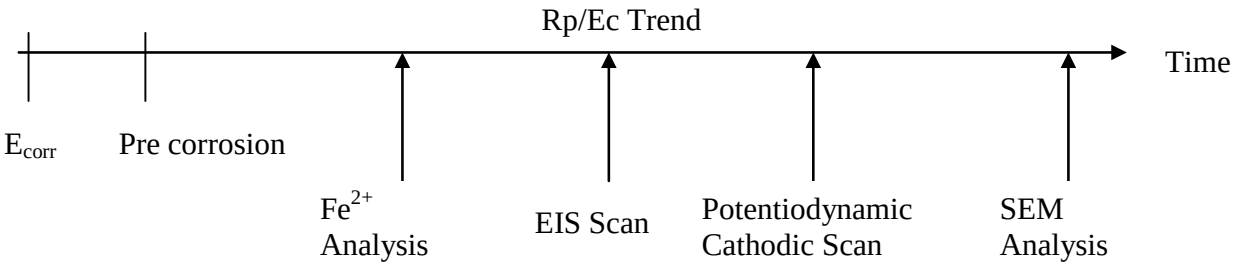

Fig. 3.6 Experimental procedures

3.6 Precorrosion

The methods for precorrosion experiments were:

1. Measure the corrosion potential for 10 minutes
2. Potentiodynamic sweep
3. Setting precorrosion time (24 hour, 48 hour) to have galvanostatic result. Gamry setting for galvanostatic are:

- Initial I(mA): 0.25
- Initial time: 0 s
- Final I (mA): 0.25
- Final time: 24 hours or 48 hours
- Sample period: 0.5 s

3.7 Analyzing the Fe^{2+} concentration

The methods for analyzing the effect of precorrosion by galvanostatic anodic polarization and the effect of temperatures on the formation rate of iron (II) carbonate film are:

3.7.1 Developer solution (1 L)

The developer solution is made by adding:

1. 200 ml distilled water
2. 1.1 g of 1.10-Phenantrolin-1-hydrat
3. 3 gram Acetic Acid
4. 2 gram $HONH_3Cl$
5. 6.8 gram $C_2H_3O_2Na*3H_2O$/4.1 gram $C_2H_3O_2Na$
6. Add up to 1 liter solution.

The procedures for analysis were:

1. Weighing bottle in tara,
2. Add 10 ml Developer Solution to a bottle and weigh it,
3. Add 200 µl solution from sample to a bottle (which already contain of Developer Solution) and weigh it,
4. For further Fe^{2+} concentration analysis, an UV spectrophotometry and calibration curves is used. Concentration of Fe^{2+} is based on UV-Spectrophotometry calibrated against a standard curve, detail presented in Appendix.

3.7.2 Electrochemical Impedance Spectroscopy (EIS) Analysis

The settings for EIS scan were:

DC Voltage	0 V vs. Eoc
AC Voltage	10 mV rms
Initial freq	500 Hz
Final freq	0.007 Hz
Points /decade	10

3.7.3 Potentiodynamic cathodic

The settings for potentiodynamic cathodic were:

Initial E	+5 mV vs. Eoc
Final E	-300 mV vs. Eoc
Scan rate	0.2 mV/s
Sample period	1 s

3.7.4 Rp/Ec Trend

The settings for Rp/Ec Trend were:

Initial E	-5 mV vs. Eoc
Final E	+5 mV vs. Eoc
Scan rate	0.05 mV/s
Sample period	1 s
Repeat time	60 min

3.7.5 Scanning Electron Microscope with EDS Analysis

SEM analysis were done in order to show the presence of both $FeCO_3$ and carbide structure on film and surface characteristics of film. In SEM analysis, the IFE's scanning electron microscope (SEM) was used; an ultra-high resolution Hitachi S-4800 which equipped with Noran System Six energy dispersive spectrometer (EDS) for element analysis. The parameter of SEM picture with EDS analysis which were used: 1) 15.0 kV Accelerating voltage of secondary electron image resolution, 2) Backscattered electron image resolution amount 3.0 nm guaranteed (at 15 kV YAG detector), 3) Magnification from 2000 to 5000.

4 RESULT AND DISCUSSIONS

4.1 Galvanostatic anodic polarization

The three specimens used in experiments are X65, St33 and St52 Steels. First, the corrosion potential was measured for 10 minutes and further potentiodynamic cathodic sweep is performed to -300 mV vs E_{corr} to "activate" the surface of the electrode. The specimen is galvanostatically polarized in the anodic direction with different forced precorrosion time (24 or 48 hours) at temperatures (40^{o}C or 80 ^{o}C). The potential given in Table 4.1, 4.2 and 4.3 were achieved at the end of precorroded time. For some experiments, the unstable corrosion potential at the beginning may cause by some errors in the equipment during experiment, for example; 1) bad connection in corrosion cell to a Gamry system, 2) the water inside of the reference electrode was evaporated. The results of experiments from each specimen are presented below.

4.1.1 X65 steel

Table 4.1 is data from the experiments of X65 steel with variation of precorroded and temperatures. According to Table 4.1 it can be considered at 40°C, Fe_3C was already present on the surface sample during the precorrosion times (24 hours and 48 hours). The potential were obtained at the end of precorrosion period (24 hours) increased from -598 mV to -552 mV. The longer precorrosion times should produce more Fe_3C, therefore at 48 hours precorrosion times, the value of potential had increase 59 mV (from -660 to -601) compared to 24 hours precorrosion times which is 46 mV (from -598 mV to -552 mV). The same also with electrolyte, CO_2 saturation and other parameters which also has been proved previously [24]; as more Fe_3C is present, the more negative is E_{corr}.
Furthermore, at 80°C, Fe_3C was accumulated on surface and increased corrosion process rapidly. It can be seen from Table 4.1 that the potential increased from -720 mV to -655 mV at the end of 24 hours precorrosion times. However, the potential were obtained at the end of 48 hours precorrosion times (-654 mV) smaller than the potential at 24 hours precorrosion times (-655 mV). It may cause by some error in the equipment during the beginning period.

Table 4.1 The experiment results of X65 steel with variation of Precorrosion times and temperature

No	T (°C)	E_{corr} (mV)	$I_{-300\ mV}$	t (Precorrosion)	E_G (mV)
1	40^{o}C	-598 mV	-252 µA	24 hours	-552 mV
2		-660 mV	- 302 µA	48 hours	-601 mV
3	80^{o}C	-720 mV	-810 µA	24 hours	-655 mV
4		-666 mV	-681 µA	48 hours	-654 mV

Definition:

T : Temperature (°C)
E_{corr} : Corrosion Potential (mV)
$I_{-300\ mV}$: Current at applied potential (µA)

t : Precorroded (Hours)
E_G : Potential obtained in the end of applied galvanostatic current of 0.25 mA

Fig. 4.1 shows the comparison of potential X65 steel applied in current 0.25 mA for 24 hours precorrosion times at different temperature (40°C and 80°C). The potential were obtained at the end of precorrosion period (24 hours) increased from -598 mV to -552 mV. The same condition is found at 80°C, the potential was -655 mV which obtained at the end of 24 hours precorrosion time. Therefore, if compared from the value of corrosion potential, the potential increased from -720 mV to -655 mV.

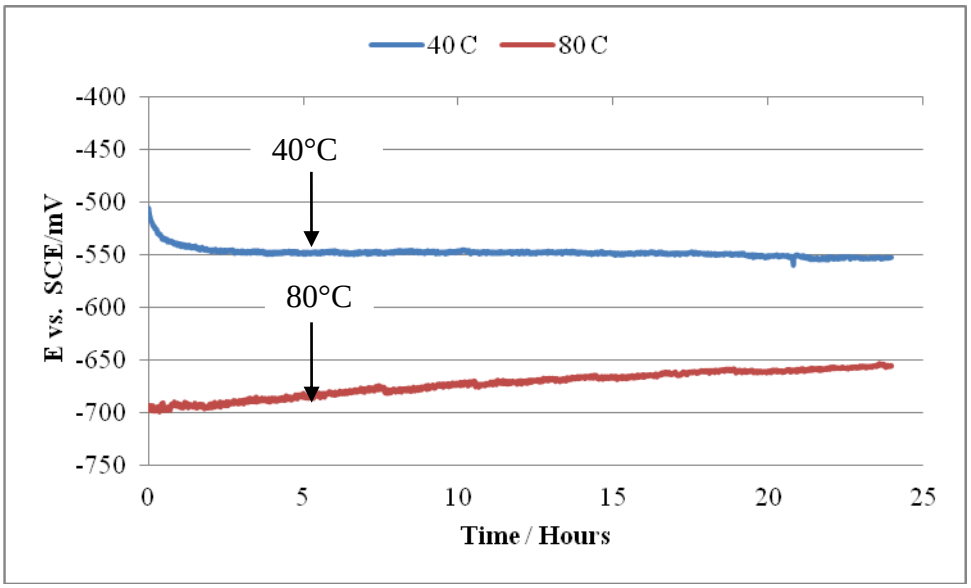

Fig. 4.1 Potentials of X65 steel with applied current at 0.25 mA for 24 hours exposure time

The potential increased during applied galvanostatic anodic polarization. The potential of 40°C obtained at the end of 48 hours precorrosion times; -601 mV and indicated that the potential increased from -660 mV to -601 mV. The same condition is found at 80°C; the potential was increased from -666 mV to -654 mV even though at the beginning the potential was unstable and is shown in Fig. 4.2.

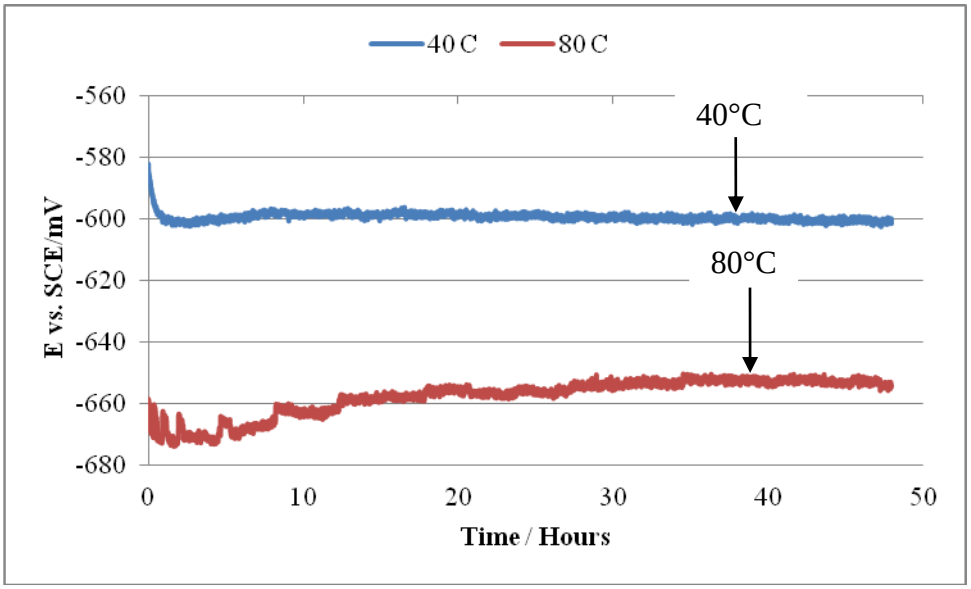

Fig. 4.2 Potentials of X65 steel with applied current at 0.25 mA for 48 hours exposure time

4.1.2 St52 steel

The 24 hours and 48 hours precorrosion times with variation of temperatures of St52 Steel is presented in Table 4.2. Based on Table 4.2, the corrosion potential at 40°C at the beginning (before galvanostatic) was -397 mV. The value was very high and indicated that was some errors during experiment. It can be viewed from irregular and random mess of line in Fig. 4.3. The condition may caused by; 1) bad connection in corrosion cell to a gamry system, 2) bubbling in reference electrode. Afterwards, the galvanostatic was conducted with 24 hours precorrosion times and obtained -533 mV at the end of precorrosion period. The comparison of 48 hours precorrosion times showed the corrosion potential at the beginning (before galvanostatic) was more stable (-668 mV) than the corrosion potential of 24 hours precorrosion times. The potential increased from -668 mV to -592 mV at the end of 48 hours precorrosion times.

Furthermore, at 80°C, the value of potentials at the end of precorrosion period is more negative compared to 40°C. It is because at 80°C, steel is corroded faster and considered that more Fe_3C is present at precorrosion period (24 hours or 48 hours) which increasing the corrosion rate. According to table 4.4, the potential were obtained at the end of precorrosion period (24 hours) increased from -728 mV to -665 mV. However, the potential were obtained at the end of 48 hours precorrosion times decreased from -676 mV to -683 mV. The unstable of potential during 48 hours precorrosion times at 80°C is shown in Fig. 4.3.

Table 4.2 The experiment results of St52 steel with variation of Precorrosion times and temperatures

No	T (°C)	E_{corr} (mV)	$I_{-300\ mV}$	t (Precorrosion)	E_G (mV)
1	40°C	-397 mV	-5 µA	24 hours	-533 mV
2		-668 mV	-247 µA	48 hours	-592 mV
3	80°C	-728 mV	-773 µA	24 hours	-665 mV
4		-676 mV	-772 µA	48 hours	-683 mV

The potentials comparison of St52 Steel applied in current 0.25 mA for 24 hours precorrosion times at different temperature (40°C and 80°C) is shown in Fig. 4.3. The irregular and random mess of line at 40°C indicated there were some errors at the beginning of experiments but finally the potential was stable at the end of precorrosion period. The potential were obtained -533 mV at the end of 24 hours precorrosion times. Furthermore, at 80°C, the potential at beginning was more stable compared to 40°C and the potential were obtained -665 mV at the end of 24 hours precorrosion times, increased from -728 mV to -665 mV.

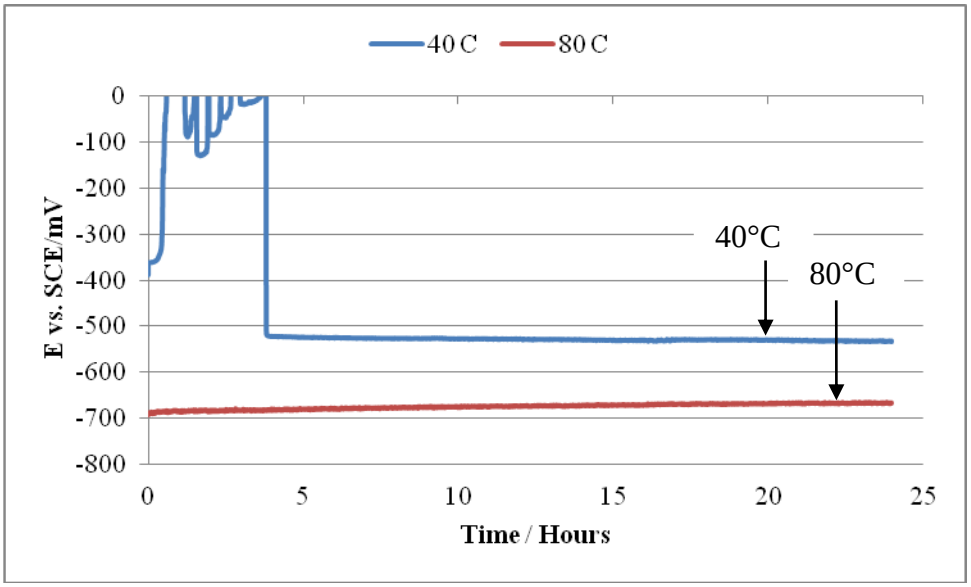

Fig. 4.3 Potentials of St52 steel with applied current at 0.25 mA for 24 hours exposure time

Fig. 4.4 shows the comparison of potential St52 steel applied in current 0.25 mA for 48 hours precorrosion times at different temperature (40°C and 80°C). The potential were -592 mV; obtained at the end of precorrosion period (48 hours) increased from -668 mV to -592 mV. Therefore, if compared from the value of potential at 80°C, -683 mV were obtained at the end of 48 hours precorrosion time and however, decreased from -676 mV to -683 mV. The decreasing of potential may cause by unstable potential in the middle of precorrosion times and shown in Fig. 4.4 below.

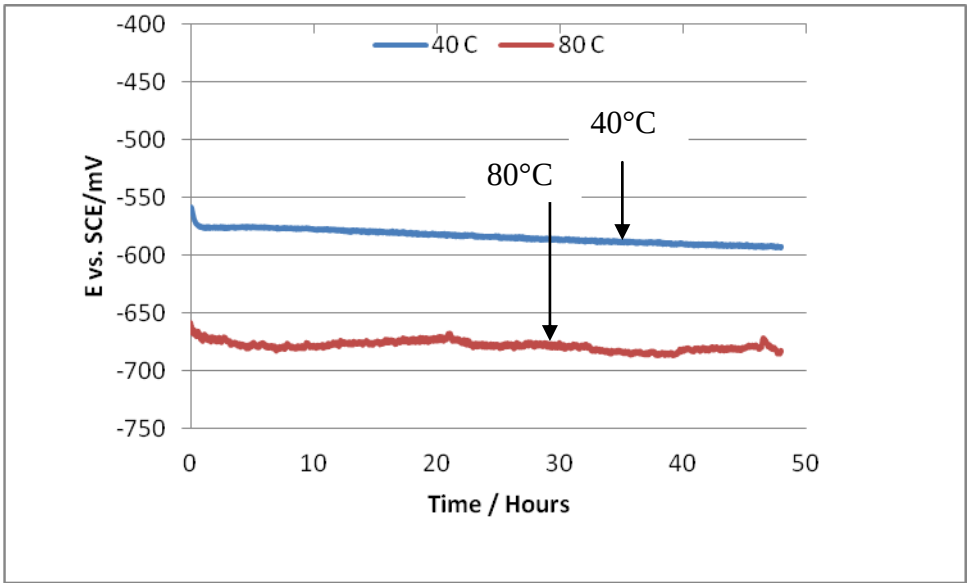

Fig. 4.4 Potentials of St52 steel with applied current at 0.25 mA for 48 hours exposure time

4.1.3 St33 steel

Table 4.3 is data from the experiments of St33steel with variation of precorrodeds and temperatures. In general, Fe_3C is already formed at the end of precorrosion period at 40°C. It can be compared between the value of potential at the end of precorrosion period and the value of corrosion potential before galvanostatic was conducted. The potential were -581 mV, obtained at 24 hours precorrosion times so that the potential increased from -640 mV to -581 mV. The same condition is also found at 48 hours precorrosion times where Fe_3C is more present on surface steel at 40°C, the potential increased from -676 mV to -620 mV.
The different condition is found at 80°C, where the potential were obtained both at the end of precorrosion times (24 hours and 48 hours) decreased. The unstable potentials which showed by irregular and random mass of lines is shown in Fig. 4.5 and 4.6.

Table 4.3 The experiment results of St33 steel with variation of precorrosion time and temperature

No	T (°C)	E_{corr} (mV)	$I_{-300\ mV}$	t (Precorrosion)	E_G (mV)
1	40°C	-640 mV	-276 µA	24 hours	-581 mV
2		-676 mV	-262 µA	48 hours	-620 mV
3	80°C	-678 mV	-1µA	24 hours	-688 mV
4		-650 mV	-1 µA	48 hours	-693 mV

The potentials comparison of St33 applied in current 0.25 mA for 24 hours precorrosion times at different temperature (40°C and 80°C) is shown in Fig. 4.5. The potential at 80°C was shown irregular line and it may indicate there was some bad connection between instruments in a corrosion cell and Gamry system until the end of experiments. The potential were obtained -688 mV at the end of 24 hours precorrosion times, decreased from -678 mV to 688

mV. However, compared to 40°C, the potential was more stable and obtained -581 mV at the end of 24 hours precorrosion times, increased from -640 mV to -581 mV.

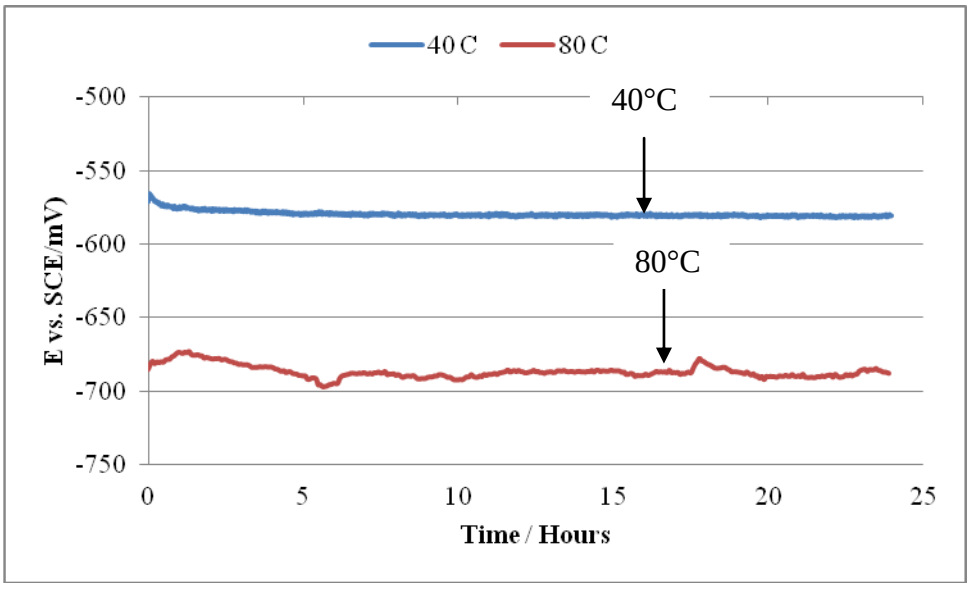

Fig. 4.5 Potentials of St33 steel with applied current at 0.25 mA for 24 hours exposure time at different temperature

Fig. 4.6 shown the potential comparisons of St33 at 48 hours precorrosion times at 80°C. The unstable potential condition at 80°C with 24 hours precorrosion times is also found at 48 hours precorrosion times. The irregular line showed up and down the potential until the end of experiment. High temperature caused the water inside reference electrode disappeared faster rather than 40°C and it may affect due to galvanostatic measurement. The potential were obtained -693 mV at the end of 48 hours precorrosion times, the potential decreased compared to corrosion potential before galvanostatic; from -650 mV to -693 mV. The decreasing of potential indicated there were some errors during precorrosion measurement. But, however, the steel was corroded faster at 80°C and it may indicate that Fe_3C is formed at the end of 48 hours precorrosion times. Furthermore, compared to potential at 40°C, the potential was more stable and reached -620 mV at the end of 48 hours precorrosion times.

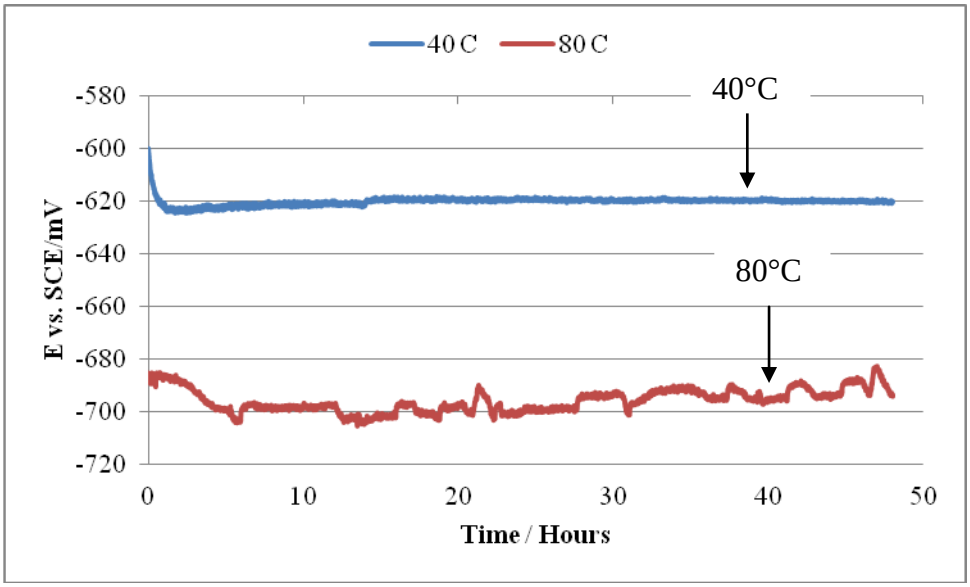

Fig. 4.6 Potentials of St33 steel with applied current at 0.25 mA for 48 hours exposure time at different temperature

4.1.4 Summary comparison of 3 steels

The summary of the potentials trend for X65, St52 and St33 steels at 24, 48 hours precorrosion time and temperature 40°C, 80°C is presented in Table 4.4.

Table 4.4 The trend of potentials for X65, St52 and St33 at 40°C and 80°C

T (^{0}C)	Precorrosion time (Hours)	The value of potentials before and after precorrosion time (mV)			The trend of potentials before and after precorrosion time (mV)		
		X65	St52	St33	X65	St52	St33
40	24	(-598/-552)	(-397/-533)	(-640/-581)	Increased (+46)	Decreased (-136)	Increased (+59)
	48	(-660/-601)	(-668/-592)	(-676/-620)	Increased (+59)	Increased (+76)	Increased (+56)
80	24	(-720/-655)	(-728/-665)	(-678/-688)	Increased (+65)	Increased (+63)	Decreased (-10)
	48	(-666/-654)	(-676/-683)	(-650/-693)	Increased (+12)	Decreased (-7)	Decreased (-43)

According to Table 4.4, in general, the potentials of steels increased at the end of precorroded time. The increasing of potentials was caused by Fe_3C formation during precorrosion period which stimulated corrosion process. The condition was supported in theory that increase in corrosion rate during the precorrosion period were caused by several factors: (1) removal of a protective oxide films, (2) galvanic coupling to the uncorroded Iron carbide (cementite) film,

(3) increase in the true specimen surface area, and (4) acidification of the solution inside the corrosion product film [15].
However, the decreasing of potentials at the end of precorroded time may cause by some errors in the equipment during experiment, for example; 1) bad connection in corrosion cell to a Gamry system, 2) the water inside of the reference electrode was evaporated. Furthermore, if the reference electrode was filled with water just before experiment that could explain the errors and also time between polishing and mounting could be a reason.

4.2 Fe^{2+} Analysis

In general, Fe^{2+} concentration of 3 steels decreases by time after the addition of $NaHCO_3$ due to precipitation. The equilibrium reactions are presented in Eq. 3 and 4. High supersaturation of Fe^{2+} concentration will lead to a higher precipitation which will make better formation of protective scale. Therefore, Fe^{2+} concentration is useful to predict the formation of protective scale. Based on Table 4.5, Fe^{2+} concentration increases due to corrosion process before $NaHCO_3$ addition. But, after $NaHCO_3$ addition, Fe^{2+} concentration decreases with increasing time because of precipitation. Thus, compared to the result of Rp/Ec trend, it showed that the corrosion rate were decreased at the end of 191 hours (or less for some experiments) and it may consider that the protective $FeCO_3$ film were formed on surface steel due to a higher supersaturation and better precipitation which lead to a decrease in corrosion rate. The iron analysis results of 3 steel with variation of forced precorrosion time and temperature is showed in Table 4.5.

Table 4.5 Iron analysis results of X65, St52 and St33 steels with variation of corrosion time at forced precorrosion 24 or 48 hours at 40°C or 80°C

T (^{0}C)	Forced Precorrosion Time (Hours)	Steel	Fe^{2+} before addition of $NaHCO_3$ (ppm)	Fe^{2+} after addition of $NaHCO_3$ accordance interval time of analysis (ppm)						
				2 Hours	10 Hours	24 Hours	48 Hours	96 Hours	192Hours	216 Hours
40	24	X65	85	57	41	17	14	8	5	3
		St52	100	75	60	41	39	28	15	N/A
		St33	76	34	21	17	13	8	6	N/A
40	48	X65	93	49	37	19	12	9	6	3
		St52	70	45	27	15	11	8	7	5
		St33	129	71	47	31	17	13	9	N/A
80	24	X65	137	46	39	32	25	14	6	3
		St52	153	43	38	29	24	14	3	N/A
		St33	162	42	38	31	19	6	7	4
80	48	X65	81	67	43	37	27	19	12	9
		St52	125	43	39	37	29	16	11	6
		St33	111	47	39	36	21	12	9	3

Due to lack of CO_2 supply (empty gas cylinder) then the experiments were stopped before this stage

4.3 Electrochemical impedance spectroscopy

In this experiment, EIS characterization was carried out under following parameter: DC Voltage 0 V vs. Eoc, AC voltage 10 mV rms, frequency range from 500 Hz to 0.007 Hz with points/decade: 10. The solution used was 1g/kg NaCl 50 wt% MEG, and 100 mmol/kg $NaHCO_3$.

4.4.1 EIS scan results of 3 steels

The Nyquist plot for X65, St52 and St33 steels showed the highest polarization resistance mostly was obtained at the end of 216 hours as shown in Figures below. An increase in the polarization resistance indicated the protective film was formed and a lower corrosion rate was observed. The larger diameter was obtained at the end of 216 hours indicated the corrosion rate decreased more rapidly at the end of 216 hours of EIS measurement. The high frequency semi-circle shows that the protective $FeCO_3$ film has formed on surface steel and lead to a decrease in corrosion rate.

EIS scan result of X65 steel (Precorroded 48 hours at 40 ℃)

The electrolyte resistance (Rs) and polarization resistance (Rp) values were obtained from the curve below. The values of Rs = 62 Ω and Rp = 2040 Ω for X65 steel in precorroded 48 hours at 40°C is shown in Fig. 4.7.

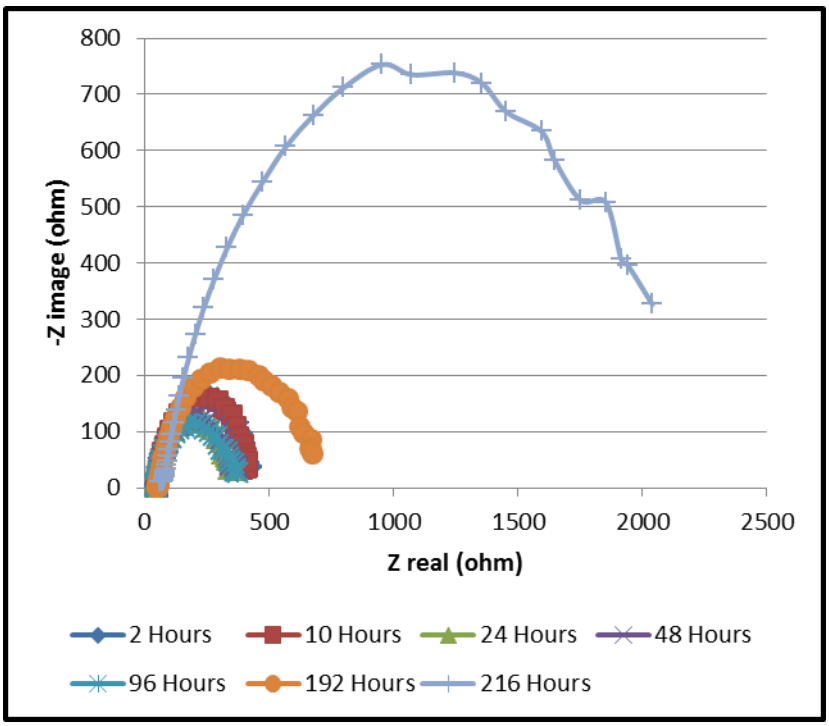

Fig. 4.7 Nyquist plots result of X65 steel in precorroded 48 hours at 40°C after 216 hours of immersion in solution

EIS scan result of St52 steel (Precorroded 48 hours at 40 ℃)

The electrolyte resistance (Rs) and polarization resistance (Rp) values were obtained from the curve below. The values of Rs = 62 Ω, Rp = 726 Ω for St52 steel in precorroded 48 hours at 40°C is shown in Fig. 4.8.

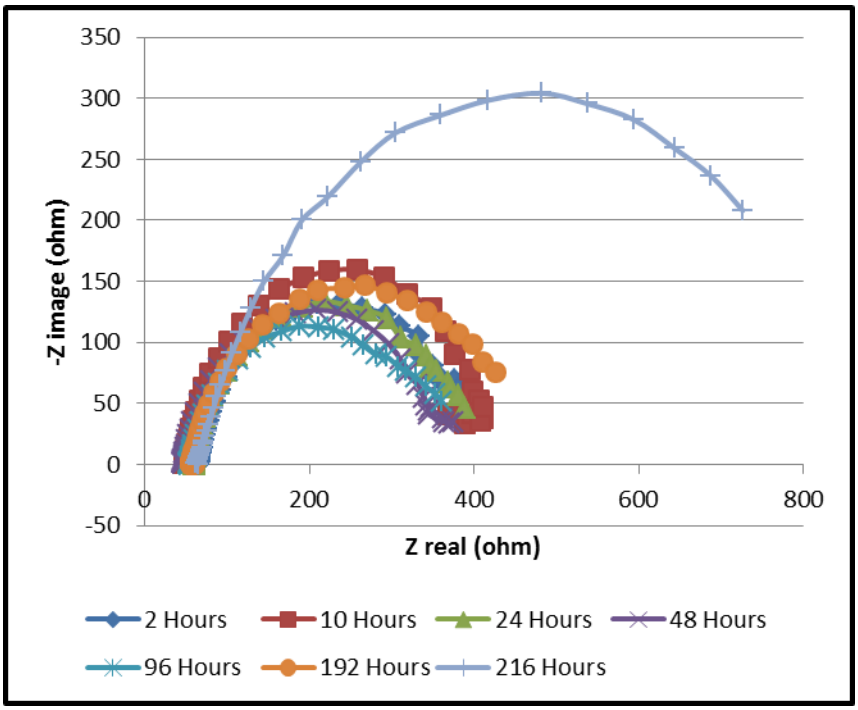

Fig. 4.8 Nyquist plots result of St52 steel in precorroded 48 hours at 40°C after 216 hours of immersion in solution

EIS scan result of St33 (Precorroded 24 hours at 40 ℃)

The electrolyte resistance (Rs) and polarization resistance (Rp) values were obtained from the curve below. The values of Rs = 49 Ω, Rp = 3019 Ω for St33 steel in precorroded 24 hours at 40°C is shown in Fig. 4.9.

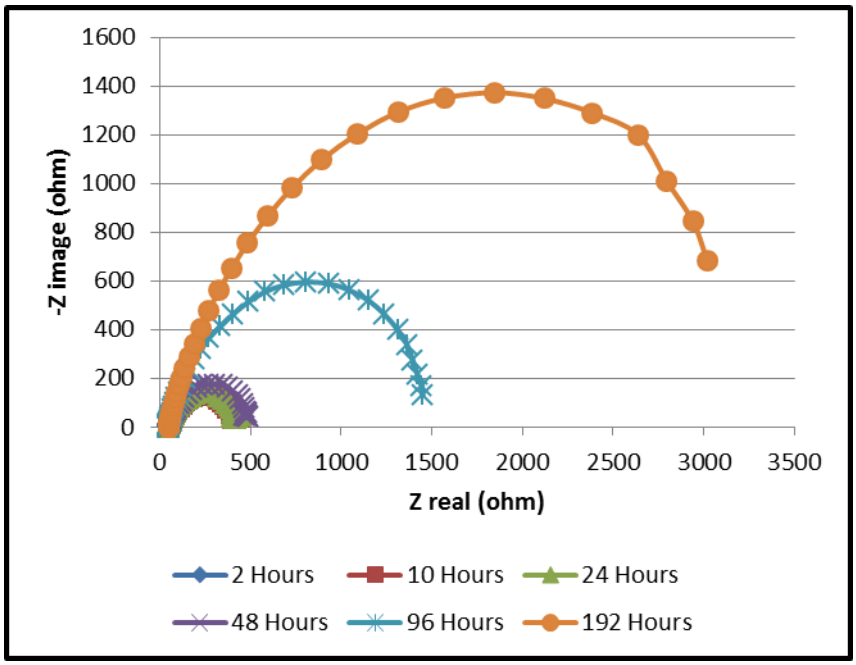

Fig. 4.9 Nyquist plots result of St33 steel in precorroded 24 hours at 40°C after 192 hours of immersion in solution

EIS scan result of St33 (Precorroded 48 hours at 40 ℃)

The electrolyte resistance (Rs) and polarization resistance (Rp) values were obtained from the curve below. The values of Rs = 48 Ω, Rp = 1772 Ω for St33 steel in precorroded 48 hours at 40°C is shown in Fig. 4.10.

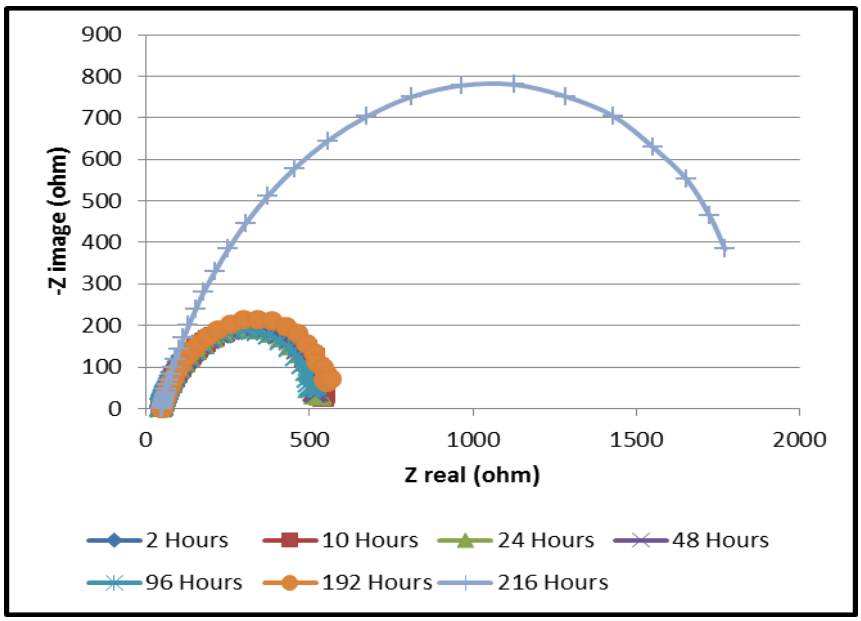

Fig. 4.10 Nyquist plots result of St33 steel in precorroded 48 hours at 40°C after 216 hours of immersion in solution.

EIS scan result of St52 (Precorroded 24 hours at 80°C)

The Nyquist plots at 80°C showed the linear function at the end of 216 hours of exposure time. The linear function is normally seen for diffusion process which shown in Fig. 4.11, 4.12, 4.13.

The electrolyte resistance (Rs) and polarization resistance (Rp) values were obtained from the curve below. The values of Rs = 30 Ω, Rp = 1249 Ω for St33 steel in precorroded 48 hours at 80°C was shown in Fig. 4.11.

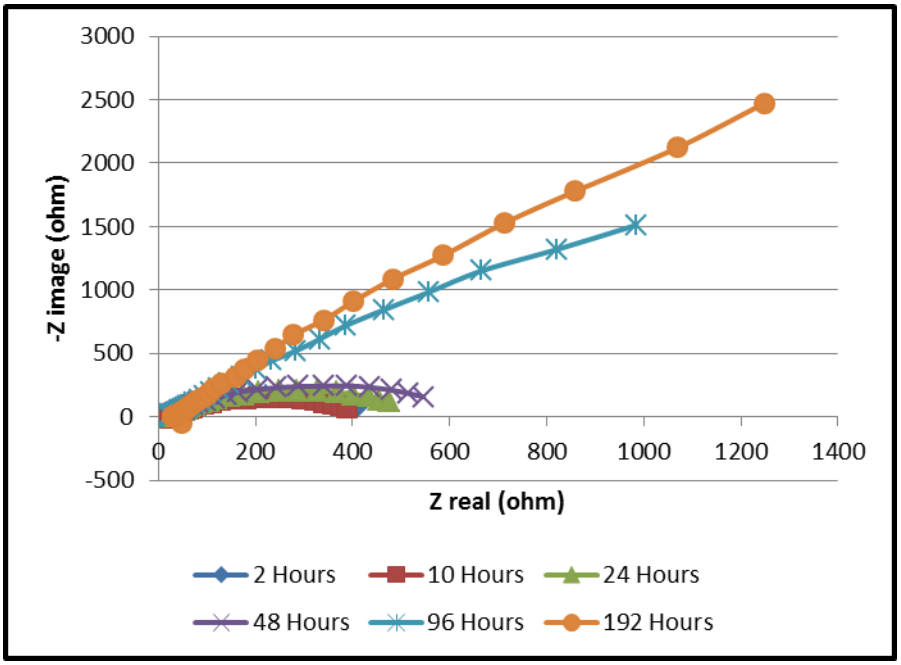

Fig. 4.11 Nyquist plots result of St52 steel in precorroded 24 hours at 80°C after 216 hours of immersion in solution

EIS scan result of St33 steel (Precorroded 24 hours at 80°C)

The electrolyte resistance (Rs) and polarization resistance (Rp) values were obtained from the curve below. The values of Rs = 26 Ω, Rp = 990 Ω for St33 steel in precorroded 48 hours at 80°C was shown in Fig. 4.12.

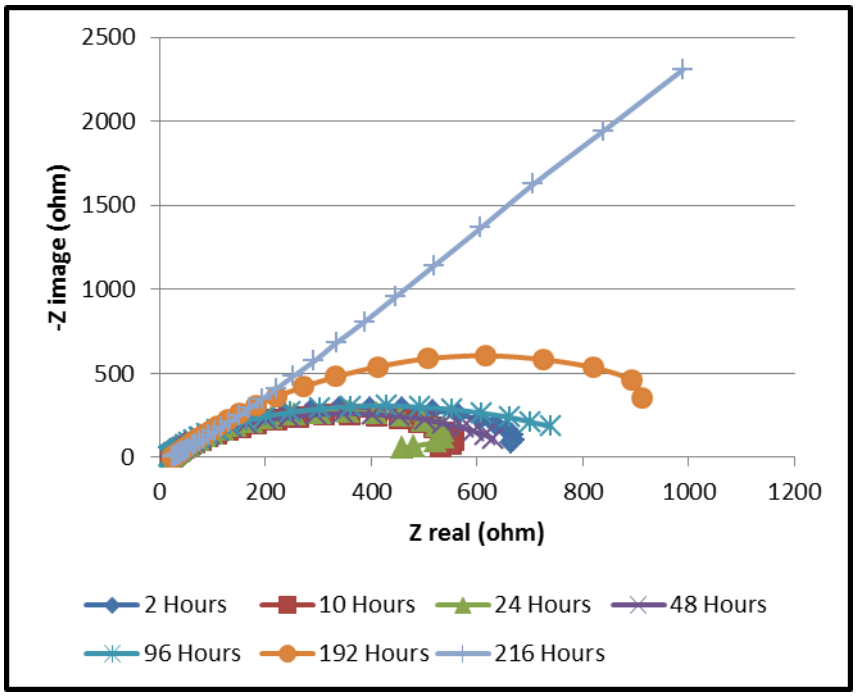

Fig. 4.12 Nyquist plots result of St33 steel in precorroded 24 hours at 80°C after 216 hours of immersion in solution

EIS scan result of St33 steel (Precorroded 48 hours at 80°C)

The electrolyte resistance (Rs) and polarization resistance (Rp) values were obtained from the curve below. The values of Rs = 55 Ω, Rp = 3517 Ω for St33 steel in precorroded 48 hours at 80°C was shown in Fig. 4.13.

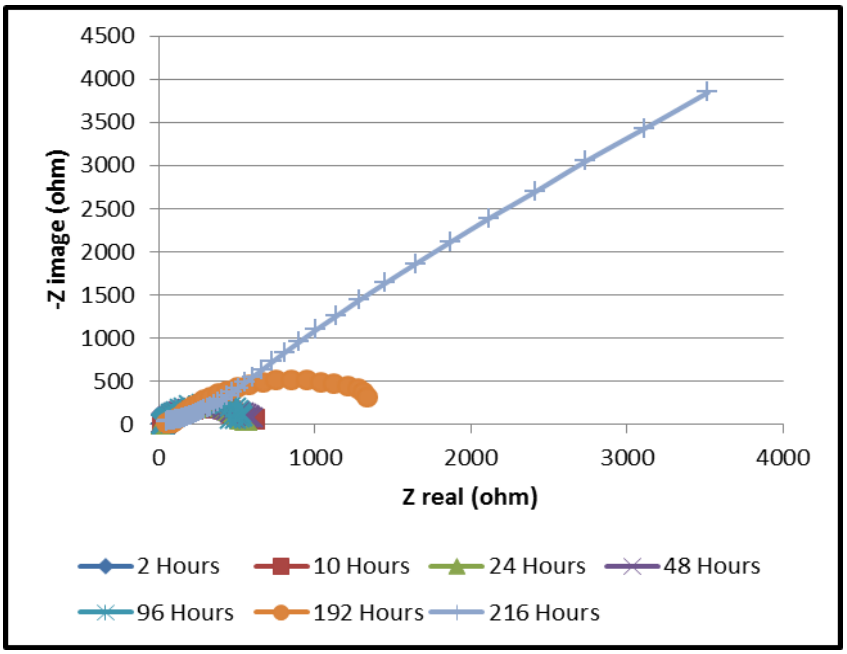

Fig. 4.13 Nyquist plots result of St33 steel in precorroded 48 hours at 80°C after 216 hours of immersion in solution

Some Nyquist plots were not as expected, probably due to bad connection in cell system and especially at 80^0C, the high temperature caused the water inside the reference electrode evaporated more rapidly during EIS measurement which affected to the measurement process. Another condition which may cause by: 1) The changed of surface scale during measurements and affected to the low frequency impedance reading, 2) The effect of steel voltage. The bad formation of Nyquist plot diagrams is presented in Appendix.

4.4.2 Summary of EIS scan results

The summary of Rs, Rp and corrosion rate values of X65, St52 and St33 steels is presented in Table 4.6. The corrosion rate can be calculated from Eq. 9.

$$B = \frac{b_a b_c}{2.303\,(b_a + b_c)} \qquad (8)$$

$$I_{corr} = \frac{B}{R_p} \qquad (9)$$

Where :

B	=	Tafel constant (volts/decade)
b_a	=	the anodic beta coefficient in volts/decade
b_c	=	the cathodic beta coefficient in volts/decade
R_p	=	polarization resistance
I_{corr}	=	the corrosion current in amps

According to Table 4.6, St52 steel has the highest corrosion rate on 48 hours precorrosion time at 40°C. The same condition is also found in St33 steel that the corrosion is higher than the other steel on 24 hours precorrosion time at 80°C.
Assume B = 30 mV/decade, therefore the corrosion rate can be calculated from Eq.10 which is using interpolation equation from Eq.9 at known B.

$$I_{corr}^{*} = I_{corr1} * \frac{B}{B_2} \qquad (10)$$

Where:

I_{corr}^{*}	=	the corrosion current of EIS scan (amps)
I_{corr1}	=	the corrosion current of Rp/Ec trend (amps)
B	=	Tafel constant (volts/decade)
B_2	=	Tafel constant from Rp/Ec trend (volts/decade)

Table 4.6 The Rs, Rp and corrosion rate values of X65, St52 and St33 steels for 24 hours and 48 hours precorrosion time at 40°C and 80°C

Specimen	Precorrosion time (Hours)	T (°C)	Time of immersion (hours)	Rs (ohm)	Rp (ohm)	Time of immersion (hours)	Corrosion Rate (mm/year) measurement by EIS Scan	Corrosion Rate (mm/year) measurement by Rp/Ec trend
X65	24	40		N/A	N/A		N/A	0.01
St52				N/A	N/A		N/A	0.07 (stop at 95 hours)
St33			*75	49	962	*75	0.03	0.03
X65	48	40	216	62	2040	216	0.01	0.05
St52			216	62	726	216	0.04	0.13
St33			95	48	490	95	0.06	0.17
X65	24	80		N/A	N/A		N/A	0.01
St52			216	30	1249	95	0.02	0.01
St33			216	26	990	216	0.03	0.01
X65	48	80		N/A	N/A		N/A	0.03
St52				N/A	N/A		N/A	0.02
St33			216	55	3517	216	0.008	0.01

Terminated earlier because of empty CO_2 cylinder

Most of the corrosion rates from EIS scan measurements are lower than those obtained by Rp/Ec trend measurements. It is different with previous experiment [7] where corrosion rate from EIS scan measurement is higher than Rp/Ec trend. Some of the corrosion rate results from EIS scan measurements are higher than those obtained by Rp/Ec trend measurements. The main reason for this may be that in Rp/Ec trend, it is impossible to separate electrolyte resistance (Rs) from polarization resistance (Rp) without doing separate experiments. Since the corrosion rate calculated from AC impedance is inversely proportional to the diameter in the Nyquist plot, the influence of solution resistance increases with increasing corrosion rates and increasing electrolyte resistance. Normally, Rs is much smaller than Rp, and minor mistake is introduced by not excluding the contribution from the electrolyte resistance when calculating the corrosion rate from Rp/Ec trend measurements [7].

4.4 Potentiodynamic cathodic

Current become the main parameter in potentiodynamic experiment, because current represents the rate with which the anodic or cathodic reactions are taking place on the working electrode. Furthermore, currents for cathodic reactions are considered to be negative and anodic currents considered being positive [32].

4.4.1 24 hours at 40^{0}C

In general, the results of potentiodynamic cathodic scan from X65, St52 and St33 steels after 24 hours precorrosion time at 40°C showed that the potential decreased with increasing time. The decreasing of potentials indicated the scale is formed on the steels which supported by the direction of cathodic reaction goes into left and indicated the low corrosion process and lead into a decrease corrosion rate. For clearer description of potentiodynamic cathodic scan is presented in Fig.s 4.14, 4.15 and 4.16.

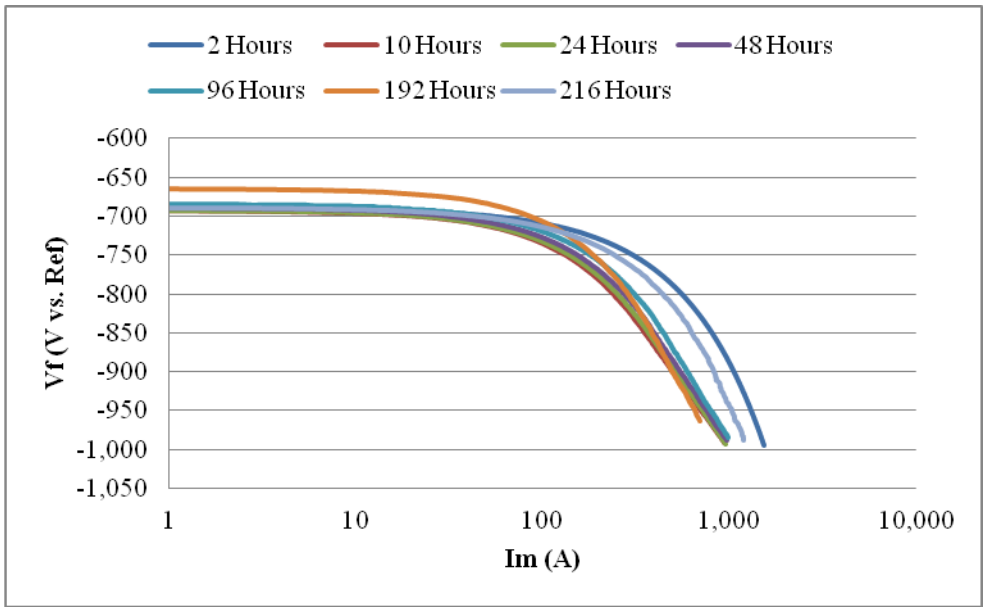

Fig. 4.14 Potentiodynamic cathodic sweeps of X65 steel (Precorroded 24 Hours at 40^{0}C) after 2-216 hours

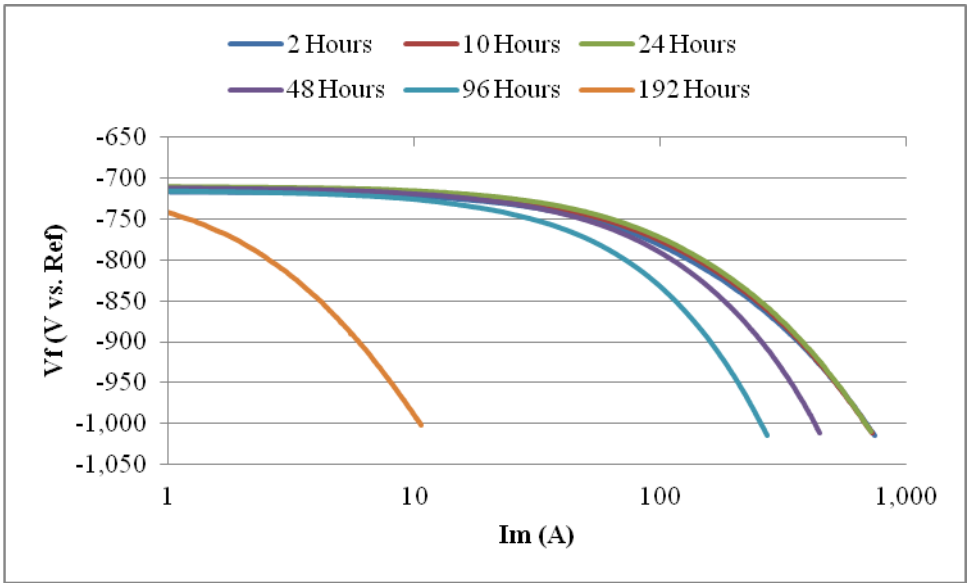

Fig. 4.15 Potentiodynamic cathodic sweeps of St52 steel (Precorroded: 24 Hours at 40^{0}C) after 2-192 hours

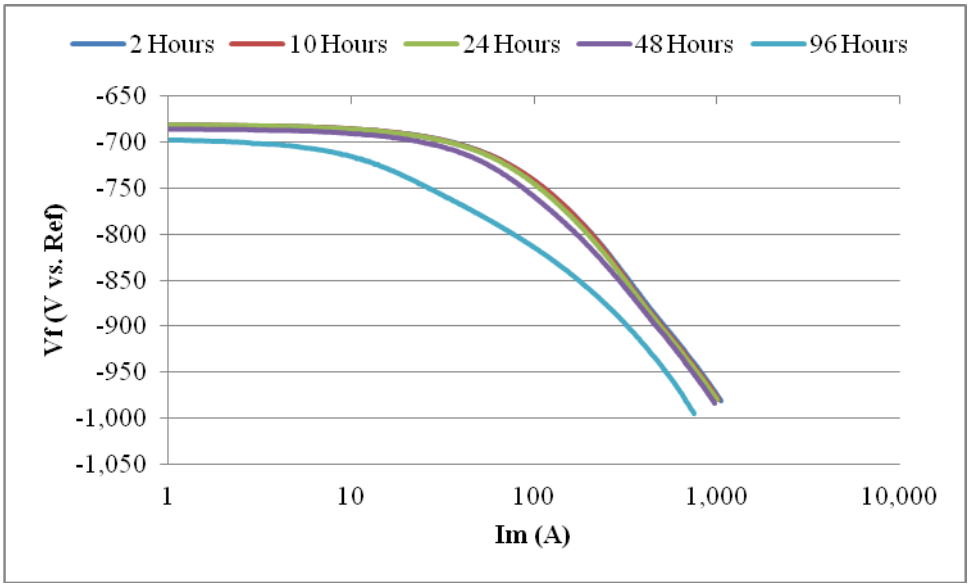

Fig. 4.16 Potentiodynamic cathodic sweeps of St33 steel (Precorroded: 24 Hours at 40^{0}C) after 2-96 hours

4.4.2 48 Hours at 40°C

The potentials for St52 and St33 steels decreased after 48 hours precorrosion time at temperature 80°C. The decreasing of potentials indicated scale has formed on the steels. However, the different condition is found at X65 steel where the potential was increased. The different conditions may cause by the bad connection in the cell system and water was evaporated in reference electrode which affected to potentiodynamic measurement.

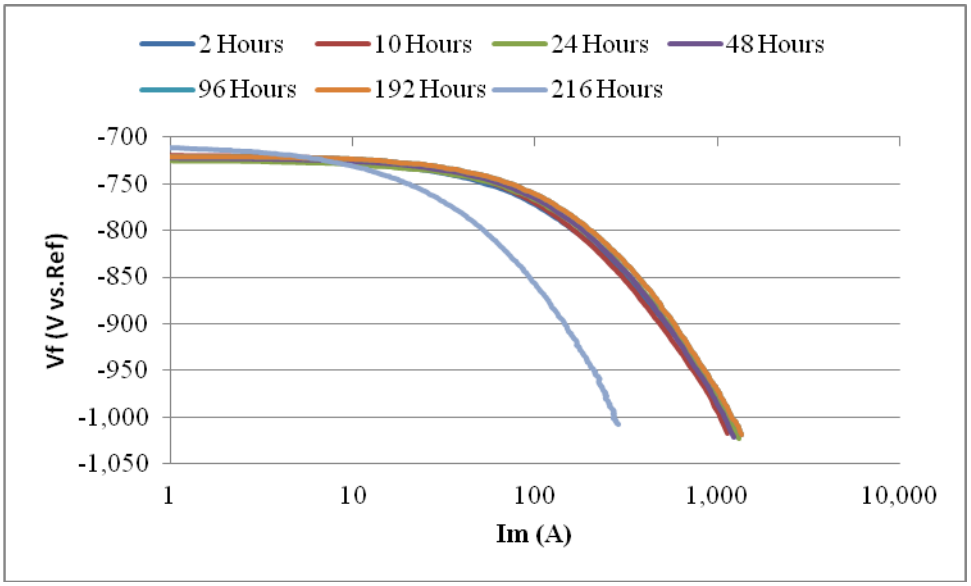

Fig. 4.17 Potentiodynamic cathodic sweeps of X65 steel (Precorroded: 48 Hours at 40^{0}C) after 2-216 hours

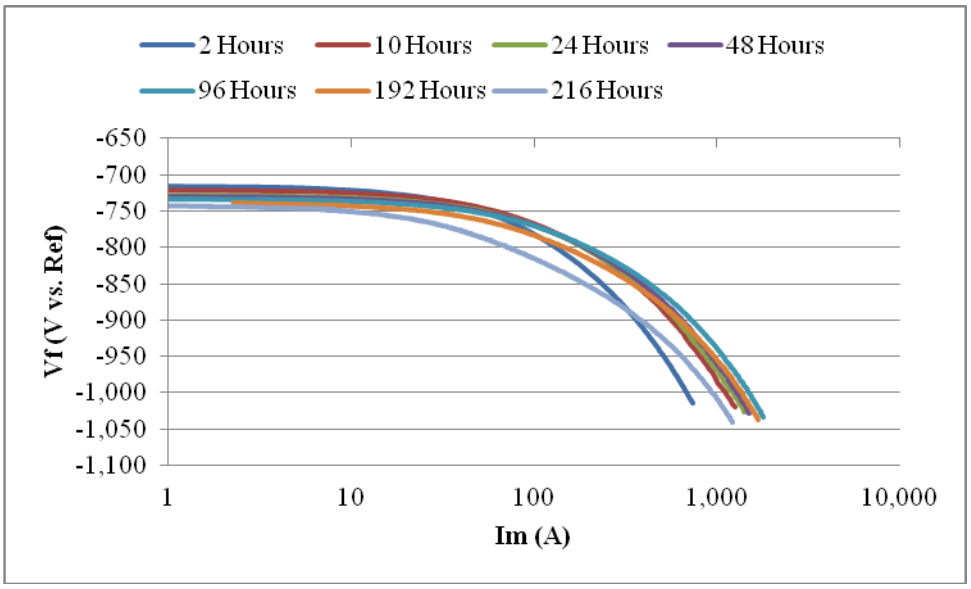

Fig. 4.18 Potentiodynamic cathodic sweeps of St52 steel (Precorroded: 48 Hours at 40^{0}C) after 2-216 hours

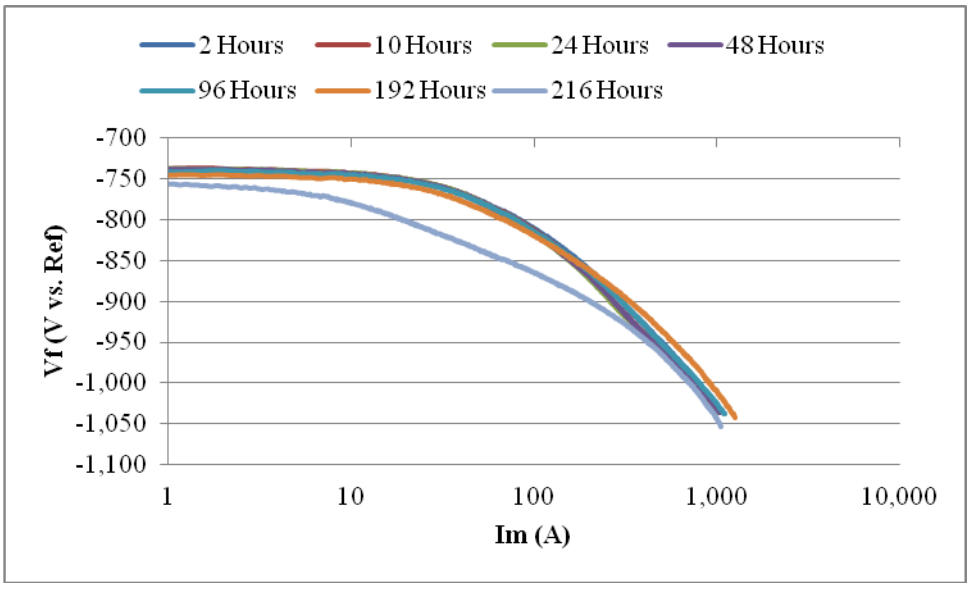

Fig. 4.19 Potentiodynamic cathodic sweeps of St33 steel (Precorroded: 48 Hours at 40^{0}C) after 2-216 hours

4.4.3 24 Hours at 80^{o}C

The results of potentiodynamic cathodic scan showed variation of potentials from 3 steels. X65 and St33 steels showed the potentials was increased by increasing time, while for St52 steel, the potential was stagnant. The condition may cause by high temperature which affects to the trend of potentials on the 3 steels. The random of lines from potentiodynamic cathodic scan may show the error was occurred during the experiment.

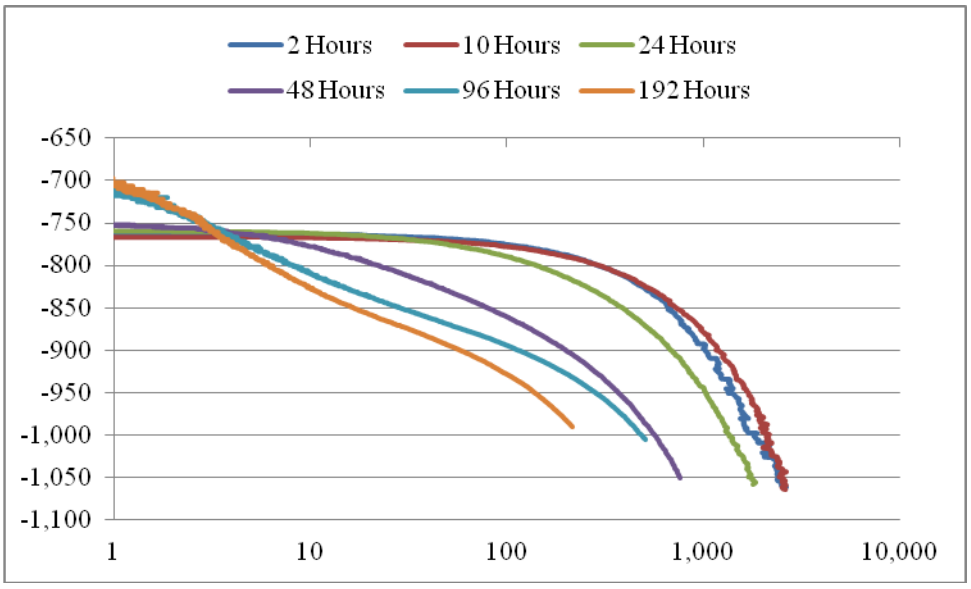

Fig. 4.20 Potentiodynamic cathodic sweeps of X65 steel (Precorroded: 24 Hours at 80^{0}C) after 2-192 hours

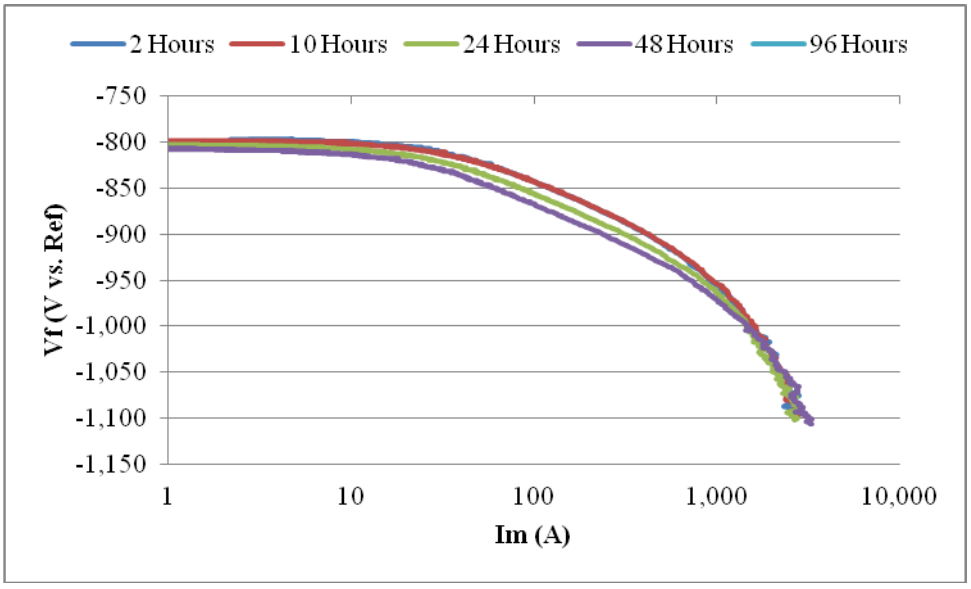

Fig. 4.21 Potentiodynamic cathodic sweeps of St52 steel (Precorroded: 24 Hours at 80^{0}C) after 2-96 hours

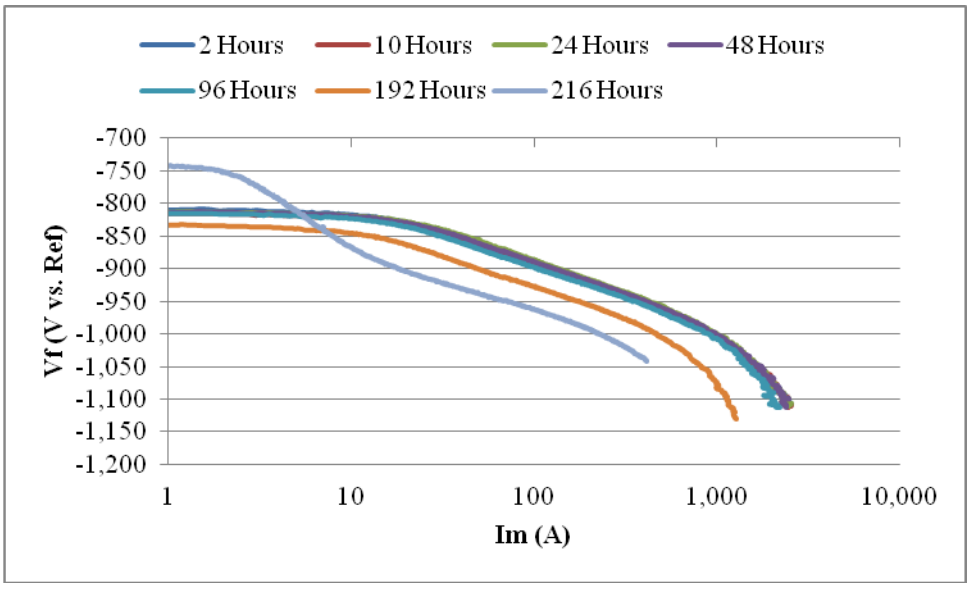

Fig. 4.22 Potentiodynamic cathodic sweeps of St33 steel (Precorroded: 24 Hours at 80^{0}C) after 2-216 hours

4.4.4 48 hours at 80^{o}C

The trend of potentials from X65 and St33 was increased after 48 hours precorrosion time at 80°C while for St52 steel, the potential was decreased. The different potentials trend may cause by the connection in the cell system and water in reference electrode because normally the potential supposed to be decreased by increasing time, because the scale has formed and decrease the corrosion rate.

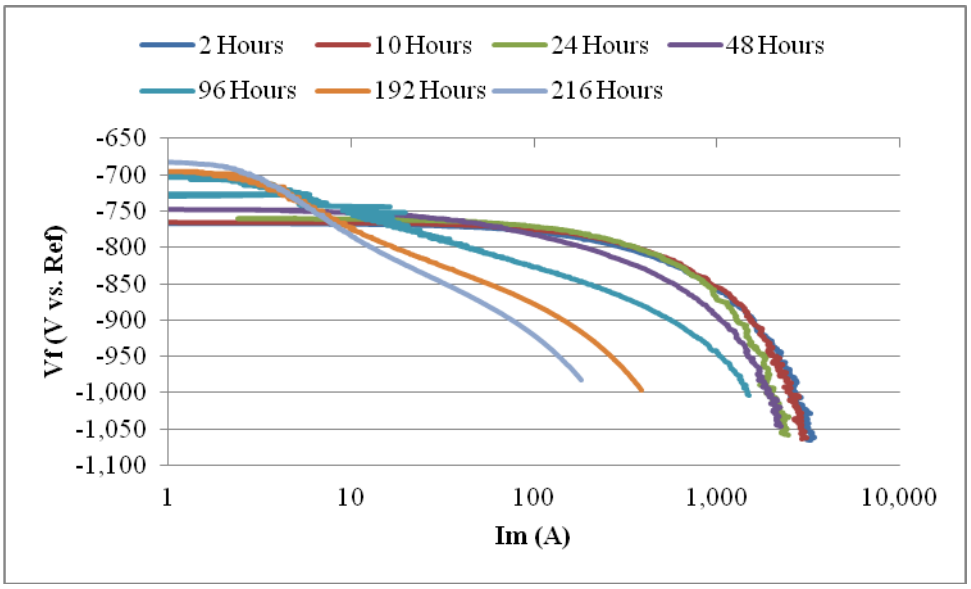

Fig. 4.23 Potentiodynamic cathodic sweeps of X65 steel (Precorroded: 48 Hours at 80^{0}C) after 2-216 hours

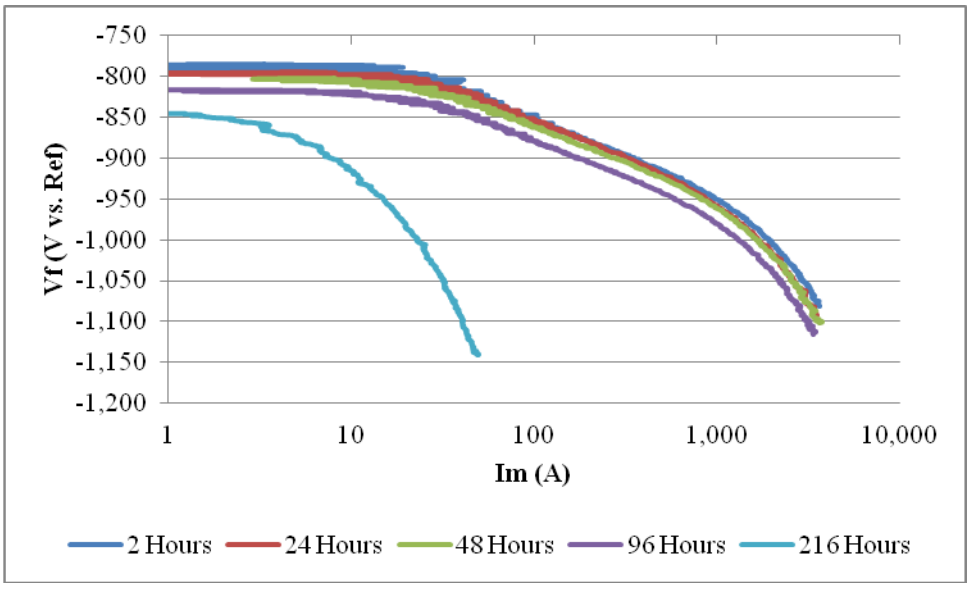

Fig. 4.24 Potentiodynamic cathodic sweeps of St52 steel (Precorroded: 48 Hours at 80^{0}C) after 2-216 hours

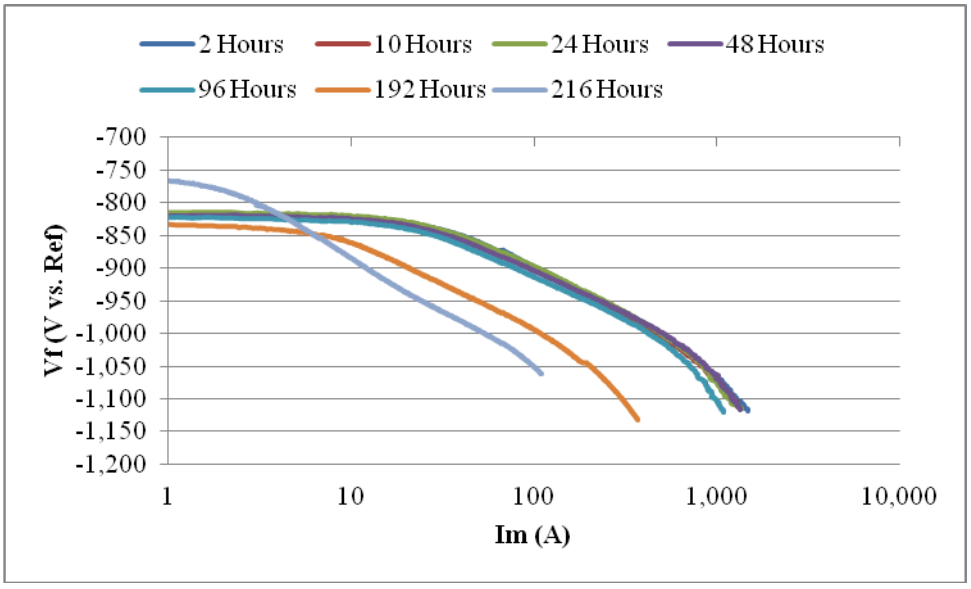

Fig. 4.25 Potentiodynamic cathodic sweeps of St33 steel (Precorroded: 48 Hours at 80^{0}C) after 2-216 hours

4.4.5 The summary of potential trends for X65, St52 and St33 steels at 40°C and 80°C

An overview is given for the potential trends of X65, St52 and St33 steels in variation of temperature. The trend of potentials from potentiodynamic cathodic scan is presented in Table 4.7. In general, the results of potentiodynamic cathodic scan from X65, St52 and St33 steels after 24 or 48 hours precorrosion time at 40°C showed that the potential decreased with increasing time. The decreasing of potentials indicated the scale is formed on the steels which indicated the low corrosion process and lead into a decrease corrosion rate. The Increased trend for X65 and St33 for both 24 and 48 hours precorrosion time at 80 ^{o}C might because of some errors.

Table 4.7 The trend of potentials from potentiodynamic cathodic scan for X65, St52 and St33 at 40°C and 80°C

T (°C)	Precorrosion Time (Hours)	The trend of potentials from potentiodynamic cathodic scan at the end of immersion time (mV)		
		X65	**St52**	**St33**
40	24	Decreased (-25) (-664/-689)	Decreased (-25) (-716/-741)	Decreased (-13) (-685/-698)
	48	Increased (+11) (-722/-711)	Decreased (-26) (-716/-742)	Decreased (-14) (-742/-756)
80	24	Increased (+56) (-762/-706)	Decreased (-3) (-803/-806)	Increased (+73) (-815/-742)
	48	Increased (+82) (-765/-683)	Decreased (-59) (-787/-846)	Increased (+65) (-832/-767)

4.5 Open circuit potential

OCP was measured after potentiodynamic cathodic scan, in order to know whether the potential was increased or decreased during the experiment. OCP is defined as free potential (same with Ecorr). Open circuit potential was measured from 2-192 hours and measured again after 192 hours of Rp/Ec trend measurement. The result of open circuit potential of 3 (three) steels is presented below.

4.5.1 24 hours at 40°C

Fig. 4.26 shown the trend of open circuit potential of 3 steels which generally decreased at the end of experiment. The open circuit potential of X65 steel decreased after 192 hours from -660 mV to -682 mV at the end of 216 hours even though the corrosion rate was increased at the end of 216 hours. The corrosion rate was decreased at the end of 216 hours for St52 and St33 as well as the open circuit potential decreased after 96 hours from -711 mV to -714 mV at the end of 192 hours and decreased from -692 mV to -703 mV at the end of 192 hours respectively. Both for St52 and St33s, the open circuit potential were measured until 192 hours because the CO_2 gas supply was stopped due to lack of CO_2.

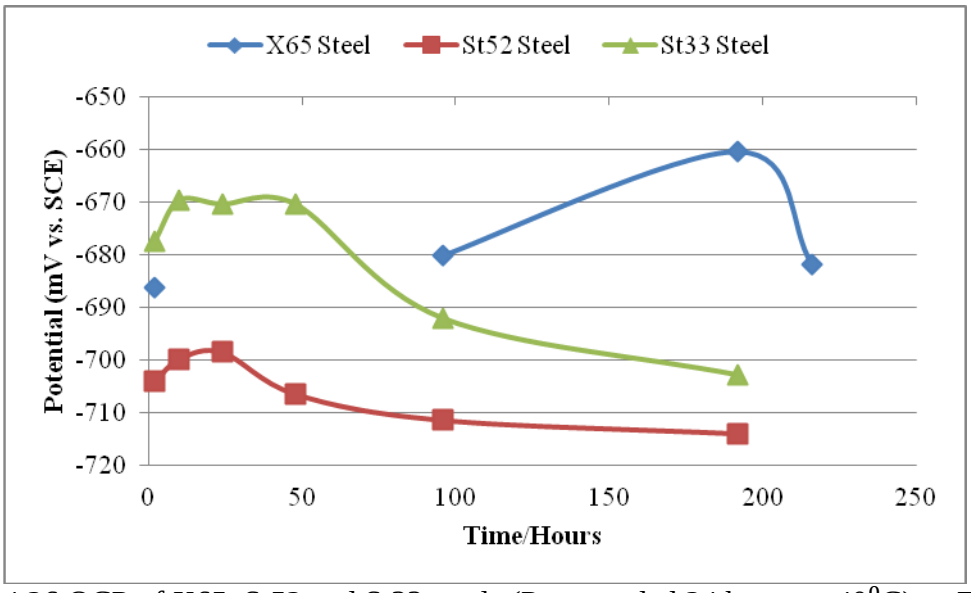

Fig. 4.26 OCP of X65, St52 and St33 steels (Precorroded 24 hours at 40^{0}C) vs Time

4.5.2 48 hours at 40^{o}C

The open circuit potential of 3 steels is shown in Fig. 4.27. According to Fig. 4.27, the potential of X65 steel is slightly increased after 192 hours from -711 mV to -699 mV at the end of 216 hours, even though the corrosion rate was decreased at the end of 216 hours. The open circuit potential for St52 and St33 decreased by increasing time, for St52 steel, the potential decreased after 192 hour from -729 mV to -734 mV at the end of 216 hours. The same condition is found in St33 that the potential decreased after 192 hour from -736 mV to -751 mV at the end of 216 hours. The corrosion rate was decreased for both of St52 and St33.

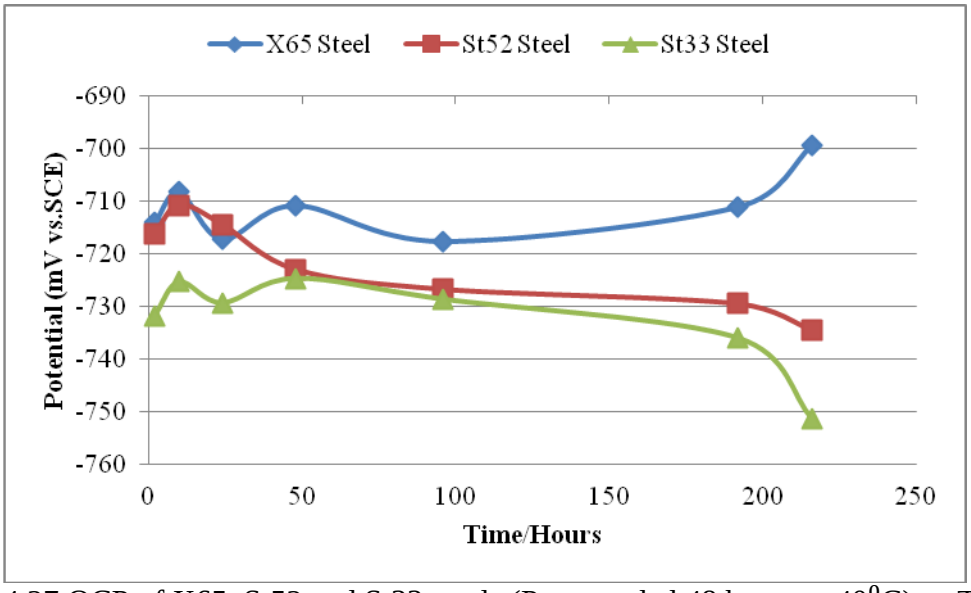

Fig. 4.27 OCP of X65, St52 and St33 steels (Precorroded 48 hours at 40^{0}C) vs Time

4.5.3 24 hours at 80°C

In general the corrosion rate was lower for 3 steels as well as the potentials after 216 hours. According to Fig. 4.28, the potential of X65 steel decreased after 192 hours from -742 mV to -773 mV as well as St52 steel, the potential decreased from -754 mV after 192 hours to -831 mV at the end of 216 hours. Compared to St33, the potential was stable from 192 hours to 216 hours.

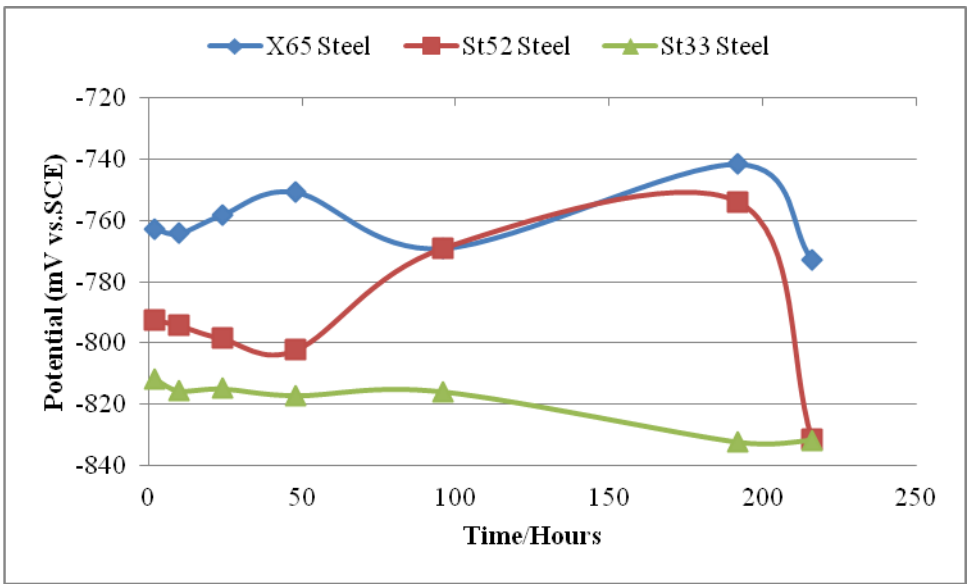

Fig. 4.28 The potential of X65, St52 and St33 steels (Precorroded 24 hours at 80°C) vs Time

4.5.4 48 hours at 80°C

Generally, the corrosion rate was decreased for three steels but the open circuit potential showed different results for each steel. OCP increased by increasing time for St52 and St33 steels as shown in Fig. 4.29. The potential increased after 192 hours for St52 steel from -841 mV to -837 mV at the end of 216 hours. The same condition is found in St33, the potential increased after 192 hours from -876 mV to -812 mV at the end of 216 hours. Furthermore, for X65 steel, the potential was decreased after 192 hours from -748 mV to -758 mV at the end of 216 hours.

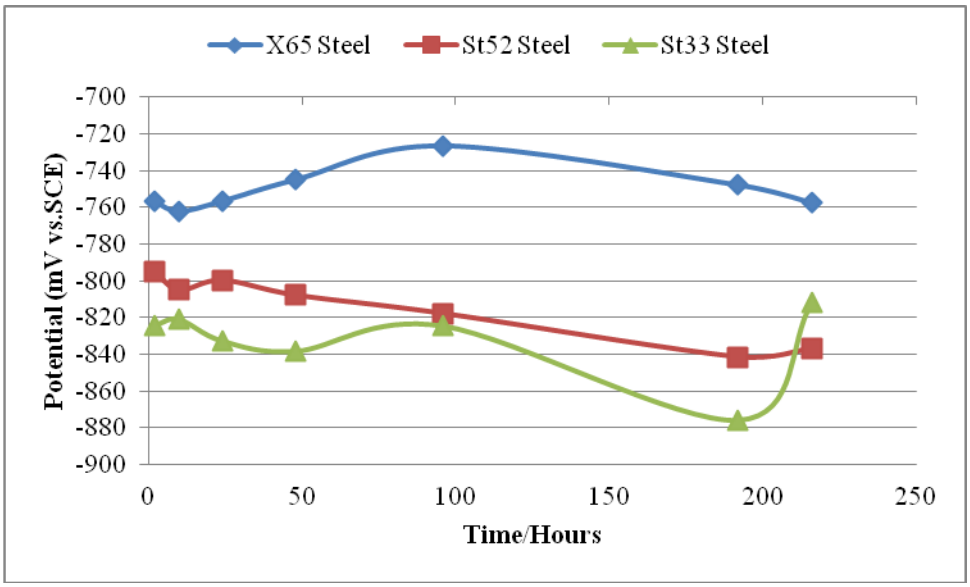

Fig. 4.29 The potential of X65, St52 and St33 steels (Precorroded 48 hours at 80°C) vs Time

4.6 Rp/Ec Trend

The technique which used to determine the polarisation resistance values of three electrodes (working electrode, reference electrode, counter electrode), which were made of the same materials to decrease the interference signal from the solution is in situ linear polarisation resistance (LPR) technique [34]. The steels (X65, St52 and St33) were immersed in solution (1g/kg NaCl 50 wt% MEG, 100 mmol/kg $NaHCO_3$). The Rp/Ec trend was measured in variation of forced precorrosion time and temperature.

4.6.1 24 Hours at 40°C

Fig. 4.30 shows the corrosion rate of 3 steels after precorroded 24 hours at temperature 40°C. The stable value of corrosion rate on X65 steel more probably incorrect measurement data which may cause by water which evaporated in water bath after 95 hours of immersion in solution. The water evaporated in water bath affects to the decreasing of temperature (approximately from 40°C to 20°C) and may lead to that condition.

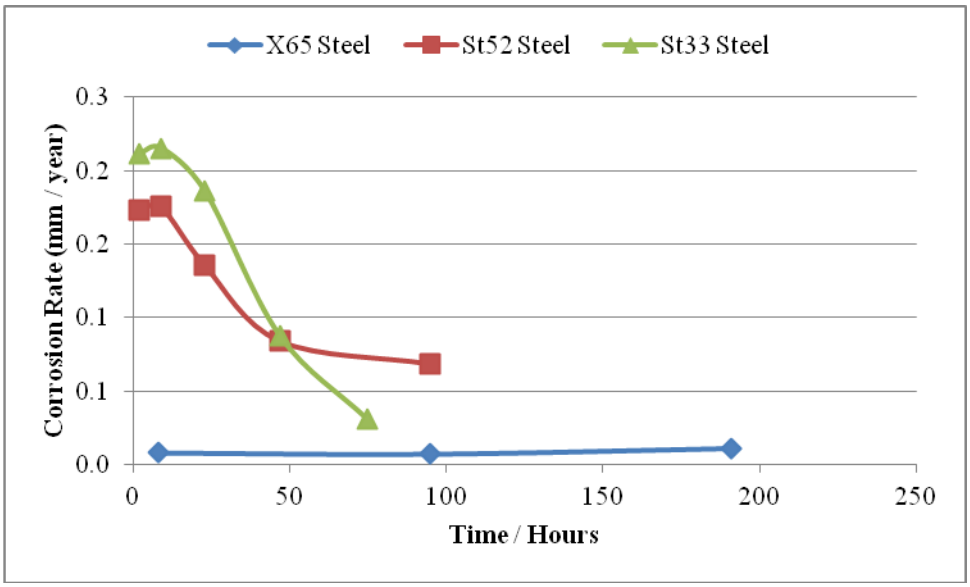

Fig. 4.30 The corrosion rate of X65, St52 and St33 steels (Precorroded: 24 hours at 40°C) vs Time

The corrosion rate of St52 steel decreased rapidly after 23 hours of immersion in the solution. The value of corrosion rate was decreased from 0.14 mm/year at 23 hours of immersion in solution to 0.07 mm/year at the end of 95 hours of immersion in solution. The same condition is also found in St33 that the corrosion rate decreased rapidly after 23 hours of immersion in the solution from 0.19 mm/year to 0.03 mm/year at 75 hours of immersion in solution. It can be considered that the protective $FeCO_3$ film may formed not only at 95 hours but also at 75 hours. However, the experiment is supposed to be conducted until 191 hours but the CO_2 gas was evaporated in the middle of both experiments. Therefore, the experiment was stopped due to the lack of CO_2 gas.

4.6.2 48 Hours at 40°C

The corrosion rate of 3 steels is shown in Fig. 4.31. The corrosion rate was decreased rapidly after 95 hours of immersion in solution for both experiments of X65 steel and St52 steel. The corrosion rate of X65 steel decreased from 0.16 mm/year to 0.05 mm/year at the end of 191 hours of immersion in solution and for St52 steel decreased from 0.23 mm/ year to 0.13 mm/year at 191 hours of immersion in the solution. It is indicated that the protective $FeCO_3$ is formed after 95 hours which decrease the corrosion rate.

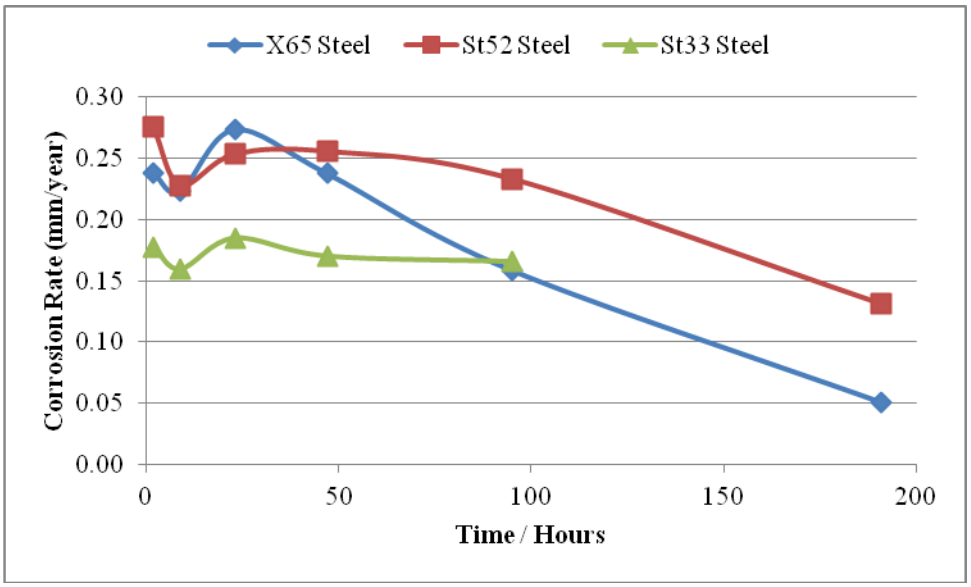

Fig. 4.31 The corrosion rate of X65, St52 and St33 steels (Precorroded 48 hours at 40°C) vs Time

Furthermore, compared to the corrosion rate of St33, the corrosion rate was stable. It can be viewed from the value of corrosion rate from 47 hours to 95 hours of immersion in the solution (0.17 mm/year). The condition may cause by the oxygen leakage inside the cell and the experiment was stopped after 95 hours of immersion in solution because of the lack CO_2 gas in tube.

4.6.3 24 Hours at 80°C

Temperature becomes the important parameter which accelerates processes in corrosion, mostly transportation process. Therefore, the increased temperature accelerates rapidly the kinetics of precipitation and protective scale formation which will decrease the corrosion rate [15]. Furthermore, as shown in Fig. 4.32, the corrosion rate of 3 steels decreased rapidly at temperature 80°C. The corrosion rate of X65 steel decreased rapidly after 9 hours of immersion in solution from 0.70 mm/year to 0.01 mm/year at the end of 191 hours of immersion in solution.

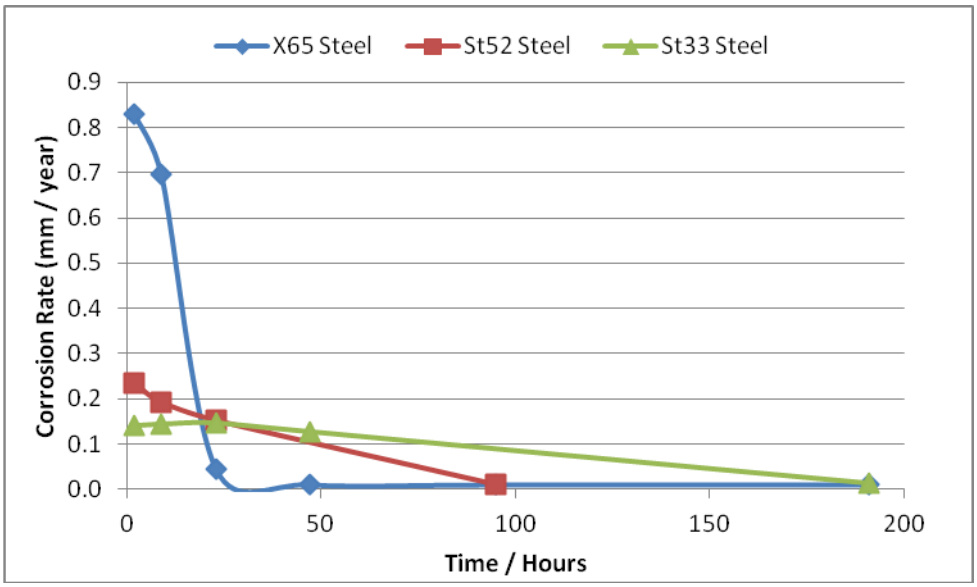

Fig. 4.32 The corrosion rate of X65, St52 and St33 steels (Precorroded 24 hours at 80oC) vs Time

The protective $FeCO_3$ film is formed for both of experiments which can be viewed from the values of corrosion rate for St52 steel and St33. The corrosion rate of St52 steel decreased after 2 hours of immersion in the solution from 0.23 mm/year to 0.01 mm/year at the end of 95 hours of immersion in solution. The data of corrosion rate at 191 hours of immersion in the solution was not presence because of the error in computer system when the experiment was conducted. The same condition is also found in St33 experiment for the data of corrosion rate at 95 hours which missed because of some errors in the computer system. However, the protective $FeCO_3$ film may form at 95 hours, because the value of corrosion rate at the end of 47 hours decreased rapidly from 0.13 mm/year to 0.01 mm/year at the end of 191 hours.

4.6.4 48 Hours at 80^{o}C

The corrosion rates of 3 examined steels are shown in Fig. 4.33. The corrosion rate of X65 steel increased at the end of 9 hours of immersion in the solution from 0.84 mm/year to 0.94 mm/year. The condition is similar found in the literature [6]; that flow may affect CO_2 corrosion in the case of protective scales does not form. The condition is typically happened at low pH (the pH during experiment was measured to 4.11). Thus, the main role of turbulent flow is to enhance transport of species towards and away from metal surface and may lead to the increasing of corrosion rate. Furthermore, after 9 hours of immersion in solution, the corrosion rate decreased from 0.94 mm/year to 0.03 mm/year at the end of 191 hours of immersion in solution. The decreasing of corrosion rate is indicated the formation of protective $FeCO_3$ film on surface steel.

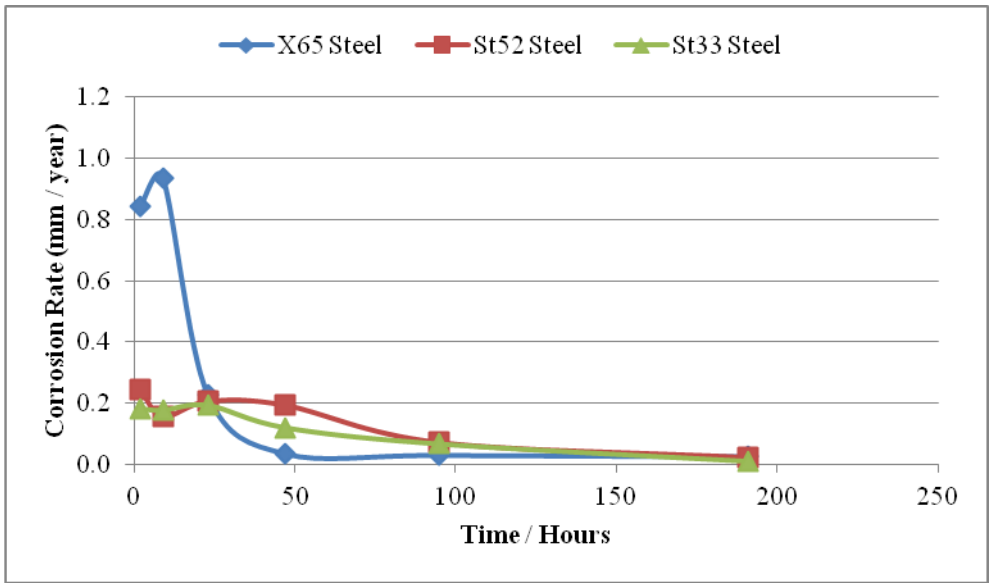

Fig. 4.33 The corrosion rate of X65, St52 and St33 steels (Precorroded 48 hours at 80^0C) vs Time

The dense protective $FeCO_3$ film is formed close to the metal at 80°C and leads to a decrease in corrosion rate quickly (amount 20-40 hours) [8]. The theory is proven by both experiment of St52 steel and St33. The corrosion rate in St52 steel decreased after 2 hours of immersion in the solution from 0.25 mm/year to 0.16 mm/year at the end of 9 hours of immersion in solution and increased again at the end of 23 hours of immersion in the solution (from 0.16 mm/year to 0.21 mm/year). Furthermore, the corrosion rate decreased rapidly after 47 hours of immersion in the solution from 0.19 mm/year to 0.02 mm/year at the end of 191 hours of immersion in solution. The same condition is also found in the St33 that the corrosion rate from 23 hours to 191 hours decreased rapidly from 0.19 mm/year to 0.02 mm/year.
Afterwards, in order to check the reliability of LPR measurement, the Fe^{2+} concentration analysis, EIS analysis, Potentiodynamic cathodic analysis and OCP was measured after 192 hours of Rp/Ec trend measurement.

4.6.7 Summary of Rp trend from X65, St52 and St33 steels

The summary of corrosion rate results at the end of exposure time with variation of precorrosion time and temperature is presented in Table 4.8.In general, corrosion rate decreased at the end of 191 hours (or less for some experiments) of immersion in solution. It is indicated that the protective scale $FeCO_3$ successfully formed after precorrosion period (approximately $FeCO_3$ formed during 95 hours). The variation of corrosion rate results depends on the chemical composition of steel. For example, X65 has lower corrosion rate due to its lower carbon content compared to St52. But, temperature is also become a parameter that needed to be considered in protective scale $FeCO_3$ formation.

Table 4.8 The corrosion rate results of X65, St52 and St33 steels with Variation of Precorrosion Time and Temperature

T (°C)	Precorrosion Time (Hours)	Time of immersion in solution (Hours)	The Results of Corrosion Rate at the end of exposure time (mm/year)		
			X65	St52	St33
40	24	191	0.01	0.07 (stop at 95 hours)	0.03 (stop at 75 hours)
	48	191	0.05	0.13	0.17 (stop at 95 hours)
80	24	191	0.01	0.01 (stop at 95 hours)	0.01
	48	191	0.03	0.02	0.01

4.7 SEM and EDS Analysis

The SEM with EDS analysis results of X65 steel with precorrosion time 24 hours at temperature 40°C was shown in Fig. 4.34. EDS analysis revealed that Fe_3C was formed on surface steel which increased corrosion process and after 95 hours, $FeCO_3$ was deposited and accumulated on surface steel which act as protective scale. The protective scale was useful to decrease the corrosion rate and it was proven by a decrease in corrosion rate from 0.98 mm/year at the end of 8 hours to 0.88 mm/ year at the end of 95 hours. But, however, compared to the results of corrosion rate based on Rp/Ec trend, the corrosion rate was increased again from 0.88 mm/ year to 1.34 mm/year at the end 191 hours. The increasing of corrosion rate was more likely caused by decreasing temperature (because the water was evaporated in water bath).

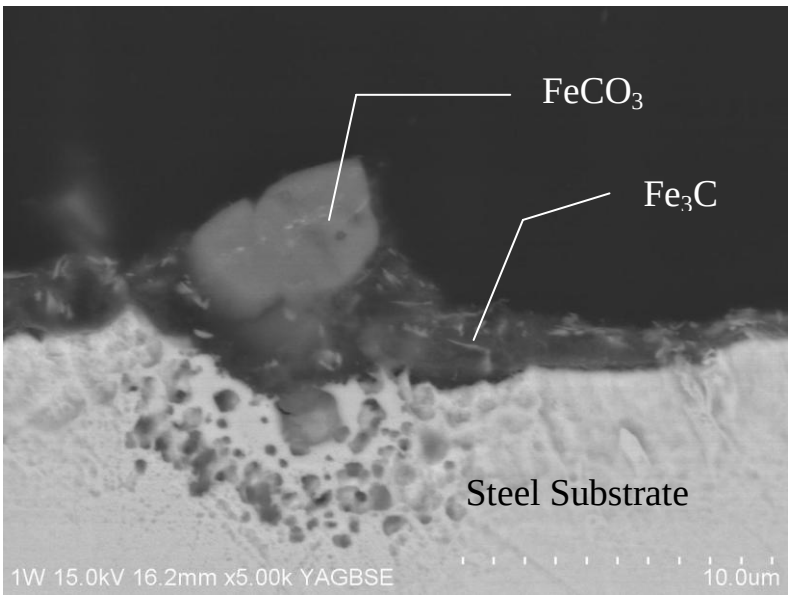

Fig. 4.34 SEM picture with EDS analysis of X65 at forced precorrosion time 24 hours and temperature 40°C after 216 hours exposure time

Based on Fig. 4.35, EDS analysis revealed more $FeCO_3$ and Fe_3C were formed on St52 steel at precorrosion time 24 hours and temperature 40°C. The formation of more $FeCO_3$ on surface steel was useful to decrease the corrosion rate and compare to the Rp/Ec trend at the end of 95 hours; the corrosion rate of St52 steel (0.22 mm/year) was lower than X65 steel (0.88 mm/year). The chemical composition should be considered, because St52 has higher carbon content than X65 so that it was expected that St52 will corrode faster than X65 which form more Fe_3C. The decrease in corrosion rate on St52 steel from 0.26 mm/year at the end of 47 hours to 0.22 mm/year at the end of 95 hours showed that $FeCO_3$ was formed during 95 hours of immersion in solution and act as protective scale on surface steel.

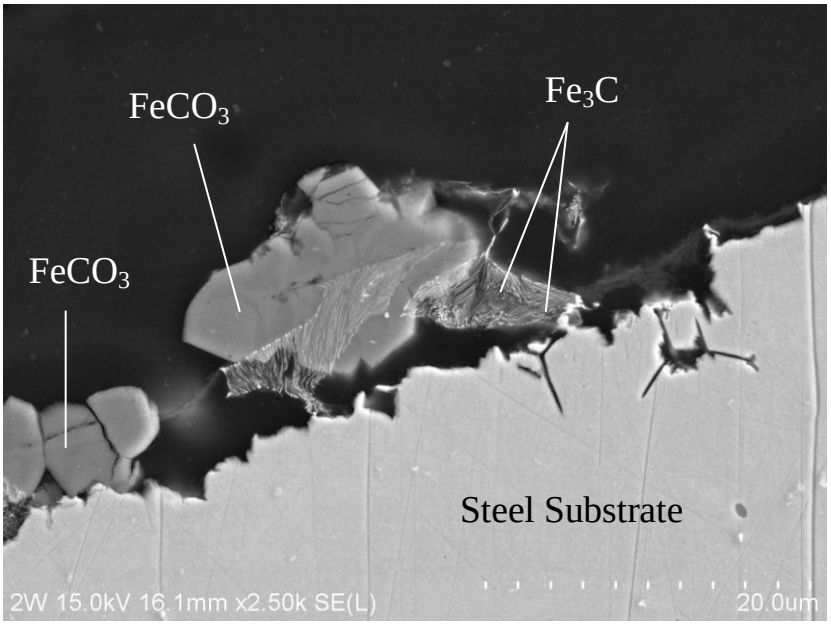

Fig. 4.35 SEM picture with EDS analysis of St52 at forced precorrosion time 24 hours and temperature 40^0C after 192 hours exposure time

The SEM analysis was applied for St33 steel at forced precorrosion time 24 hours at 40°C was shown in Fig. 4.36. According to the Fig. 4.36, EDS analysis showed more Fe_3C formed on surface steel but there was no $FeCO_3$. The condition was reasonable due to experiment stopped at 75 hours because of the CO_2 on the CO_2 gas tube was exhausted in the middle of experiment. Therefore, it may conclude that it took time 95 hours to form $FeCO_3$ on surface steel. Thus, the decreasing of corrosion rate from 0.27 mm/year to 0.10 mm/year at the end of 75 hours was more caused by the high Cr content on St33 steel which reduce the corrosion rate.

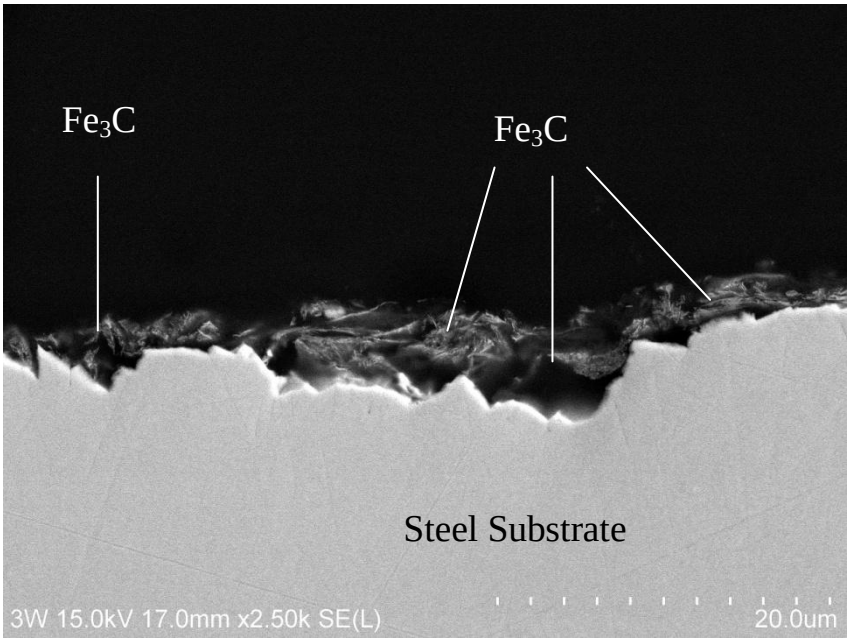

Fig. 4.36 SEM picture with EDS analysis of St33 at forced precorrosion time 24 hours and temperature 40^0C after 75 hours exposure time

Temperature gives significantly affect to the $FeCO_3$ formation on the steel substrate. It was proven by SEM with EDS analysis in Fig. 4.37 and 4.38. At temperature 80°C, $FeCO_3$ much more formed on surface steel rather than at temperature 40°C. Fig. 4.37shown the SEM with EDS analysis of St33 at forced 24 hours precorrosion time at 80°C.

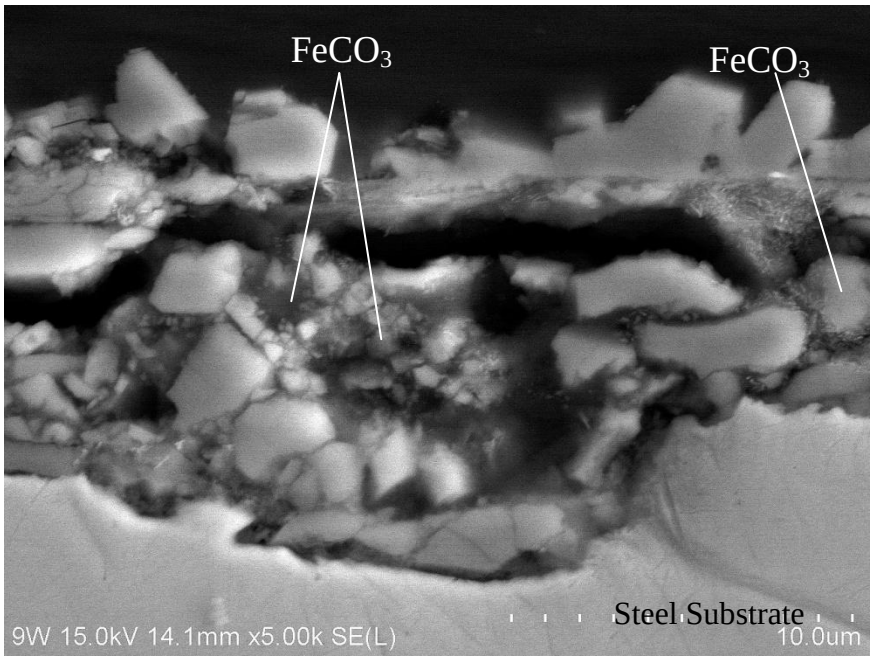

Fig. 4.37 SEM picture with EDS analysis of St33 at forced precorrosion time 24 hours and temperature 80^0C after 216 hours exposure time

Ideally, the longer precorrosion time and higher temperature will form more dense and rapid $FeCO_3$ on surface steel. It was supported in theory [8]; at 80°C, a dense protective $FeCO_3$ film was formed close to the metal and it decreases the corrosion rate quickly (20-40 hours). It was proven by the SEM with EDS analysis result for St52 steel at 48 hours precorrosion times and

temperature 80°C. $FeCO_3$ was much more formed on the steel surface rather than at temperature 40°C. Furthermore, with more $FeCO_3$ formation, it will lead into a decrease in corrosion rate and it was supported by Rp/Ec trend that the corrosion rate decreased rapidly after 47 hours of immersion in the solution from 0.61 mm/year to 0.08 mm/year at the end of 191 hours of immersion in solution. $FeCO_3$ formation on St52 steel was shown in Fig. 4.38.

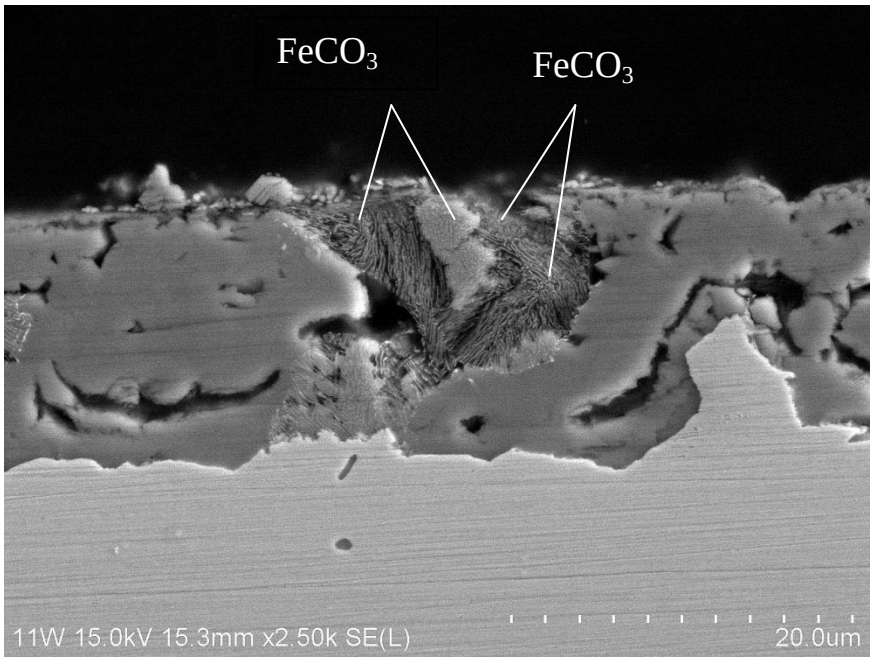

Fig. 4.38 SEM picture with EDS analysis of St52 at forced precorrosion time 48 hours and temperature 80^0C after 216 hours exposure time

5 CONCLUSIONS

- The potentials of steels increased at the end of precorroded time. The increasing of potentials was caused by Fe_3C formation during precorrosion period which stimulated corrosion process.
- The steel is corroded faster at temperature 80°C than at temperature 40°C.
- Fe^{2+} concentration of the 3 steels decreases by time after the addition of $NaHCO_3$ due to precipitation. High supersaturation of Fe^{2+} concentration will lead to a higher precipitation which will make better formation of protective scale.
- The highest polarization resistance of 3 steels mostly obtained at the end of 216 hours of EIS measurement giving the lowest of corrosion rate.
- Potentiodynamic cathodic scan from X65, St52 and St33 steels after 24 or 48 hours precorrosion time at 40°C showed that the potential decreased with increasing time indicated the low corrosion process.
- The decreasing potential from potentiodynamic cathodic scan and OCP after 216 hours of immersion in solution indicated protective scale formation on surface steel.
- Both for 40°C and 80°C, the protective scales seemed to be formed on surface steel at least after 75 hours exposure time.
- St33 has the lowest corrosion rate compared to X65 and St52 steels due to its high Cr content which more protective to corrosion.
- At temperature 80°C, more rapid protective $FeCO_3$ is formed on surface compared with temperature at 40°C.

6 RECOMMENDATION FOR FURTHER WORK

One sample is required 216 hours exposure time with total experiment time is around 2 weeks with preparation and the precorrosion period. During the 2 weeks experiment for each sample, some of the experiment showed poor results and some of them were stopped in the middle of experiments due to errors such as bad connection in cell system, water evaporated in reference electrode, and other things. Some of the SEM and EDS analysis is not reliable because the equipment has not properly calibrated. The recommendation for further work in order to prevent the unreliably results are:

- Check reference electrode frequently, before and after experiment
- Check the connection in cell system
- Check the availability of CO_2 content in CO_2 gas cylinder
- Check solution to improve the water evaporation prevention by installing proper cap on water bath for example.
- Make sure the SEM and EDS analysis equipment has been properly calibrated before used.
- Parallels should be run to see the reproducibility of the results

7 REFERENCES

[1] C. De Waard, D.E. Milliams: Prediction of Carbonic Acid in Natural Gas Pipelines. First International Conference on the Internal and External Protection of Pipes. (1975) Paper F-1.

[2] C. De Waard, U. Lotz, D.E. Milliams: Predictive Model for CO_2 Corrosion Engineering in Wet Natural Gas Pipelines. Corrosion 47 (1991) 976-985.

[3] C. De Waard, U. Lotz: Prediction of CO_2 Corrosion of Carbon Steel, in Prediction of CO_2 Corrosion in the Oil and Gas Industry. Institute of Materials Publisher, UK (1994) pp. 30-49.

[4] C.A. Palacios, J.R. Shadley: Characteristics of Corrosion Scales on Steel in a CO_2-Saturated NaCl Brine. Corrosion 47 (1991) 122-127.

[5] S. Slåtten: CO_2 Corrosion of Carbon Steel with Low Temperature. NTNU, Trondheim (2007)

[6] S. Nesic: Key Issues Related to Modelling of Internal Corrosion of Oil and Gas Pipelines – A Review. Corrosion Science 49 (2007) page 4308-4338.

[7] N.O. Ågotnes, T. Hemmingsen et.al: Comparison of Corrosion Measurements by Use of AC-impedance, LPR and Polarization Methods on Carbon Steel in CO_2 purged NaCl Electrolytes. NACE Corrosion 99, Paper No.27.

[8] A. Dugstad: The Importance of $FeCO_3$ Supersaturation of Carbon Steel. NACE Corrosion'92, Paper no. 14.

[9] J.L. Crolet, N. Thevenot, S. Nesic: Role of Conductive Corrosion Products in The Protectiveness of Corrosion Layers. Corrosion Science Section, NACE International 1998.

[10] K. Trethewey and J. Chamberlain: Corrosion for Science and Engineering: Second Edition (1995) page 281.

[11] G.I. Ogundele, W.E. White: Some Observations on Corrosion of Carbon Steel in Aqueous Environments Containing Carbon Dioxide. Corrosion 42 (1986) 71-78

[12] M.S.A. Al-Sayed: Ph.D. Thesis, UMIST, 1989

[13] K. Videm, A. Dugstad: Corrosion of Carbon Steel in an Aqueous Carbon Dioxide Environment. Part 2. Film formation. Mats. Perf. 28 (1989) 46-50

[14] S. Valen, Corrosion course: Aspects of Corrosion in Oil and Gas Systems, Corrocean, Trondheim, Norway

[15] T. Berntsen: Personnal Letter (2011)

[16] J.L. Mora Mendoza, S. Turgoose: $FeCO_3$ Influence on the Corrosion Rate of Mild Steel in Aqueous CO_2 System Under Turbulent Flow Conditions", Corrosion Science 44 (2002) 1223-1246

[17] K. Videm, A. Dugstad: The Many Facets of CO_2 Corrosion of Carbon Steels. 11th Scandinavian Corrosion Congress, Stavanger (1989) Paper F60.

[18] T. Berntsen, M. Seiersten, T. Hemmingsen: CO_2 Corrosion of Carbon Cteel at Lower Temperatures. Eurocorr 2008. Paper 1188

[19] E. Gulbrandsen, J. Morard: Why Does Glycol Inhibit CO_2 Corrosion?. NACE CORROSION 98, paper no. 221

[20] S. Nesic, Kun-Lin John Lee, Vukan Ruzic: A Mechanistic Model of Iron (II) Carbonate Film Growth and the Effect on CO_2 Corrosion of Mild Steel. Department of Mechanical Engineering, The University of Queensland, Australia.

[21] A. Dugstad: Mechanism of Protective Film Formation During CO_2 Corrosion of Carbon Steel. NACE CORROSION/98, paper no.31

[22] R. Nyborg: Iniatiation and Growth of Mesa Corrosion Attack During CO_2 Corrosion of Carbon Steel. NACE CORROSION/98, paper No.48

[23] R. Nyborg, A. Dugstad: Mesa Corrosion Attack in Carbon Steel and 0.5% Chromium Steel. NACE CORROSION/98, paper no.29

[24] S. Nesic, M. Nordsveen et al: A Mechanistic Model for Carbon Dioxide Corrosion of Mild Steel in the Presence of Protective Iron (II) Carbonate Films- Part 2: A Numerical Experiment. NACE CORROSION-Vol.59, No.6

[25] T. Berntsen, M. Seiersten and T. Hemmingsen: Effect of $FeCO_3$ Supersaturation and Carbide Exposure on the CO_2 Corrosion Rate of Carbon Steel. NACE Corrosion 2011

[26] J.W Mullin: Crystallization. 3rd ed. (Oxford, U.K : Oxford Press, 1993)

[27] P. Benezeth, J.L Dandurand, J.C Harrichoury: Solubility Product of Siderite $FeCO_3$ as a Function of Temperature (25°C-250°C). Chemical Geology 265 (2009) 3-12.

[28] E.W.J. van Hunnik, B.F.M. Pots, E.L.J.A. Hendriksen: The Formation of Protective $FeCO_3$ Corrosion Product Layers in CO_2 Corrosion. NACE CORROSION/96, paper No.6

[29] B. Kisella, Y.J. Tan, S. Balley: Electrochemical Impedance Spectroscopy and Surface Characterization Techniques to Study Carbon Dioxide Corrosion Product Scales. NACE CORROSION (1998).-Vol. 54, No.10

[30] Z.Q. Bai, C.F. Chen, M.X. Lu, and J.B. Li, Analysis of EIS characteristics of CO2 corrosion of well tube steels with corrosion scales", Applied Surface Science 252 (2006) 7578–7584.

[31] D.G. Enos, L.L. Scribner: The Potentiodynamic Polarization Scan; Technical Report 33. (1997) Solartron Instruments a division of Solartron Group Ltd

[32] Gamry Instruments, Inc: CMS100 Framework Software, Operator's Manual.

8 APPENDIX

8.1 Chemical composition of steels

8.1.1 X65 steel

Ståldata

Stål nr:	57		
Legering	X-65	Form	Rør 36", WT 31,0
Sveis		Leverandør	Shell
Prosjekt		Lagringssted	PT-2 kjeller plass 1.7
Prosjekt betegnelse		Beholdning	Mer enn 3 kg

Legeringselementer - grunnmateriale

C:	Si:	Mn:	S:	P:	Cr:	Ni:	V:	Mo:	Cu:	Al:	Sn:	Nb:
0.08	0.25	1.54	0.001	0.019	0.04	0.03	0.045	0.01	0.02	0.038	0.001	0.043

Mikrostruktur	Feritt - perlitt

Fig. 8.1 Chemical composition of X65 steel

8.1.2 St52 steel

Ståldata

Stål nr:	53		
Legering	St. 52-3	Form	Bolt 12 mm
Sveis		Leverandør	
Prosjekt	Statoil	Lagringssted	Hovedlager pallplass
Prosjekt betegnelse	St. 52	Beholdning	Mindre enn 3 kg

Legeringselementer - grunnmateriale

C:	Si:	Mn:	S:	P:	Cr:	Ni:	V:	Mo:	Cu:	Al:	Sn:	Nb:
0.13	0.38	1.29	0.008	0.015	0.07	0.09	0.035	0.01	0.34	0.05	0.015	

Mikrostruktur	Feritt - noe perlitt

Fig. 8.2 Chemical composition of St52 steel

8.1.3 St33 steel

Ståldata

Stål nr:	33		
Legering	C0.07Mn0.9Cr0.6	Form	Rør
Sveis	x	Leverandør	Saga/Mitsui
Prosjekt	KSC III	Lagringssted	
Prosjekt betegnelse	33W	Beholdning	Mer enn 3 kg

Legeringselementer - grunnmateriale

C:	Si:	Mn:	S:	P:	Cr:	Ni:	V:	Mo:	Cu:	Al:	Sn:	Nb:
0.07	0.19	0.87	0.004	0.012	0.56	0.01	0.032	0.01	0.01	0.035	0.001	

Mikrostruktur: Grov feritt - noe widmanstattenferitt

Fig. 8.3 Chemical composition of St33 steel

8.2 Fe2+ Concentration Analysis

8.2.1 Standard Calibration Curve

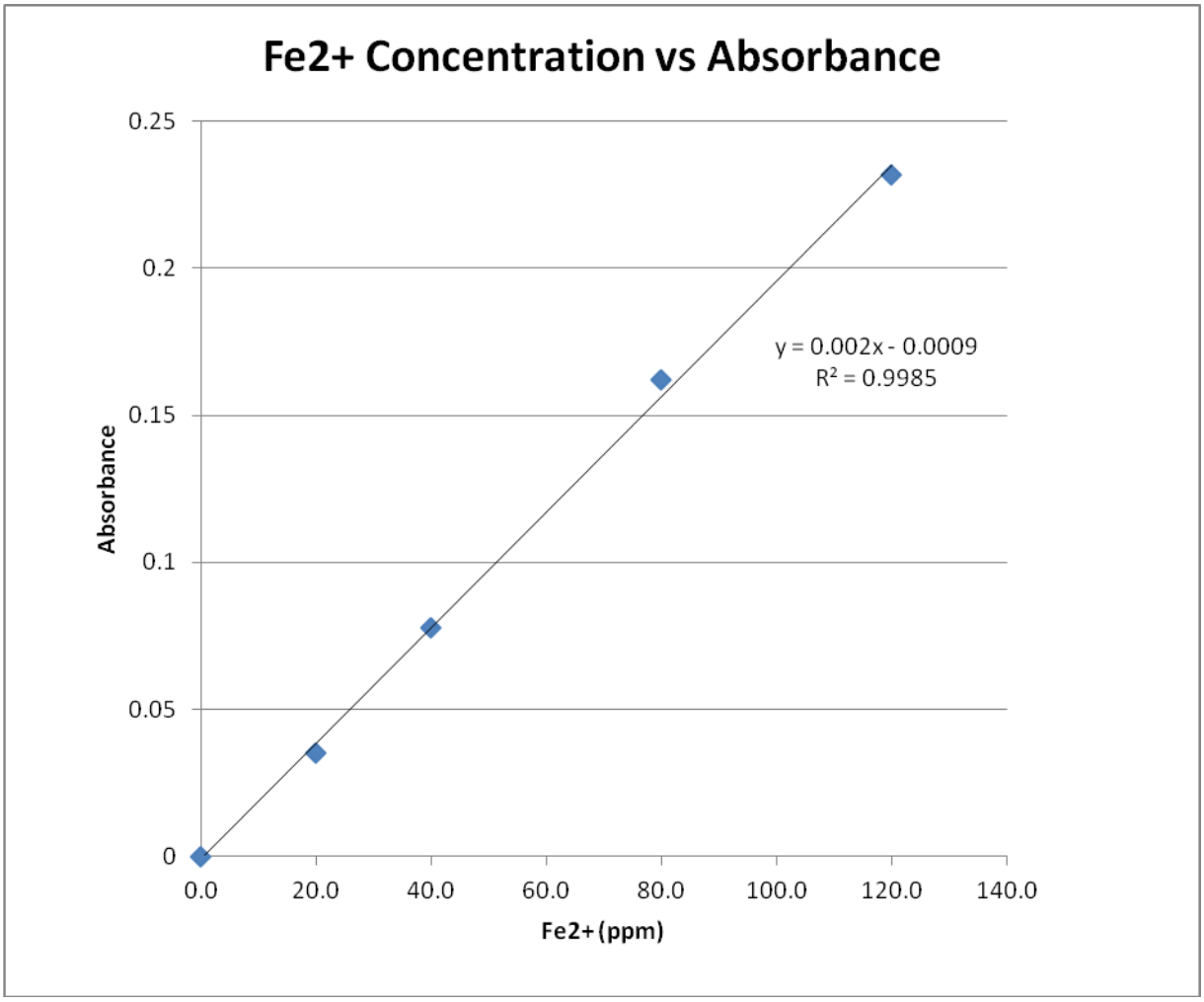

Fig. 8.4 Fe2+ Concentration vs Absorbance

8.2 Fe^{2+} concentration results of X65, St52 and St33 steels

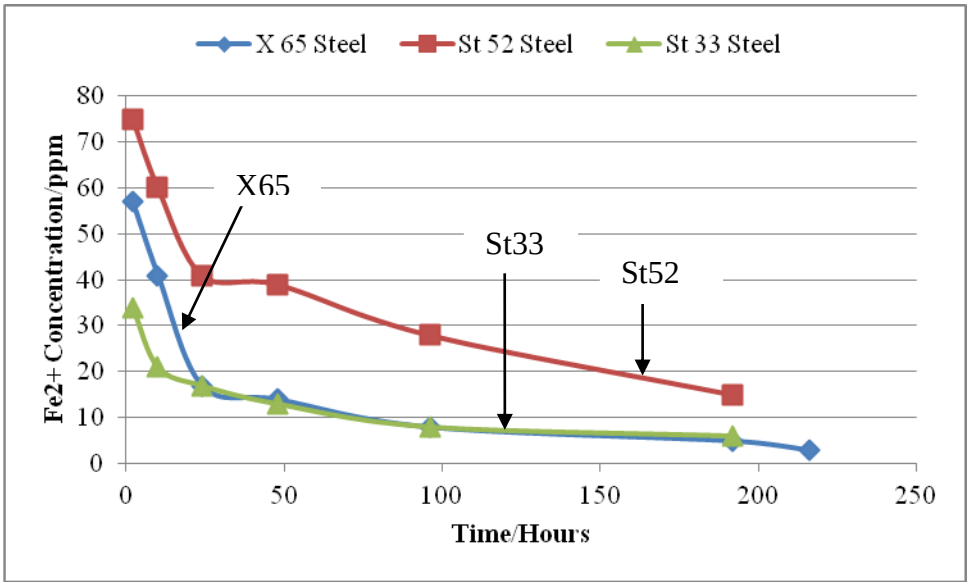

Fig. 8.5 Fe2+ concentration of X65, St52, and St33 steels (Precorroded: 24 hours at 40^0C) vs Time

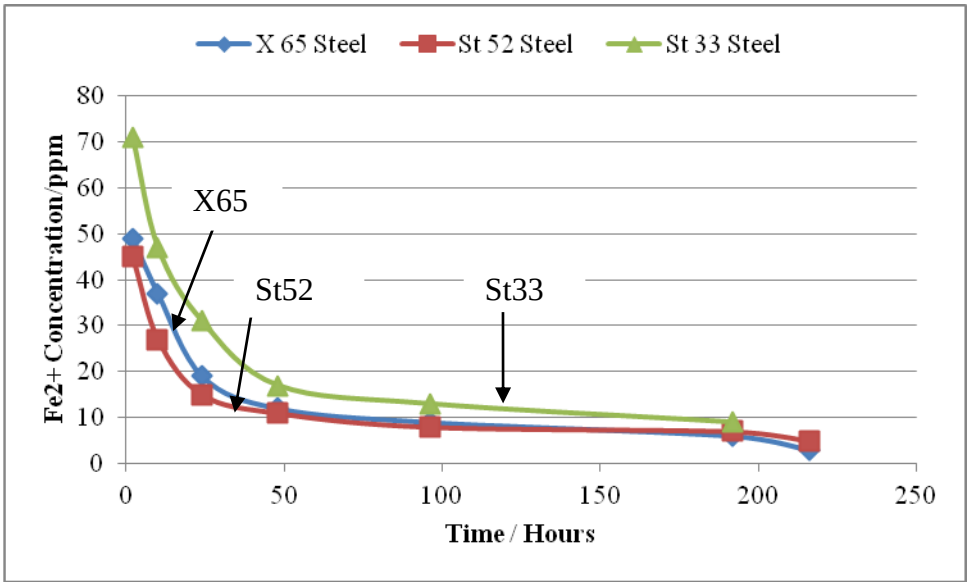

Fig. 8.6 Fe2+ concentration of 3 (three) steels (48 hours Precorrosion Times at 40^0C) vs Time

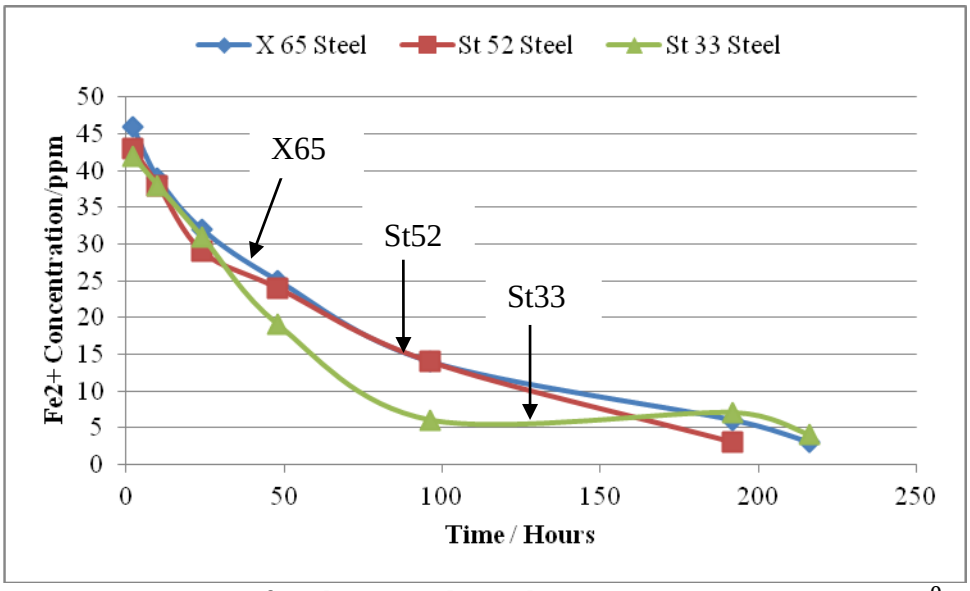

Fig. 8.7 Fe2+ concentration of 3 (three) steels (24 hours Precorrosion Times at 80^0C) vs Time

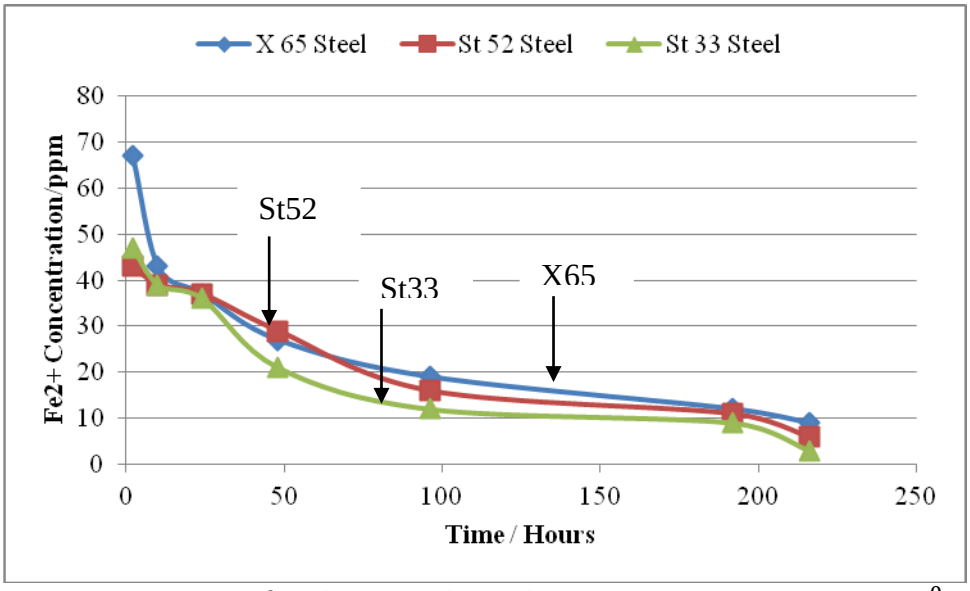

Fig. 8.8 Fe2+ concentration of 3 (three) steels (48 hours Precorrosion Times at 80^0C) vs Time

8.3 Electrochemical Impedance Spectroscopy

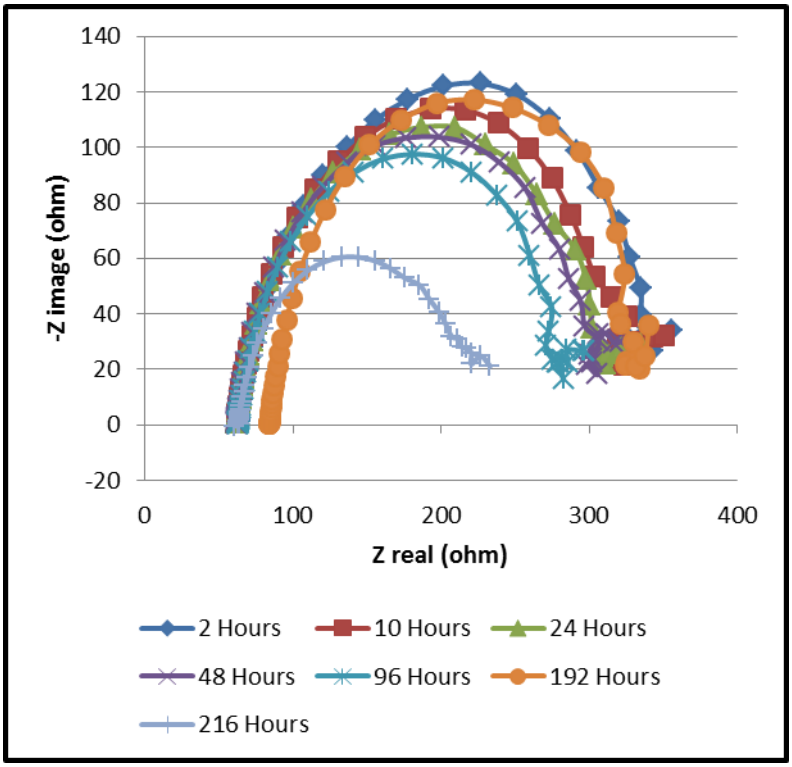

Fig. 8.9 Nyquist plots of impedance diagrams of X65 in precorroded 24 hours at 40°C after 216 hours of immersion in solution

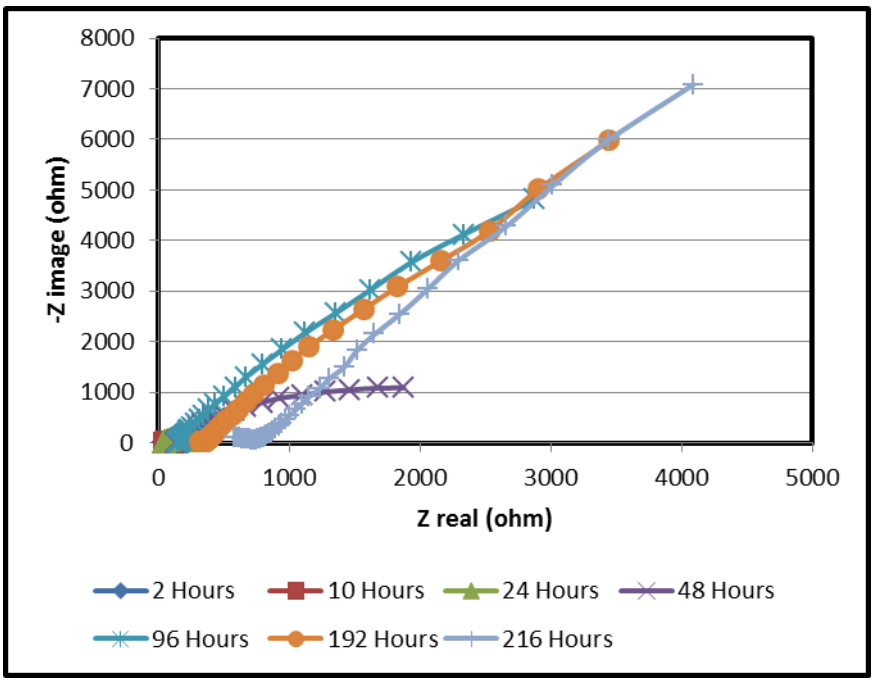

Fig. 8.10 Nyquist plots of impedance diagram result of X65 in precorroded 24 hours at 80°C after 216 hours of immersion in solution

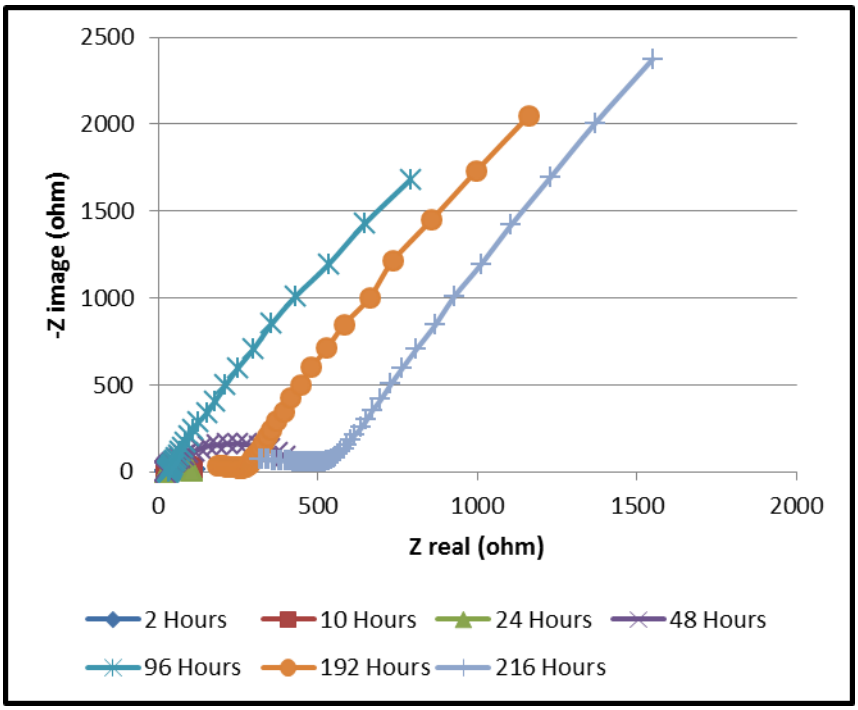

Fig. 8.11 Nyquist plots of impedance diagram result of X65 in precorroded 48 hours at 80°C after 216 hours of immersion in solution

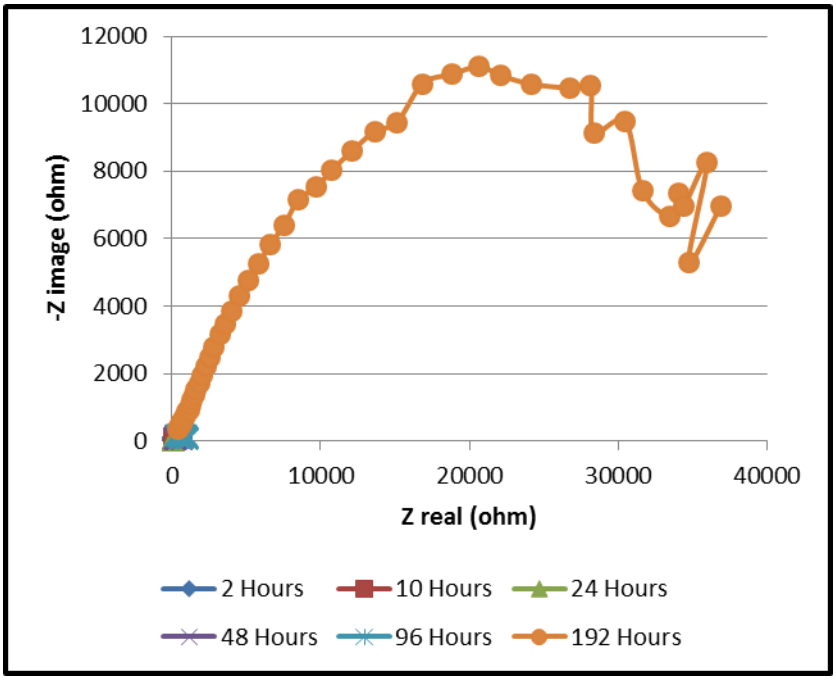

Fig. 8.12 Nyquist plots of impedance diagram result of St52 steel in precorroded 24 hours at 40°C after 216 hours of immersion in solution

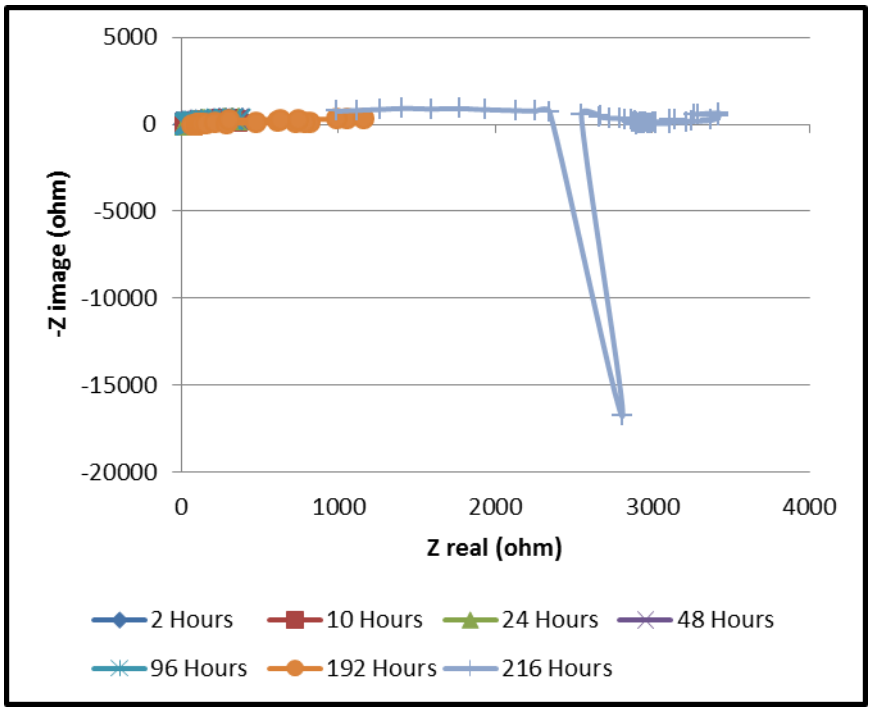

Fig. 8.13 Nyquist plots of impedance diagram result of St52 steel in precorroded 48 hours at 80°C after 216 hours of immersion in solution

8.4 Rp/Ec Trend

8.4.1 X65 steel

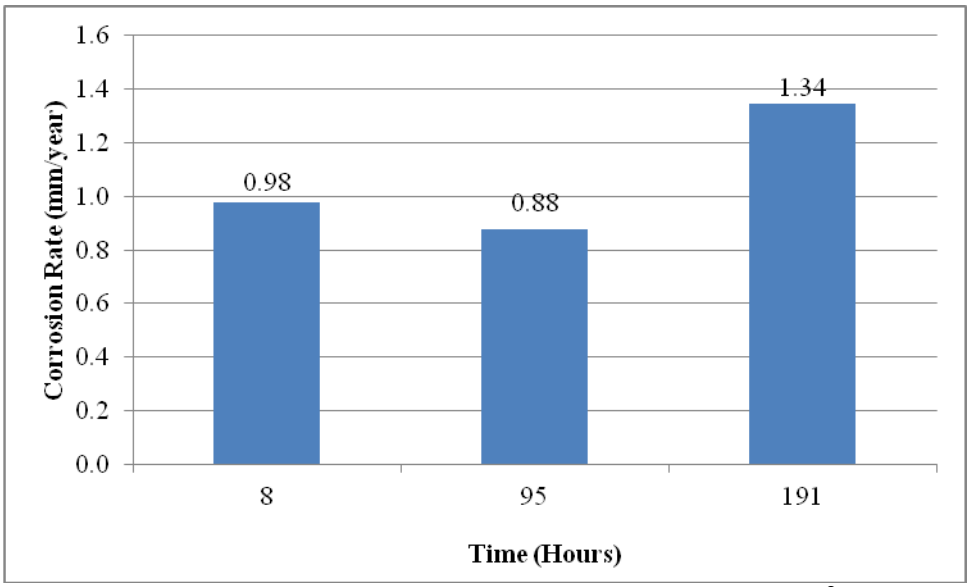

Fig. 8.14 Corrosion rate of X65 steel (Precorroded 24 hours at 40^0C) vs Time

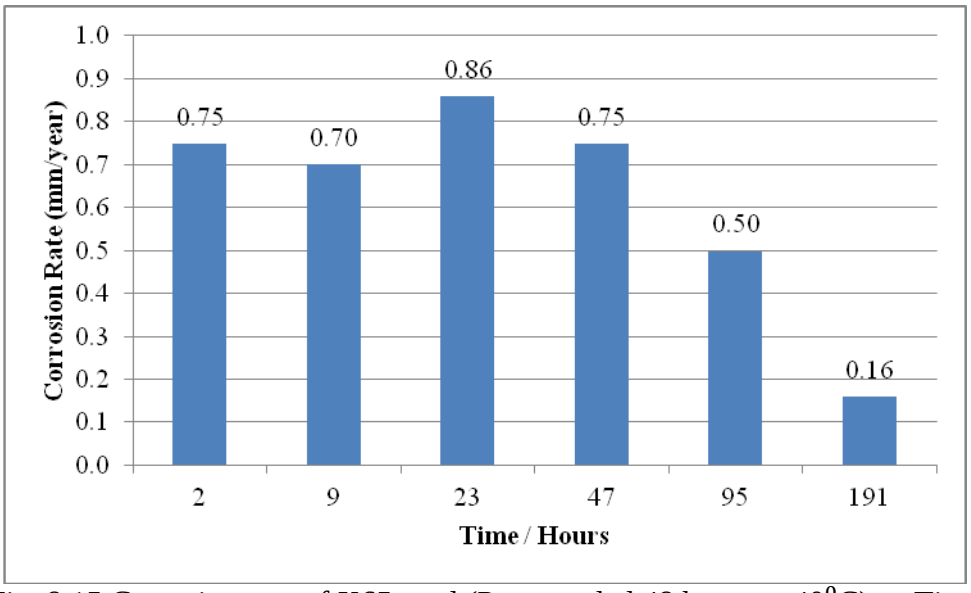

Fig. 8.15 Corrosion rate of X65 steel (Precorroded 48 hours at 40^0C) vs Time

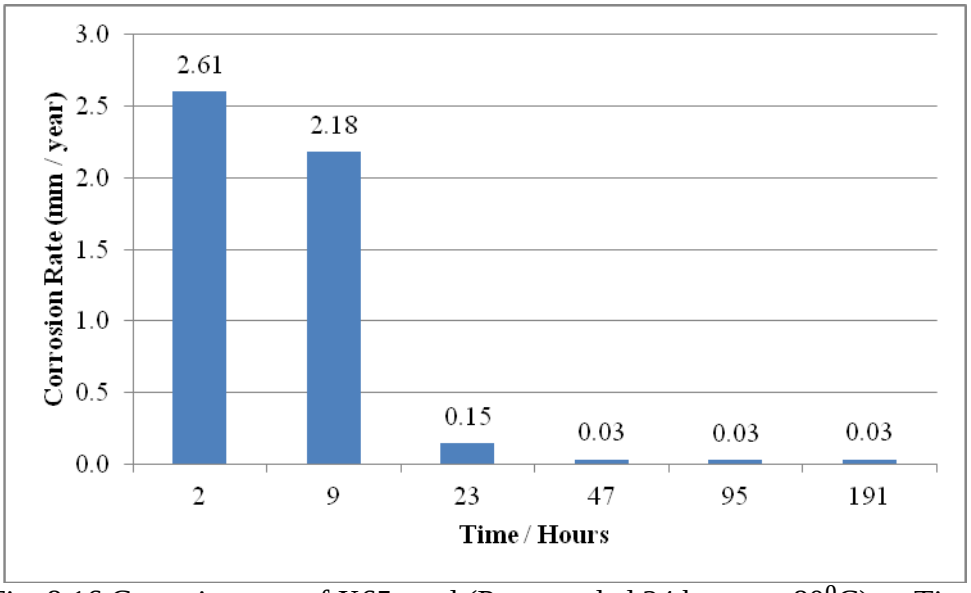

Fig. 8.16 Corrosion rate of X65 steel (Precorroded 24 hours at 80^0C) vs Time

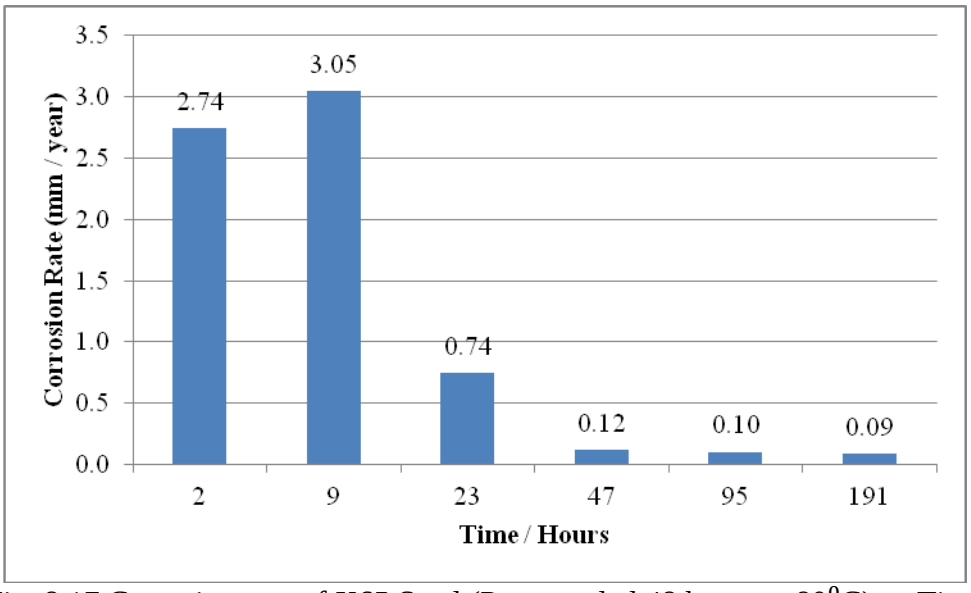

Fig. 8.17 Corrosion rate of X65 Steel (Precorroded 48 hours at 80^0C) vs Time

8.4.2 St52 Steel

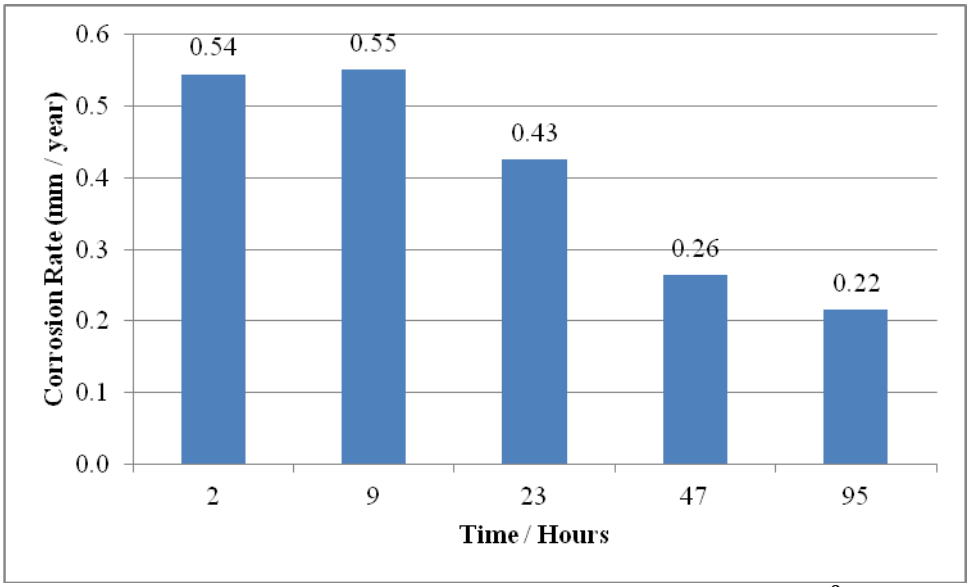

Fig. 8.18 Corrosion rate of St52 Steel (Precorroded 24 hours at 40^0C) vs Time

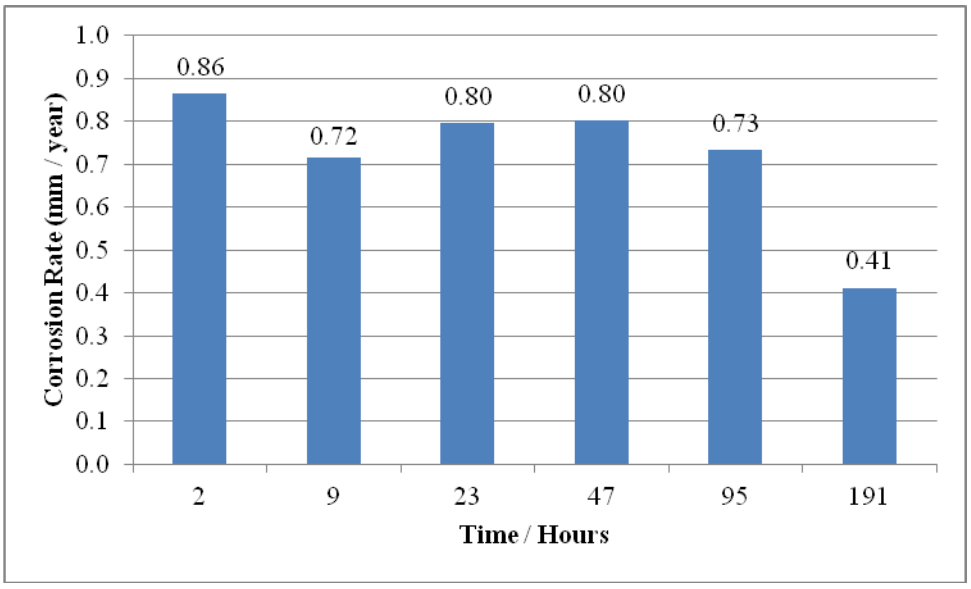

Fig. 8.19 Corrosion rate of St52 steel (Precorroded 48 hours at 40^0C) vs Time

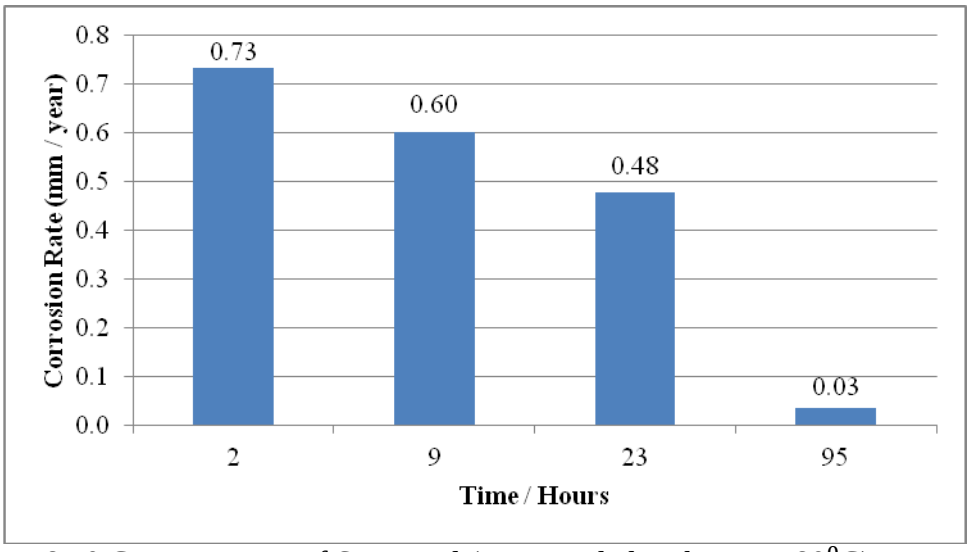

Fig. 8.20 Corrosion rate of St52 steel (Precorroded 24 hours at 80^0C) vs Time

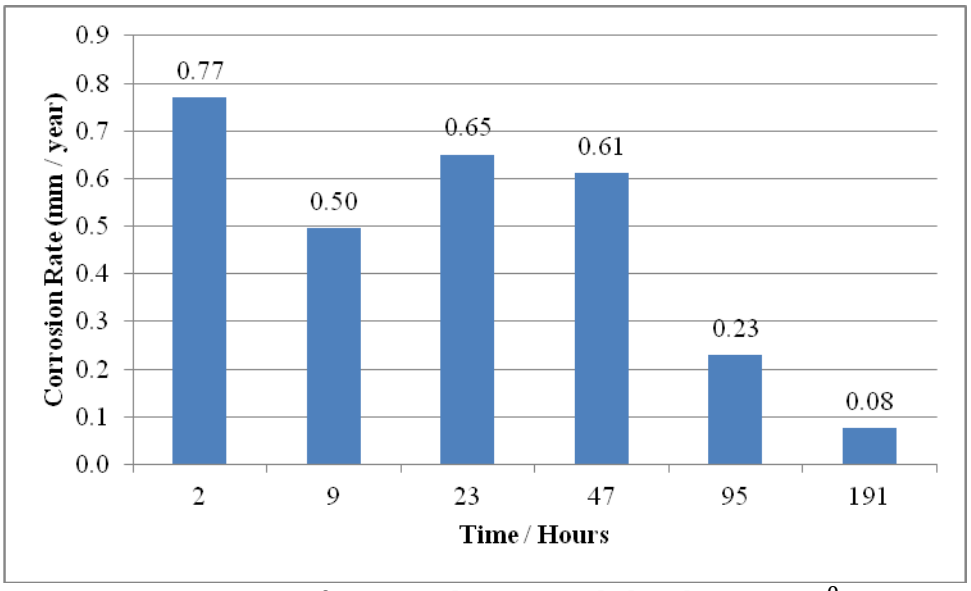

Fig. 8.21 Corrosion rate of St52 steel (Precorroded 48 hours at 80^0C) vs Time

8.4.3 St33 steel

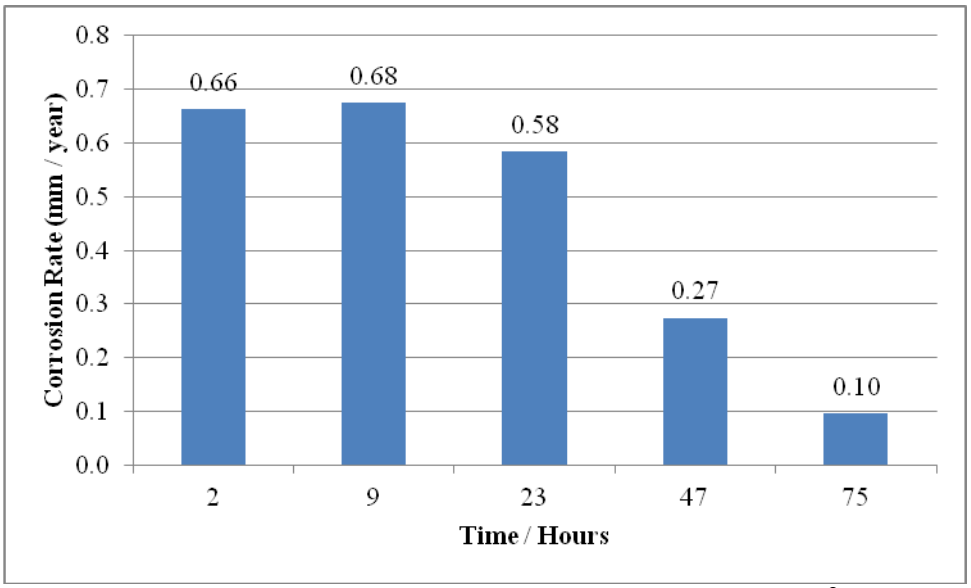

Fig. 8.22 Corrosion rate of St33 steel (Precorroded 48 hours at 80^0C) vs Time

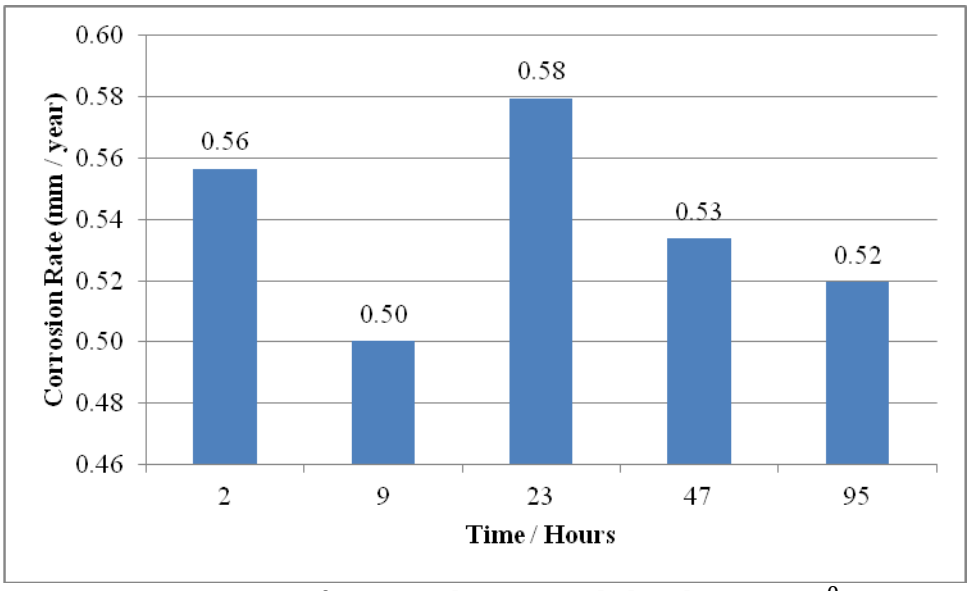

Fig. 8.23 Corrosion rate of St33 steel (Precorroded 48 hours at 40^0C) vs Time

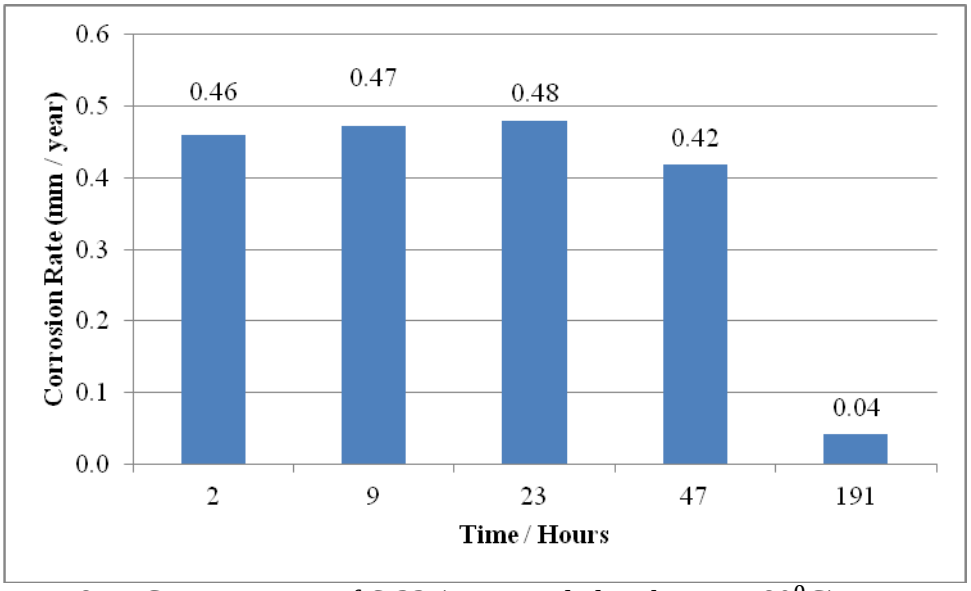

Fig. 8.24 Corrosion rate of St33 (Precorroded 24 hours at 80^0C) vs Time

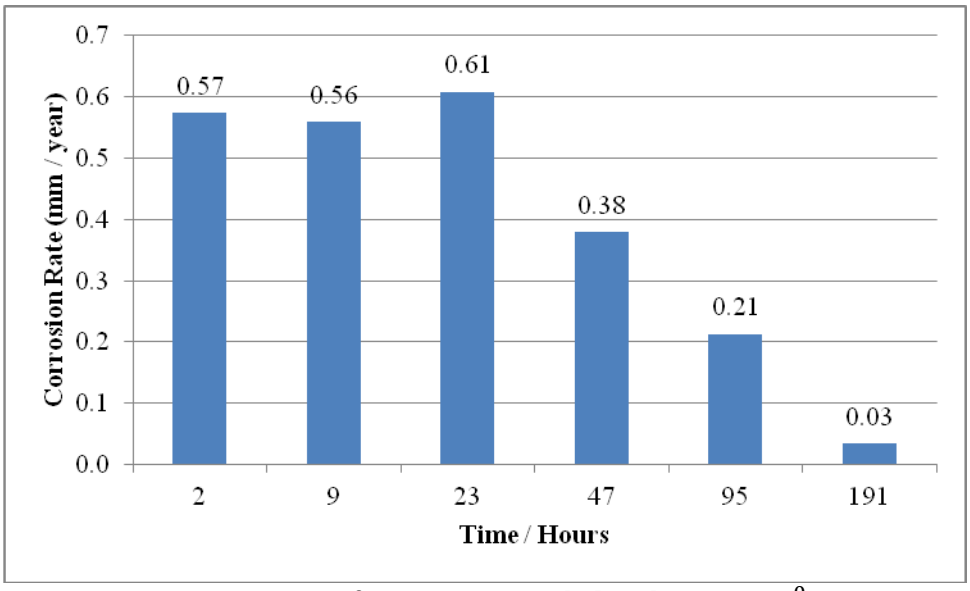

Fig. 8.25 Corrosion rate of St33 (Precorroded 48 hours at 80^0C) vs Time

8.5 SEM Analysis

The following SEM images and EDS analysis is a result of X65, St52 and St33 steels under solution 1 g/kg NaCl, 50 wt% MEG and 100 mmol/kg $NaHCO_3$ in variation of forced precorrosion time, temperature and corrosion time.

8.5.1 X65 steel at forced precorrosion 24 hours and 40°C

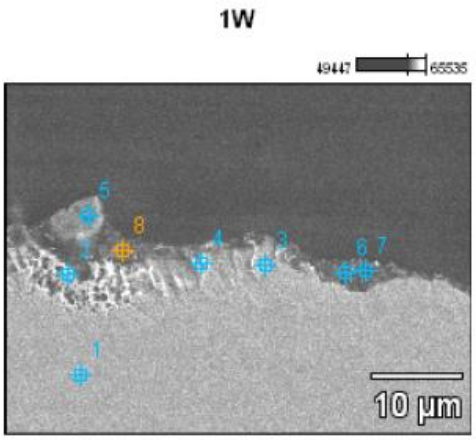

Image Name: 1W

Accelerating Voltage: 15.0 kV

Magnification: 2500

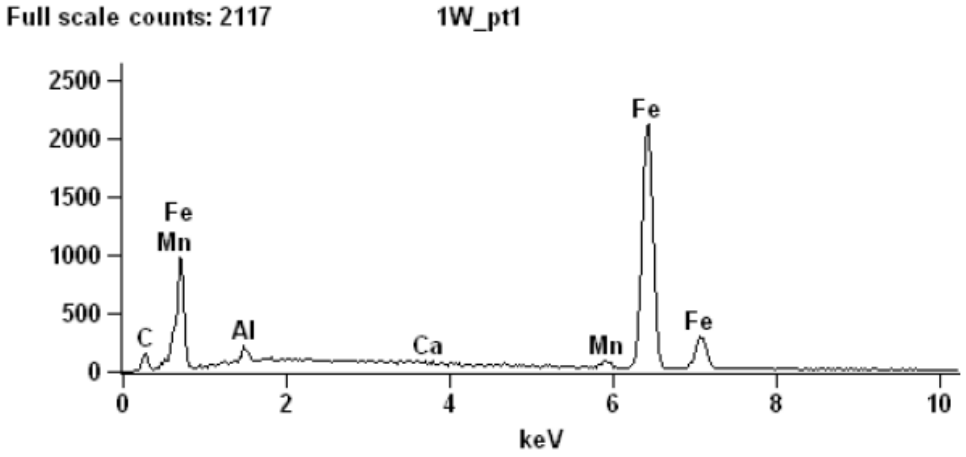
Full scale counts: 2117
1W_pt1
2500
2000
1500
1000
500
0
Fe
Mn
C
Al
Ca
Mn
Fe
Fe
0
2
4
6
8
10
keV

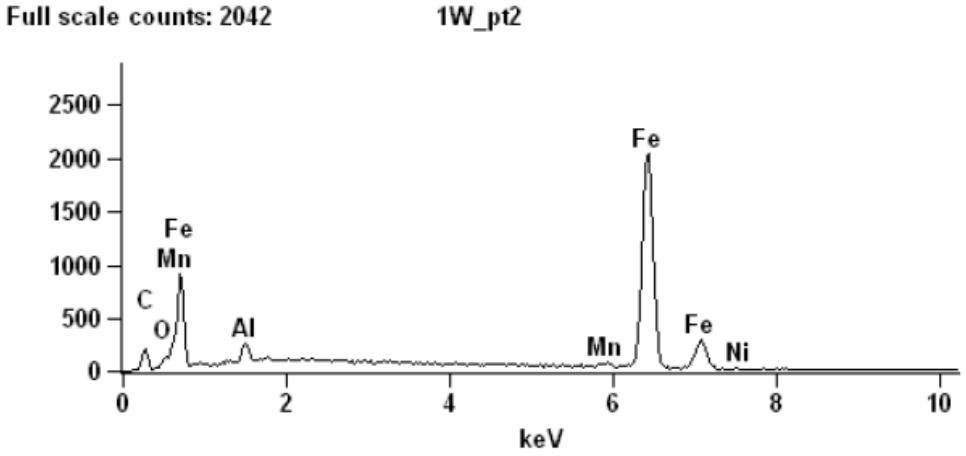
Full scale counts: 2042
1W_pt2
2500
2000
1500
1000
500
0
Fe
Mn
C
O
Al
Mn
Fe
Fe
Ni
0
2
4
6
8
10
keV

Full scale counts: 2096 1W_pt3

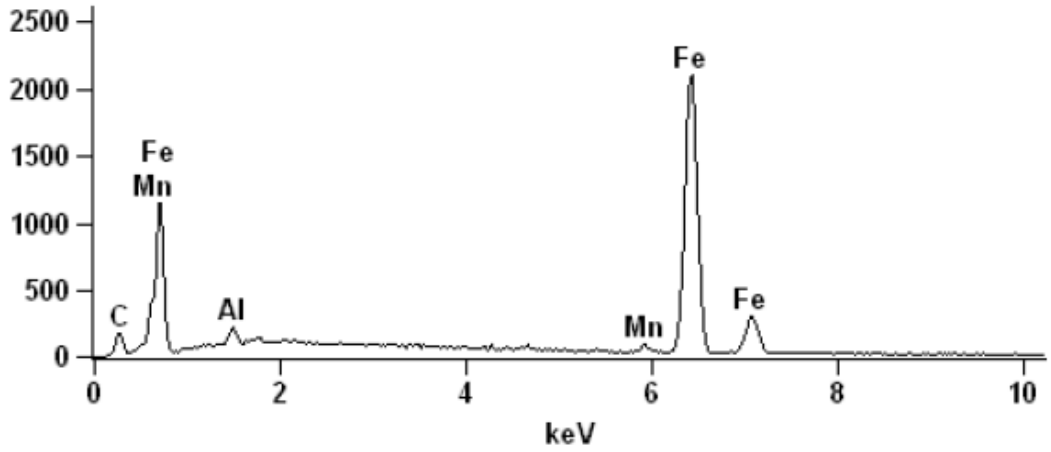

Full scale counts: 2008 1W_pt4

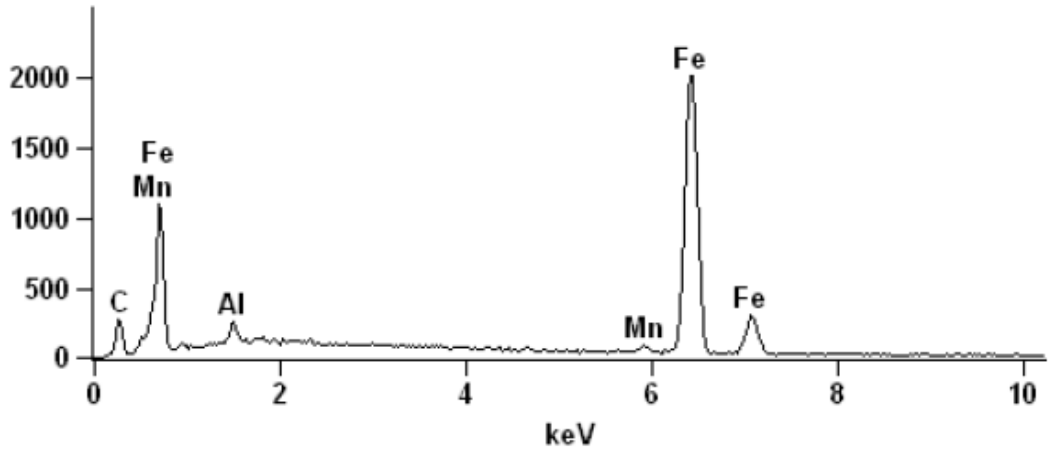

Full scale counts: 1223 1W_pt5

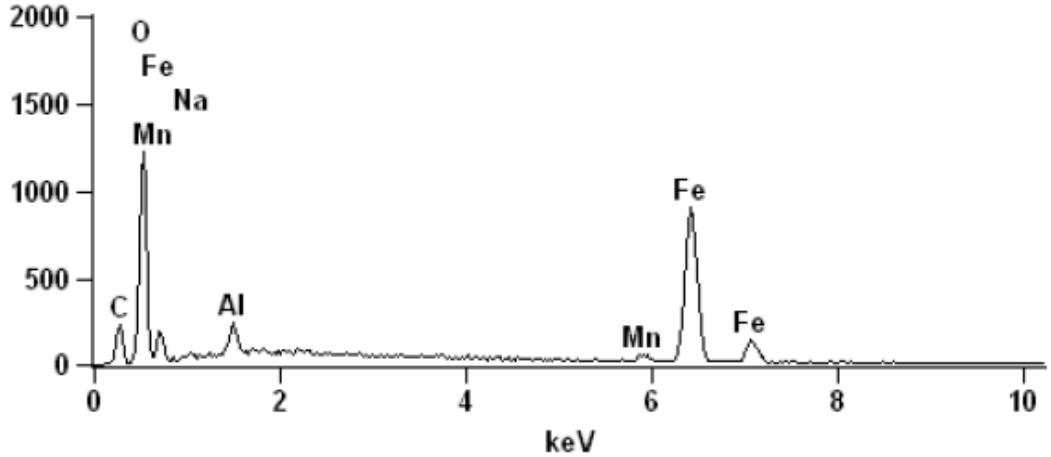

Full scale counts: 1192 1W_pt6

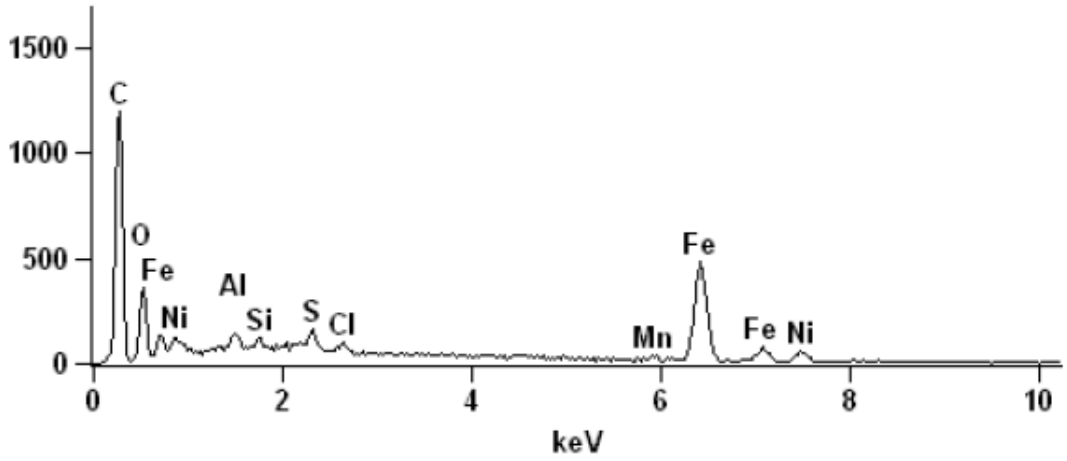

Full scale counts: 1435 1W_pt7

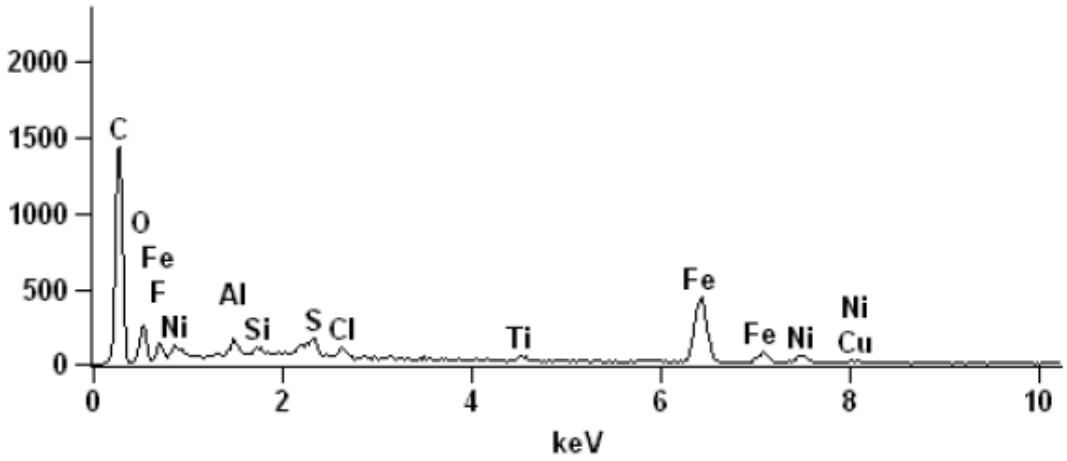

Full scale counts: 1396 1W_pt8

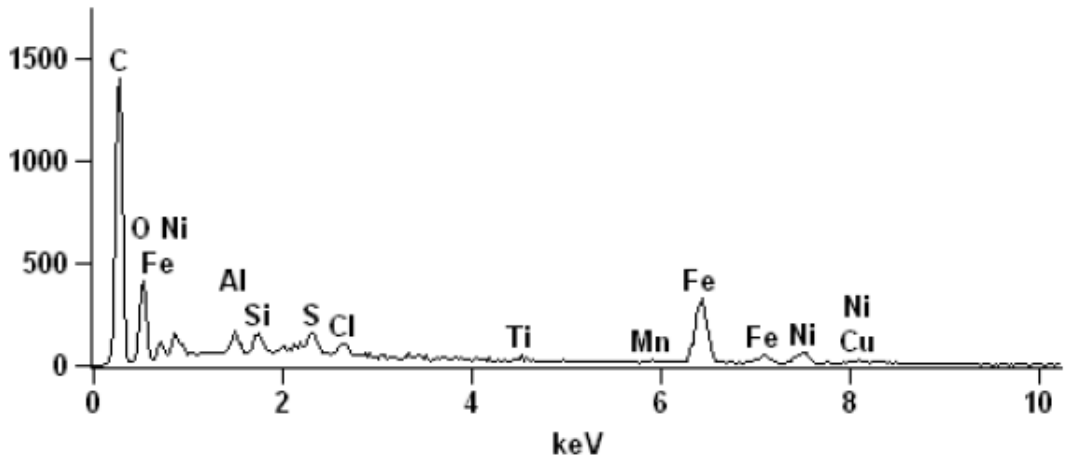

Weight %

	C-K	O-K	F-K	Na-K	Al-K	Si-K	S-K	Cl-K	Ca-K	Ti-K	Mn-K	Fe-K	Ni-K	Cu-K
1W_pt1	9.61				1.14				0.09		1.89	87.28		
1W_pt2	12.12	2.49			1.36						1.66	82.10	0.26	
1W_pt3	11.11				1.00						1.71	86.18		
1W_pt4	15.33				1.13						1.72	81.83		
1W_pt5	13.61	37.15		0.49	1.41						1.73	45.62		
1W_pt6	52.67	19.22			0.60	0.32	0.62	0.51			0.86	21.94	3.27	
1W_pt7	58.01	14.24	0.19		0.55	0.24	0.78	0.64		0.45		19.28	3.67	1.94
1W_pt8	55.03	21.88			0.49	0.51	0.77	0.70		0.31	0.50	13.60	4.44	1.78

Atom %

	C-K	O-K	F-K	Na-K	Al-K	Si-K	S-K	Cl-K	Ca-K	Ti-K	Mn-K	Fe-K	Ni-K	Cu-K
1W_pt1	32.76				1.73				0.09		1.41	64.01		
1W_pt2	37.10	5.73			1.85						1.11	54.04	0.16	
1W_pt3	36.48				1.47						1.23	60.83		
1W_pt4	45.34				1.48						1.11	52.06		
1W_pt5	25.89	53.05		0.48	1.19						0.72	18.66		
1W_pt6	71.68	19.64			0.36	0.18	0.32	0.23			0.26	6.42	0.91	
1W_pt7	77.29	14.24	0.16		0.32	0.14	0.39	0.29		0.15		5.52	1.00	0.49
1W_pt8	71.68	21.40			0.28	0.28	0.38	0.31		0.10	0.14	3.81	1.18	0.44

8.5.2 St52 steel at forced precorrosion 24 hours and 40°C

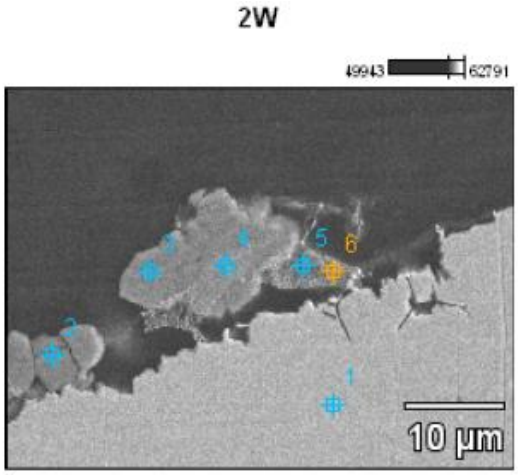

Image Name: 2W

Accelerating Voltage: 15.0 kV

Magnification: 2500

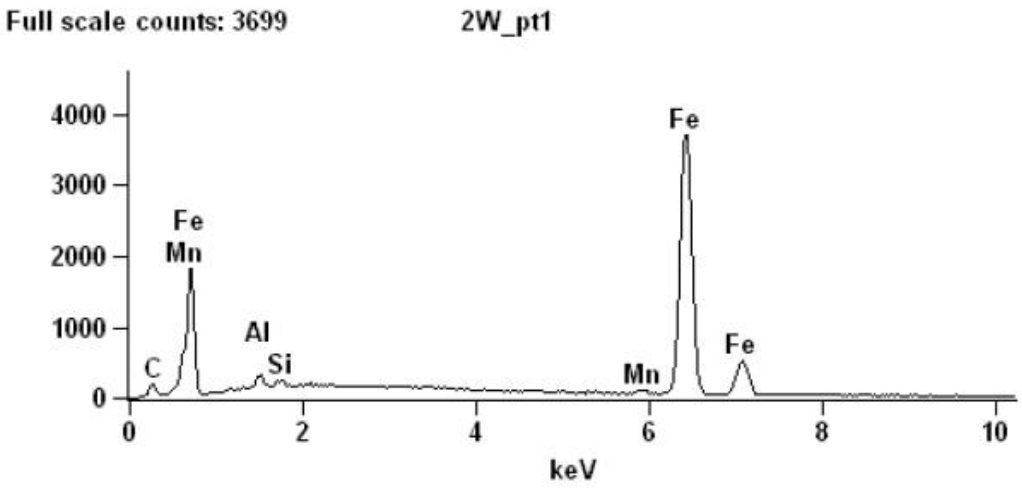

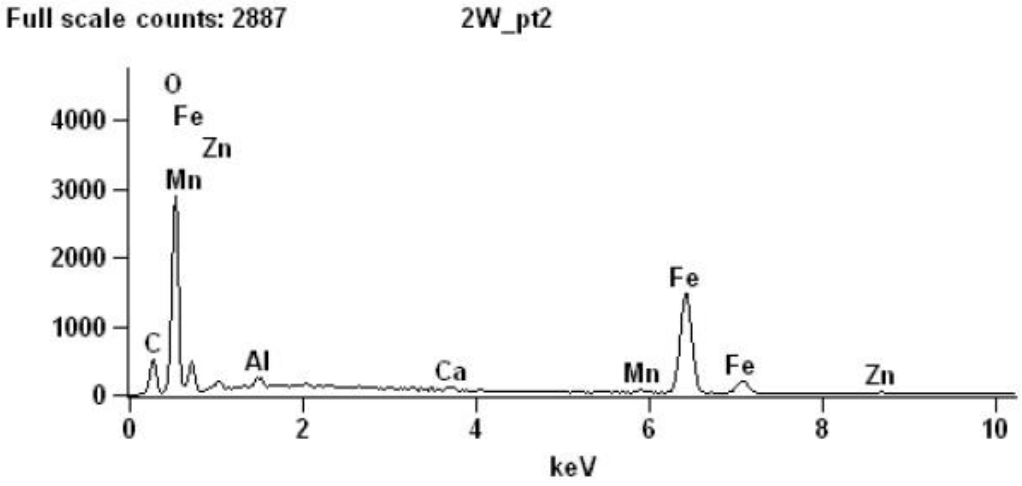

Full scale counts: 2667 2W_pt3

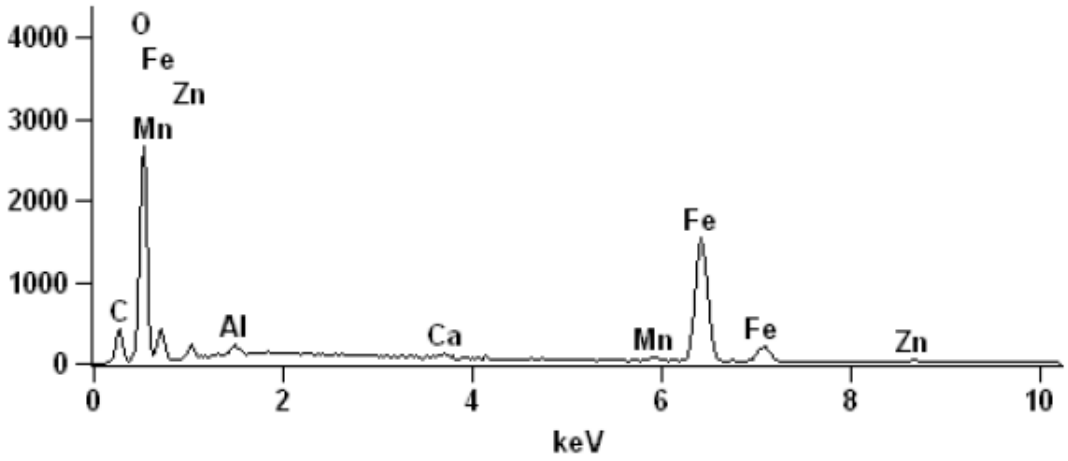

Full scale counts: 2435 2W_pt4

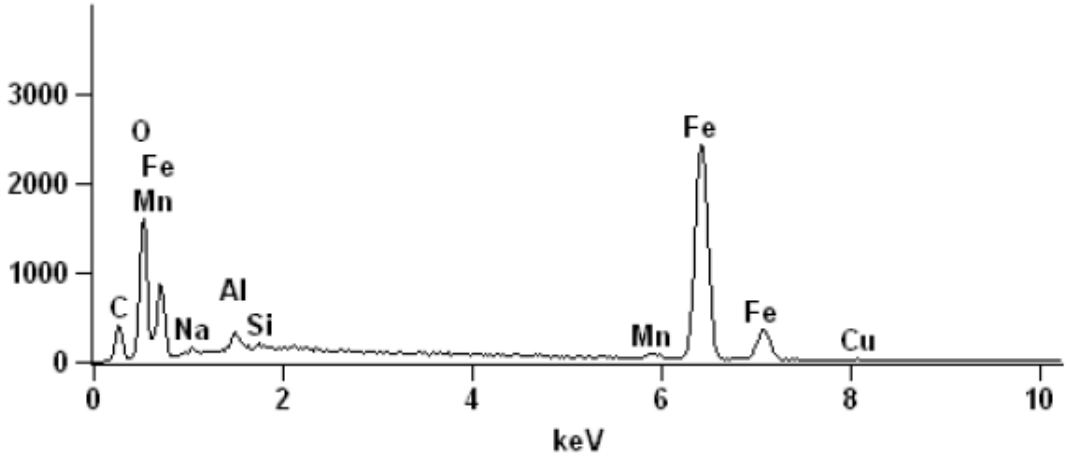

Full scale counts: 1629 2W_pt5

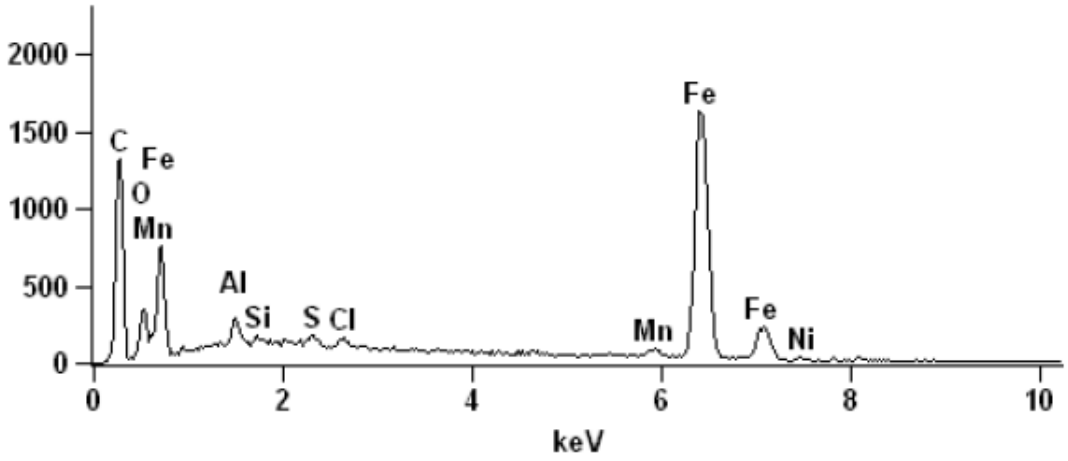

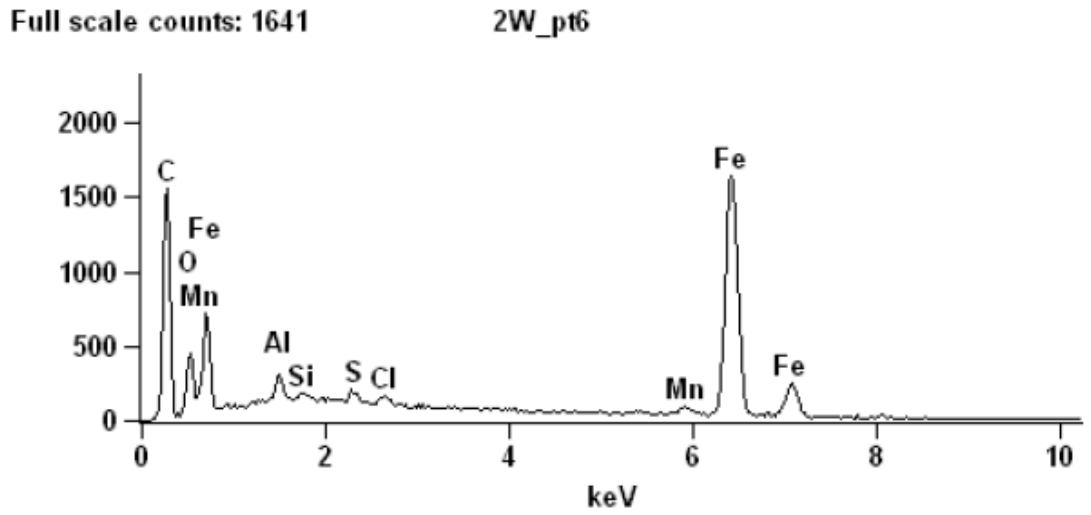

Weight %

	C-K	O-K	Na-K	Al-K	Si-K	S-K	Cl-K	Ca-K	Mn-K	Fe-K	Ni-K	Cu-K	Zn-K
2W_pt1	7.29			0.88	0.36				1.35	90.12			
2W_pt2	14.83	43.95		0.56				0.22	1.14	37.40			1.90
2W_pt3	12.97	41.73		0.46				0.33	1.18	40.57			2.75
2W_pt4	13.02	23.89	0.54	0.83	0.12				1.12	59.87		0.61	
2W_pt5	41.95	8.93		0.69	0.11	0.41	0.38		1.64	45.24	0.65		
2W_pt6	42.93	11.27		0.64	0.18	0.34	0.31		1.48	42.84			

Atom %

	C-K	O-K	Na-K	Al-K	Si-K	S-K	Cl-K	Ca-K	Mn-K	Fe-K	Ni-K	Cu-K	Zn-K
2W_pt1	26.51			1.42	0.56				1.07	70.44			
2W_pt2	26.11	58.11		0.44				0.12	0.44	14.17			0.62
2W_pt3	23.98	57.92		0.38				0.19	0.48	16.13			0.93
2W_pt4	29.00	39.95	0.63	0.82	0.12				0.55	28.68		0.26	
2W_pt5	70.49	11.27		0.52	0.08	0.26	0.21		0.60	16.35	0.22		
2W_pt6	69.78	13.75		0.47	0.12	0.21	0.17		0.53	14.97			

8.5.3 St33 steel at forced precorrosion 24 hours and 40°C

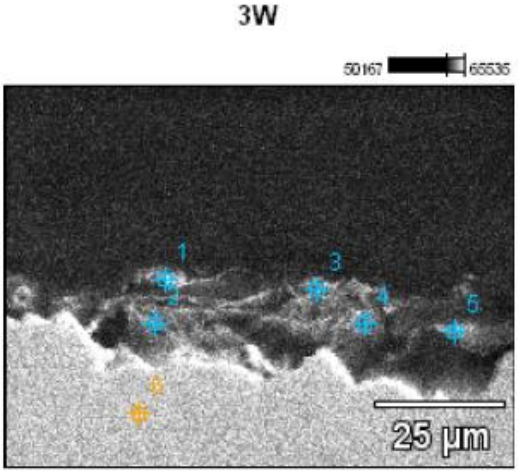

Image Name: 3W

Accelerating Voltage: 10.0 kV

Magnification: 1300

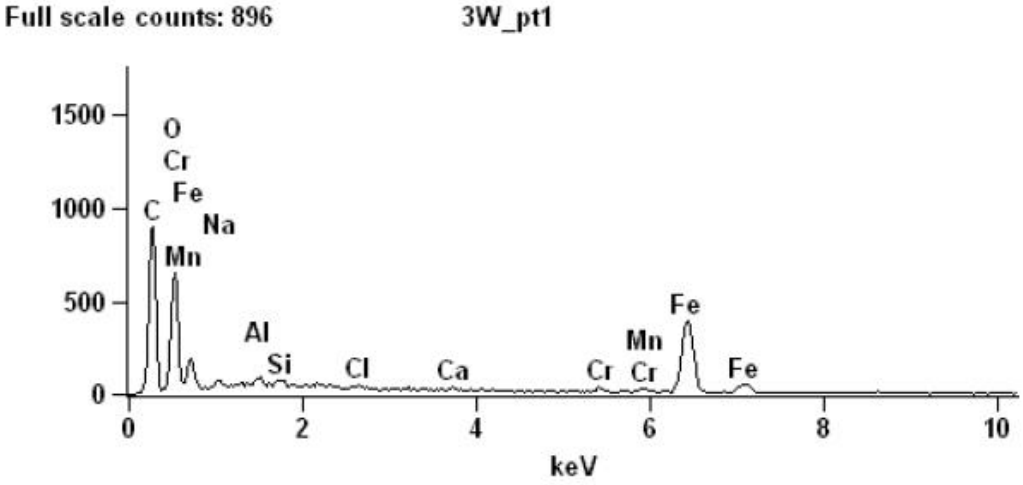

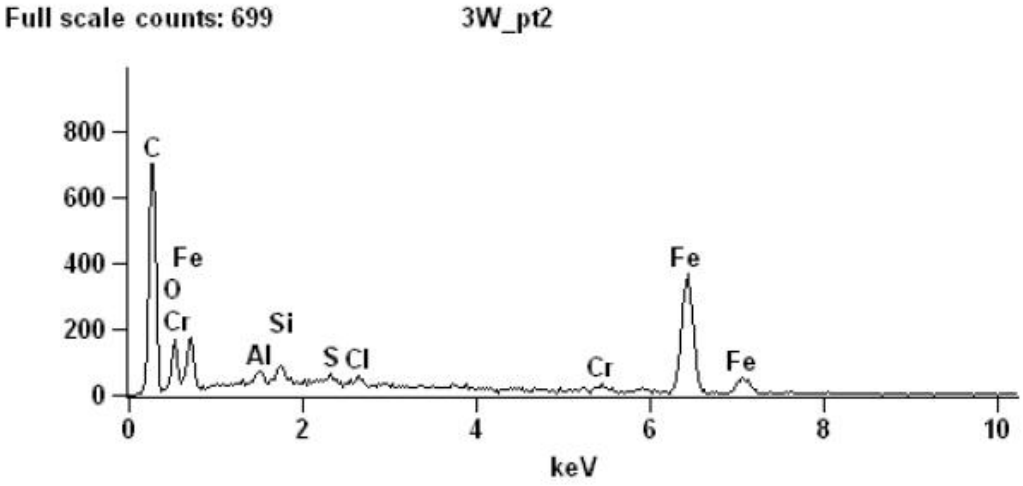

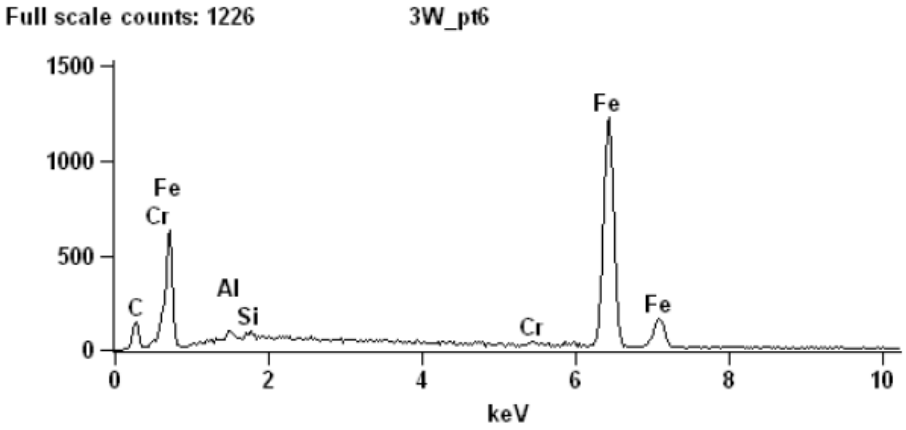

Weight %

	C-K	O-K	Na-K	Al-K	Si-K	S-K	Cl-K	Ca-K	Cr-K	Mn-K	Fe-K
3W_pt1	35.18	19.86	0.55	0.25	0.23		0.10	0.12	0.76	0.99	41.98
3W_pt2	39.92	6.36		0.26	0.39	0.17	0.39		0.70		51.81
3W_pt3	50.64	5.85		0.19	0.21	0.10	0.38		1.02		41.61
3W_pt4	44.94	5.02		0.17	0.46		0.43		1.13		47.86
3W_pt5	43.33	6.08		0.28	0.57	0.23	0.22		1.10		48.21
3W_pt6	6.19			0.23	0.08				0.45		93.06

Atom %

	C-K	O-K	Na-K	Al-K	Si-K	S-K	Cl-K	Ca-K	Cr-K	Mn-K	Fe-K
3W_pt1	58.56	24.82	0.47	0.18	0.17		0.06	0.06	0.29	0.36	15.03
3W_pt2	70.68	8.46		0.21	0.29	0.11	0.23		0.29		19.73
3W_pt3	78.44	6.80		0.13	0.14	0.06	0.20		0.36		13.86
3W_pt4	75.31	6.31		0.13	0.33		0.24		0.44		17.25
3W_pt5	73.39	7.73		0.21	0.41	0.14	0.13		0.43		17.56
3W_pt6	23.42			0.38	0.12				0.39		75.69

Full scale counts: 1261 3W_pt3

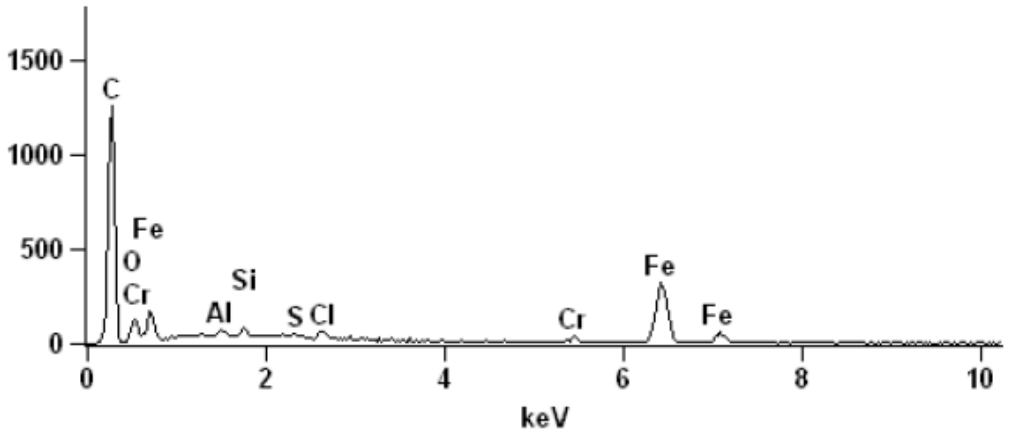

Full scale counts: 919 3W_pt4

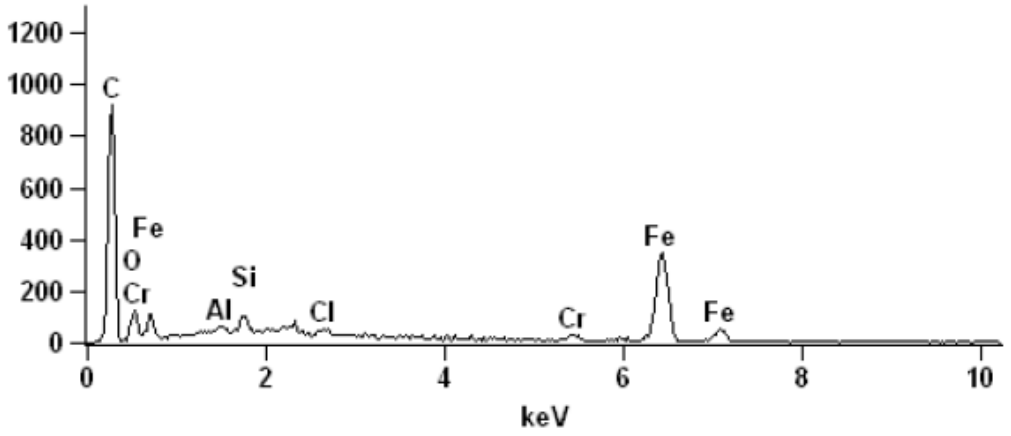

Full scale counts: 948 3W_pt5

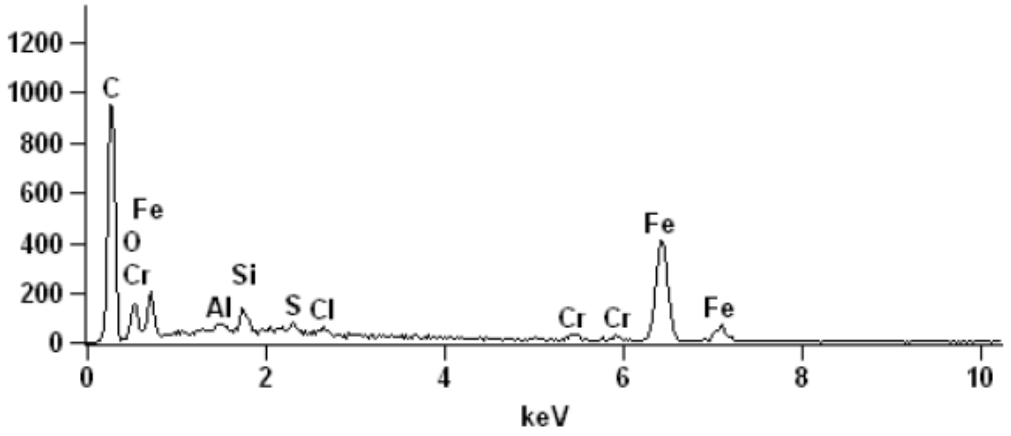

8.5.4 St33 steel at forced precorrosion 24 hours and 80°C

9W

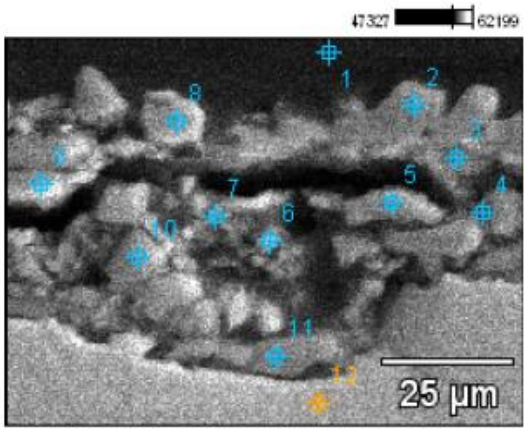

Image Name: 9W

Accelerating Voltage: 10.0 kV

Magnification: 1300

Full scale counts: 1153 9W_pt1

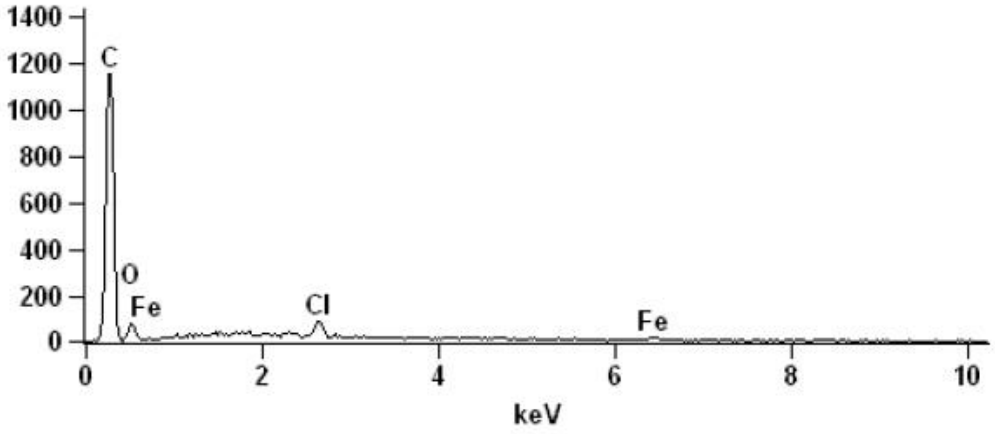

Full scale counts: 1330 9W_pt2

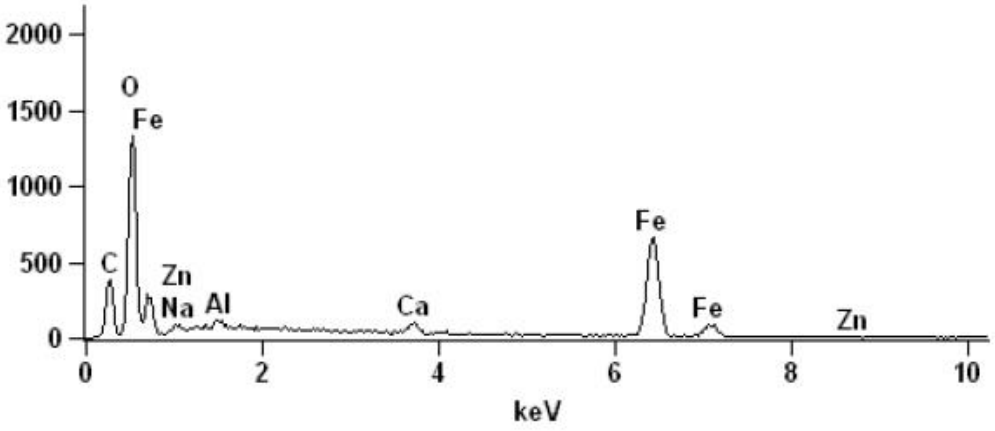

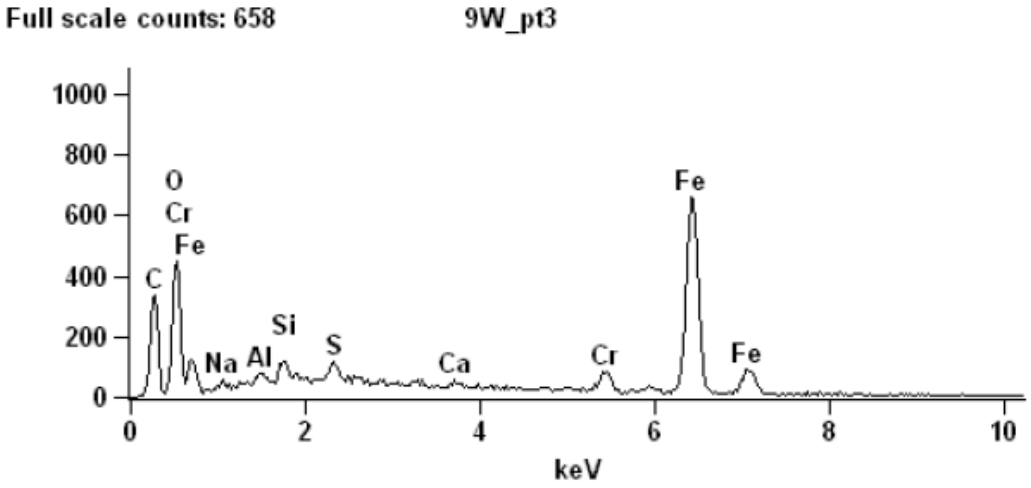
Full scale counts: 658
9W_pt3
1000
800
600
400
200
0
O
Cr
Fe
C
Si
Na
Al
S
Ca
Cr
Fe
Fe
0
2
4
6
8
10
keV

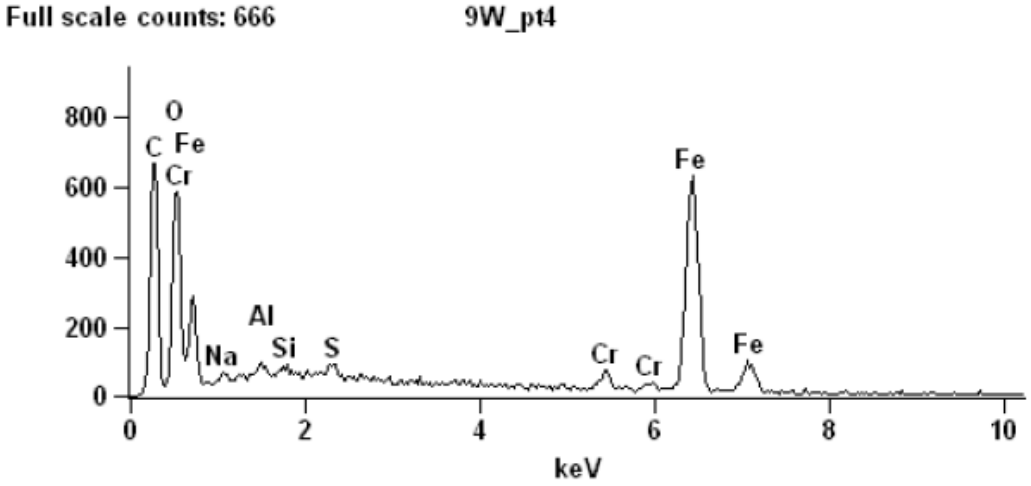
Full scale counts: 666
9W_pt4
800
600
400
200
0
O
C
Fe
Cr
Al
Na
Si
S
Cr
Cr
Fe
Fe
0
2
4
6
8
10
keV

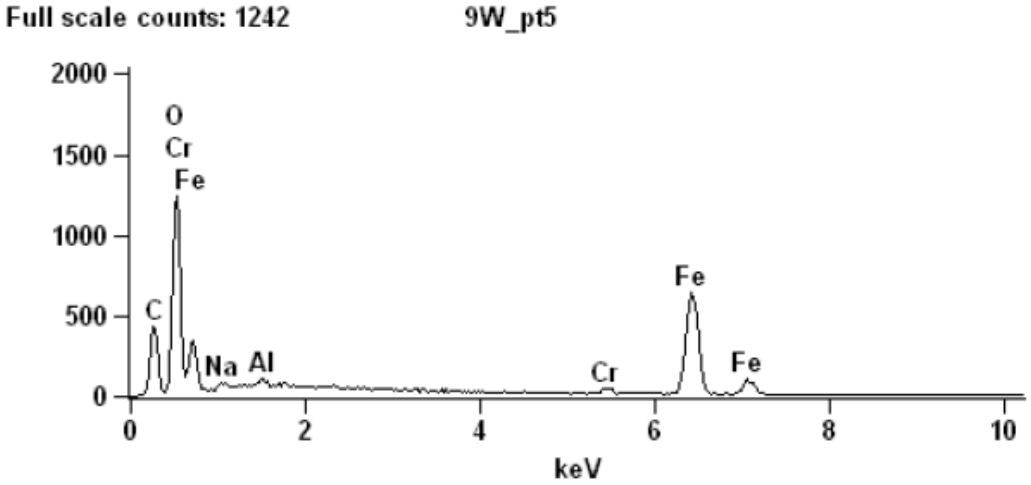
Full scale counts: 1242
9W_pt5
2000
1500
1000
500
0
O
Cr
Fe
C
Na
Al
Cr
Fe
Fe
0
2
4
6
8
10
keV

Full scale counts: 599 9W_pt6

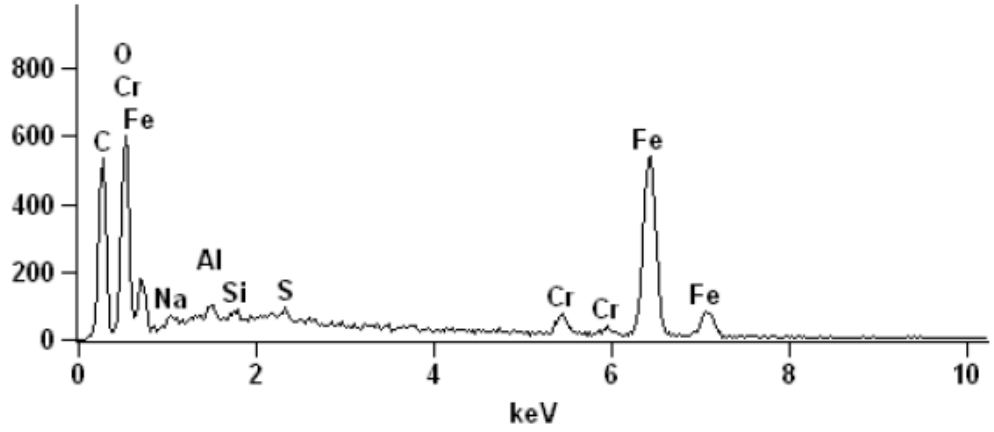

Full scale counts: 641 9W_pt7

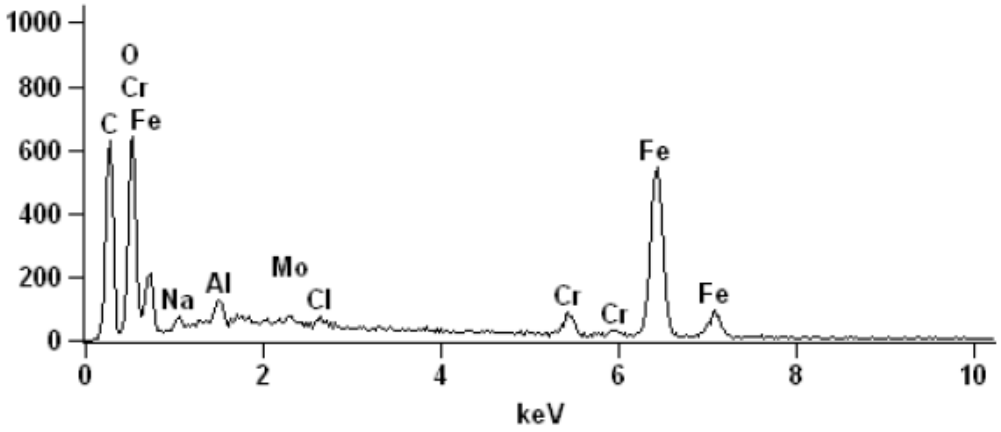

Full scale counts: 1330 9W_pt8

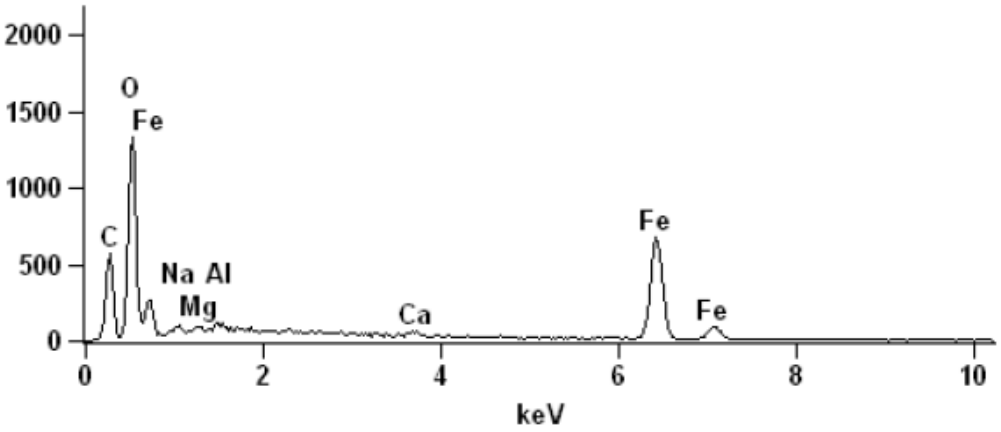

Full scale counts: 1169 9W_pt9

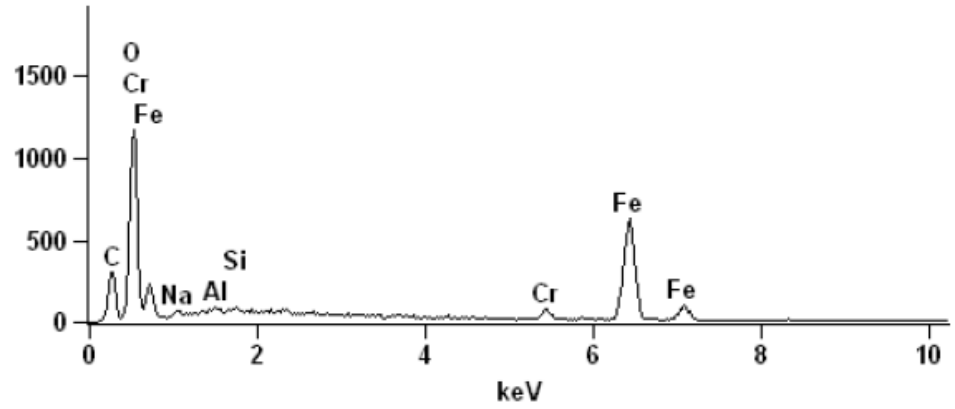

Full scale counts: 1024 9W_pt10

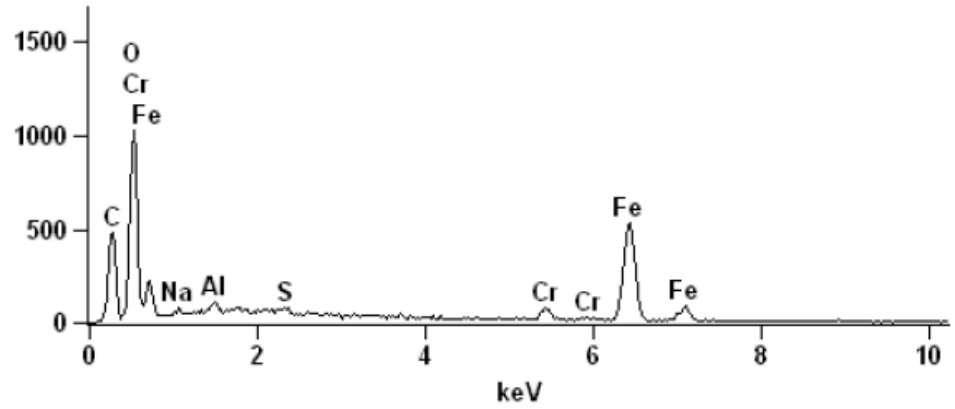

Full scale counts: 877 9W_pt11

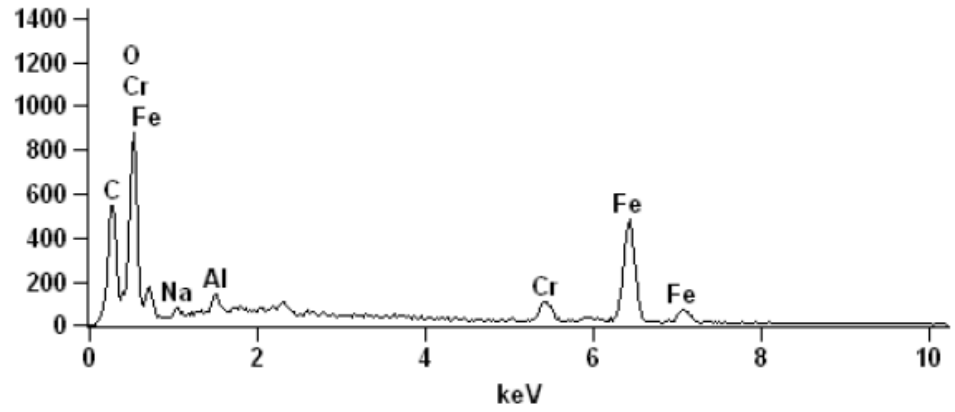

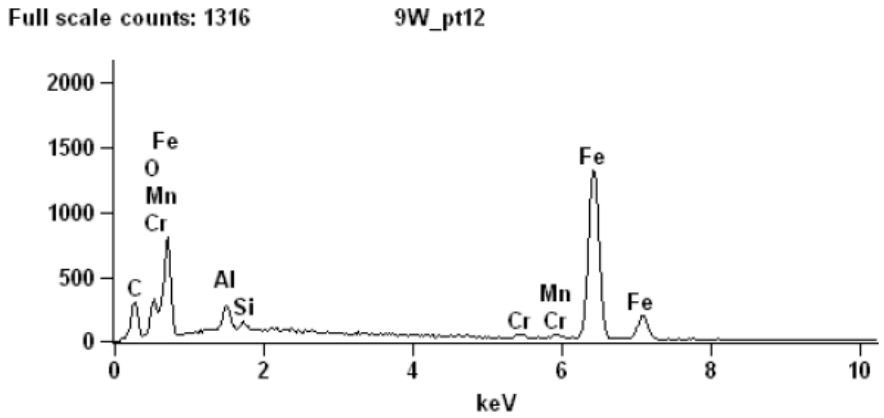

Weight %

	C-K	O-K	Na-K	Mg-K	Al-K	Si-K	S-K	Cl-K	Ca-K	Cr-K	Mn-K	Fe-K	Zn-L	Mo-L
9W_pt1	80.89	14.70						1.74				2.67		
9W_pt2	14.45	26.67	0.35		0.20				0.81			57.15	0.37	
9W_pt3	18.57	9.46	0.32		0.22	0.42	0.52		0.20	3.13		67.16		
9W_pt4	27.85	12.21	0.27		0.16	0.08	0.20			1.61		57.62		
9W_pt5	18.39	20.04	0.45		0.18					1.16		59.77		
9W_pt6	25.23	13.09	0.45		0.23	0.16	0.13			2.11		58.60		
9W_pt7	27.30	13.72	0.42		0.47			0.15		2.47		55.04		0.44
9W_pt8	19.25	26.01	0.60	0.14	0.20				0.33			53.48		
9W_pt9	14.48	20.26	0.49		0.18	0.11				1.82		62.66		
9W_pt10	22.75	20.13	0.33		0.27		0.18			2.52		53.82		
9W_pt11	24.51	17.95	0.49		0.52					4.36		52.16		
9W_pt12	9.33	3.36			0.85	0.15				0.54	0.79	84.97		

Atom %

	C-K	O-K	Na-K	Mg-K	Al-K	Si-K	S-K	Cl-K	Ca-K	Cr-K	Mn-K	Fe-K	Zn-L	Mo-L
9W_pt1	86.90	11.85						0.63				0.62		
9W_pt2	30.52	42.29	0.39		0.19				0.51			25.96	0.14	
9W_pt3	44.71	17.10	0.40		0.24	0.43	0.47		0.14	1.74		34.77		
9W_pt4	55.59	18.29	0.28		0.14	0.07	0.15			0.74		24.73		
9W_pt5	39.24	32.10	0.50		0.17					0.57		27.42		
9W_pt6	51.91	20.21	0.48		0.21	0.14	0.10			1.00		25.93		
9W_pt7	54.01	20.39	0.43		0.41			0.10		1.13		23.42		0.11
9W_pt8	37.86	38.41	0.61	0.14	0.17				0.19			22.62		
9W_pt9	32.93	34.59	0.58		0.18	0.11				0.96		30.65		
9W_pt10	45.16	30.00	0.34		0.24		0.13			1.16		22.98		
9W_pt11	48.35	26.58	0.50		0.46					1.99		22.12		
9W_pt12	30.23	8.18			1.23	0.20				0.40	0.56	59.20		

8.5.5 St33 steel at forced precorrosion 48 hours and 80°C

12W

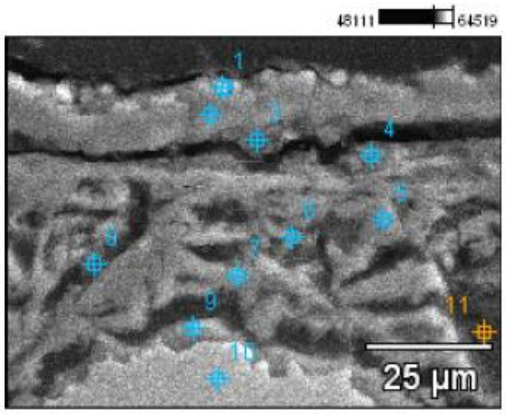

Image Name: 12W

Accelerating Voltage: 10.0 kV

Magnification: 1300

Full scale counts: 1402 12W_pt1

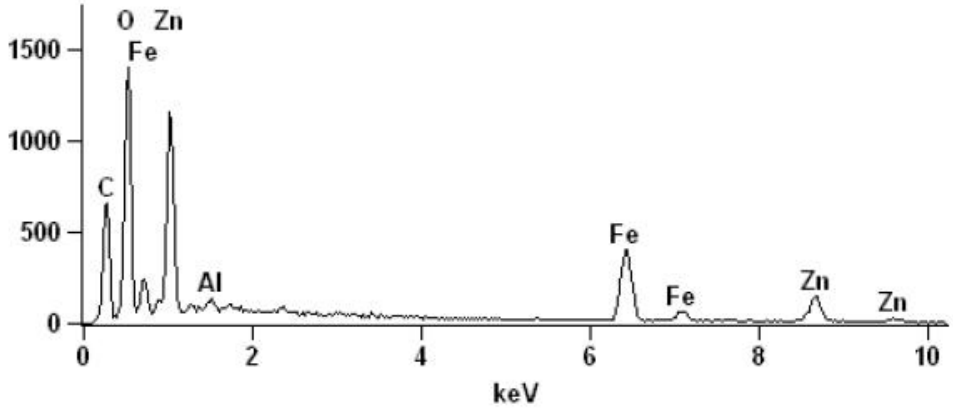

Full scale counts: 1272 12W_pt2

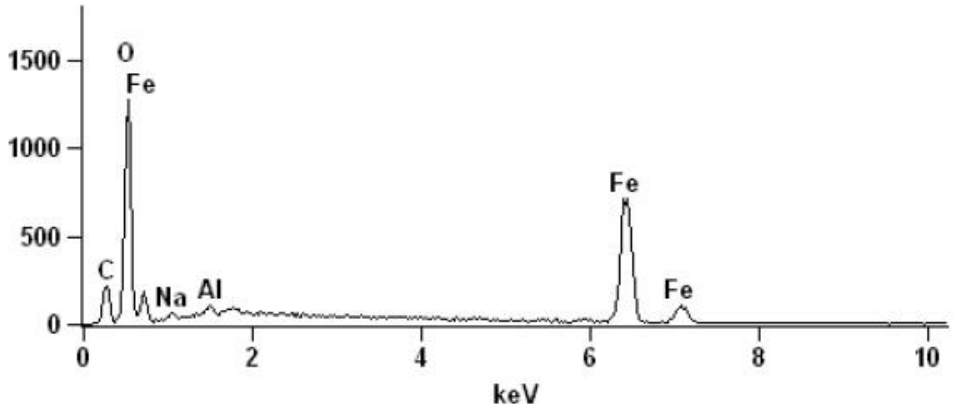

Full scale counts: 517 12W_pt3

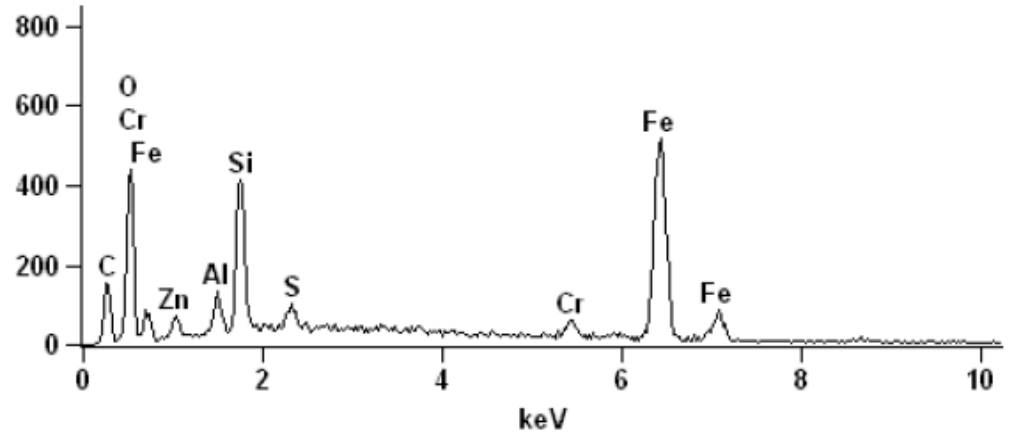

Full scale counts: 936 12W_pt4

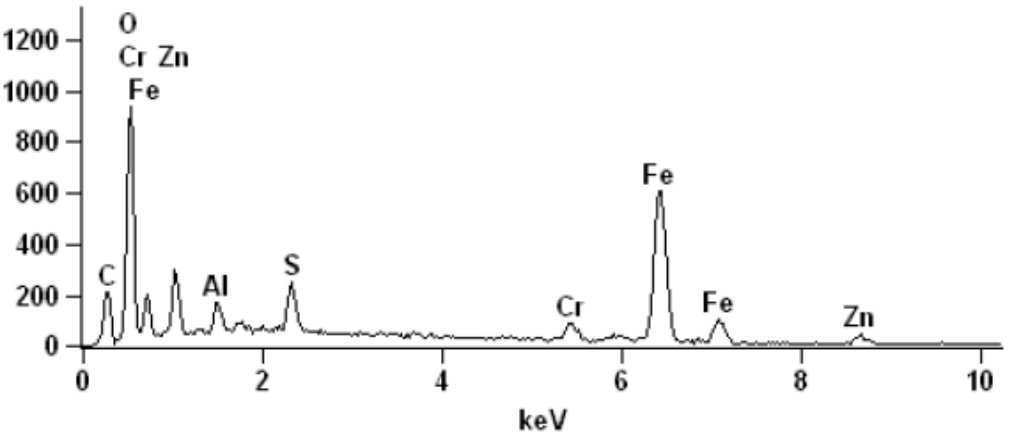

Full scale counts: 1307 12W_pt5

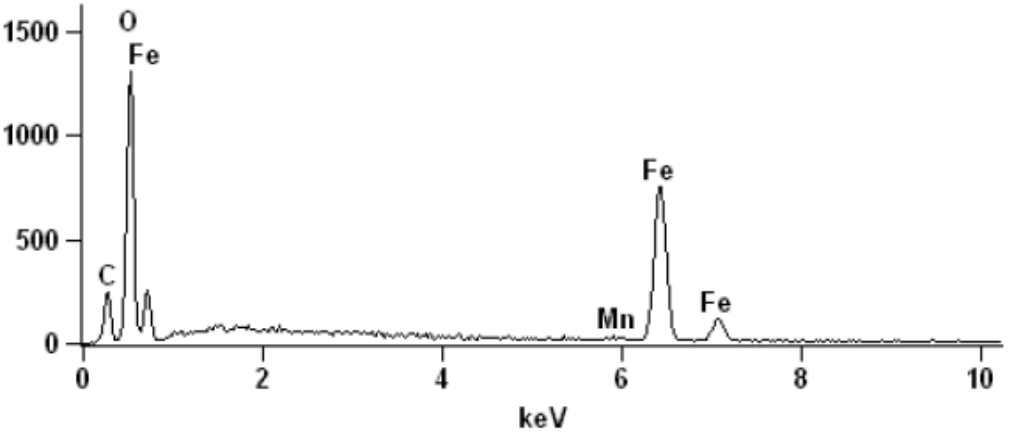

Full scale counts: 749 12W_pt6

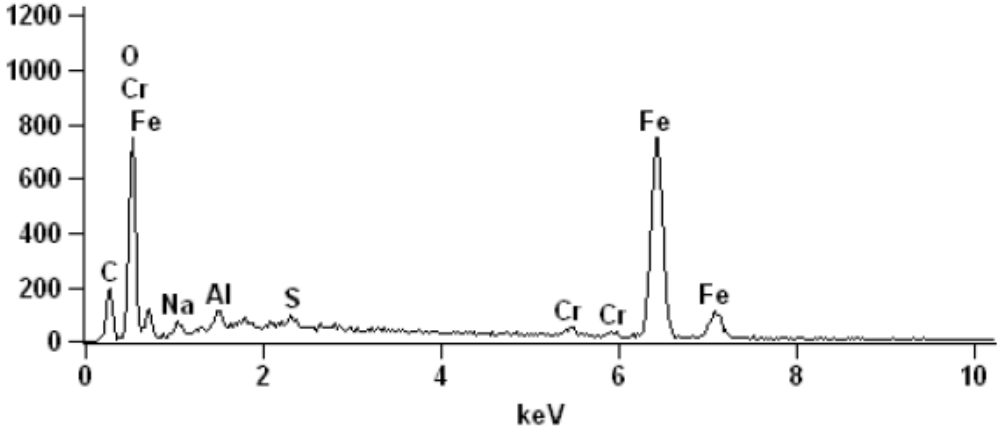

Full scale counts: 1262 12W_pt7

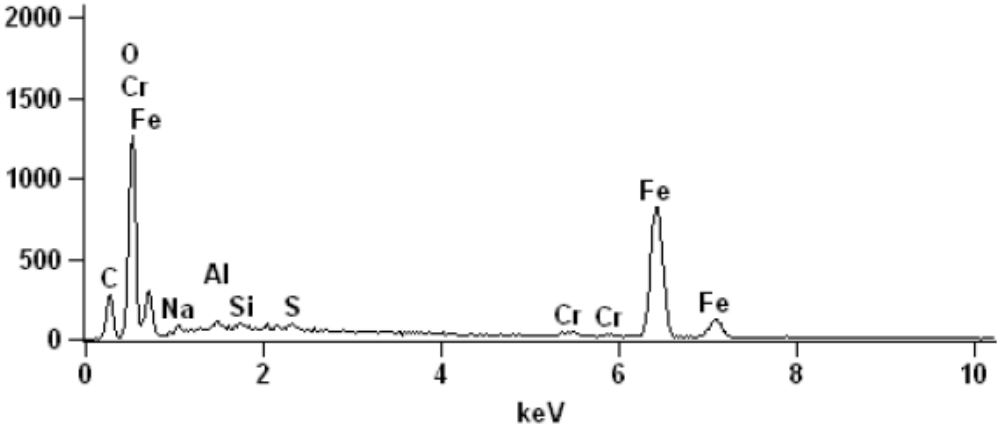

Full scale counts: 731 12W_pt8

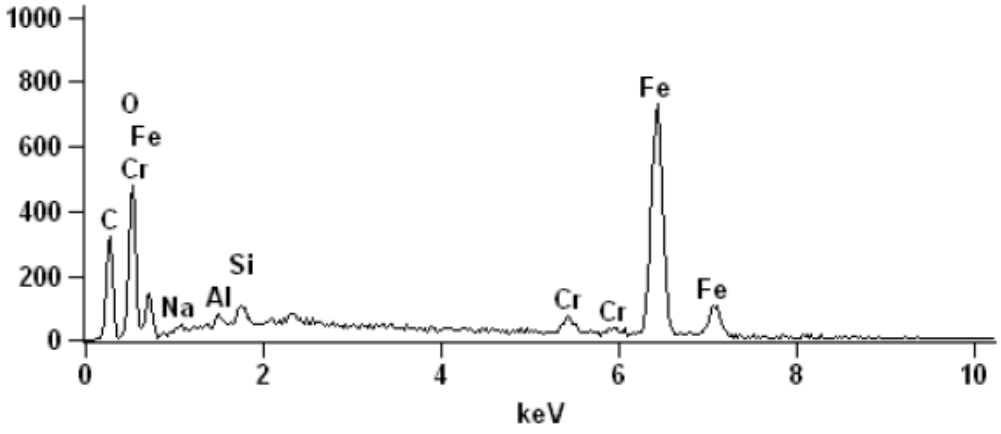

Full scale counts: 1551 12W_pt9

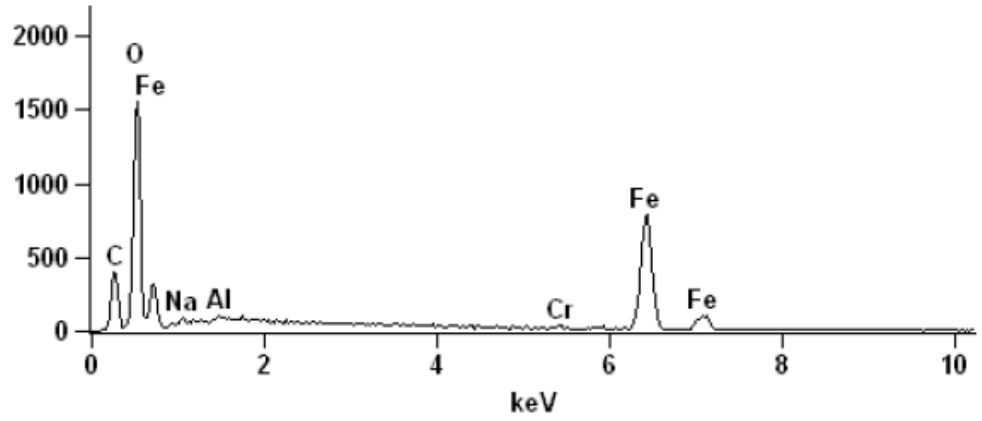

Full scale counts: 1806 12W_pt10

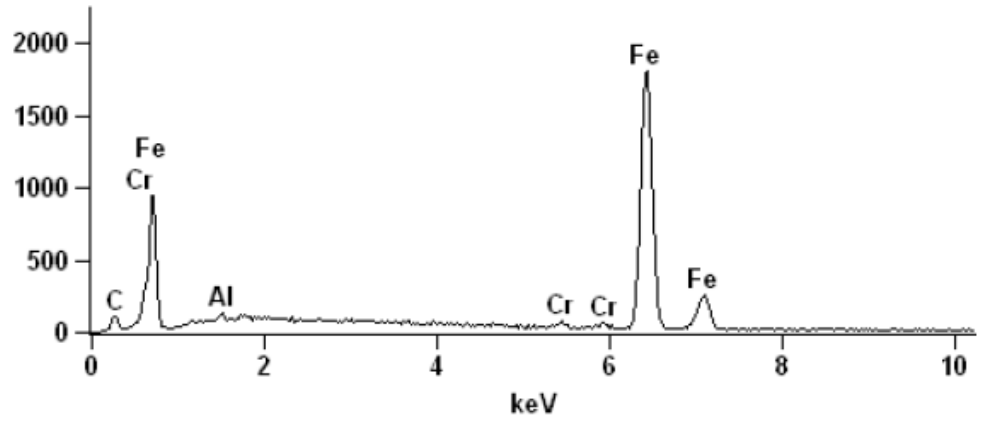

Full scale counts: 711 12W_pt11

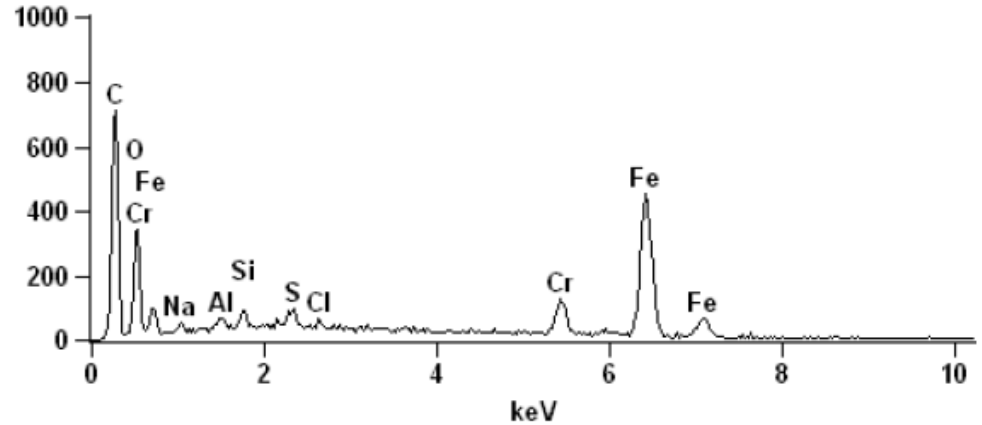

Weight %

	C-K	O-K	Na-K	Al-K	Si-K	S-K	Cl-K	Cr-K	Mn-K	Fe-K	Zn-L
12W_pt1	22.80	27.42		0.24						31.16	18.38
12W_pt2	9.42	21.61	0.39	0.35						68.23	
12W_pt3	11.73	11.41		0.89	3.23	0.64		2.01		68.03	2.06
12W_pt4	11.48	16.12		0.77		1.40		2.93		59.99	7.30
12W_pt5	9.30	21.62							0.66	68.41	
12W_pt6	9.73	12.83	0.70	0.49		0.27		1.11		74.88	
12W_pt7	11.20	18.36	0.29	0.16	0.11	0.24		0.98		68.67	
12W_pt8	15.69	9.29	0.25	0.19	0.33			1.92		72.32	
12W_pt9	14.45	23.30	0.34	0.21				0.40		61.30	
12W_pt10	3.06			0.15				0.70		96.10	
12W_pt11	32.56	10.17	0.38	0.21	0.27	0.36	0.19	4.63		51.22	

Atom %

	C-K	O-K	Na-K	Al-K	Si-K	S-K	Cl-K	Cr-K	Mn-K	Fe-K	Zn-L
12W_pt1	42.56	38.43		0.20						12.51	6.30
12W_pt2	23.15	39.89	0.50	0.39						36.07	
12W_pt3	31.03	22.68		1.05	3.66	0.63		1.23		38.72	1.00
12W_pt4	29.16	30.74		0.87		1.34		1.72		32.77	3.41
12W_pt5	23.03	40.19							0.36	36.43	
12W_pt6	26.72	26.46	1.00	0.59		0.28		0.71		44.24	
12W_pt7	27.78	34.17	0.37	0.17	0.11	0.22		0.56		36.61	
12W_pt8	40.21	17.87	0.33	0.22	0.37			1.14		39.86	
12W_pt9	31.76	38.46	0.40	0.20				0.20		28.98	
12W_pt10	12.76			0.28				0.67		86.29	
12W_pt11	61.56	14.44	0.38	0.18	0.22	0.25	0.12	2.02		20.82	